Universidade do Minho
Escola de Engenharia

Manuel Ricardo Mendes Pereira da Silva

Preparation and characterisation of novel multifuncional chitosan-based membranes to modulate cell-material interactions

Setembro de 2007

Preparation and characterisation of novel multifuncional chitosan-based membranes to modulate cell-material interactions
Manuel Ricardo Mendes Pereira da Silva
UMinho|2007

Universidade do Minho
Escola de Engenharia

Manuel Ricardo Mendes Pereira da Silva

Preparation and characterisation of novel multifuncional chitosan-based membranes to modulate cell-material interactions

Tese de Doutoramento
Ramo de Ciência e Tecnologia de Materiais - Área de Biomateriais

Trabalho efectuado sob a orientação do
Professor Doutor Rui Luís Gonçalves dos Reis
Professor Doutor João Filipe Colardelle da Luz mano

Setembro de 2007

Acknowledgments

Several years have been passed from the moment that I started this thesis and I could not finish it without express my gratitude to all the people that was present in the countless moments of this journey. It is interesting to realise the powerful metaphor: the last page to be written is exactly the first one by order of appearance of a thesis.

I would like to acknowledge my supervisor, Prof. Rui Reis, the director of the 3B's Research Group, for given me the opportunity to joint this enterprise and to participate in the construction of this research group, almost by spontaneous generation, revealing that the human capital is the most important one, as well as for the broad sight he gave me about the science world. I would also like to thank my co-supervisor, Prof João Mano, for the scientific discussions, philosophical brainstormings and for his good mood and refined humour.
I would like express my gratitude to Prof. Julio San Roman for receiving me in his lab and to have assigned the exceptional hands-on-lab supervisor Carlos Elvira (El Pine). Thank you both for your guidance in the macromolecular chemistry world and for your friendship. (Gracias por hacer del viejito laboratorio de Madrid un hogar de amistades).

I also acknowledge the Portuguese Foundation for Science and Technology (FCT) for the scholarship SFRH/BD/6862/2001and the Fundação Calouste Gulbenkian for supporting my attendance to some of the International Biomaterials Conferences.

I would like to dedicate a special thank to my dear colleagues and friends of the 3B's wide world, which, if I had to nominate everyone and explain the individual reasons behind my gratitude, I would considerable increase the expenses with the printing of this manuscript. Your support, scientific inventiveness and friendship were critical to withstand the harder moments. A todos aqueles que completaram o significado das palavras amizade e entreajuda.

Gracias a todos mis queridos compañeros del CSIC, con quienes viví momentos inolvidables, por las partidas de tetris y la copa Leoncio, el San Alberto, la fiesta de Navidad, os echo mucho de menos. Agradezco especialmente a Paloma, por su sonrisa, a Cesar, por su fuerte carácter y humor, y a Miguel, por haberme invitado a cenar en su casa, además en la mesa. Gracias por haberme enseñado una España profunda y una de sus mayores glorias, el Beni.

A todos os amigos e amigas cujas vidas entraram em algum momento em rota de fusão com a minha e cujas memórias me provocam o sorriso irreprimível da consciência, encontros que se estendem desde os tempos do infantário ao dia de hoje, mesmo àqueles com os quais as vicissitudes do possível não me permitiram um convívio mais continuado.

Não poderia deixar de agradecer à Rita, pela marca indelével que deixou na minha personalidade, na minha história, pelo apoio afectivo e efectivo em momentos difíceis deste percurso, pelos choros e alegrias.

Quero também expressar a minha profunda gratidão e apreço à minha mãe, ao meu pai e aos meus irmãos Leninha, Eduardo e Cristina pelo apoio incondicional, pela compreensão implícita; aos meus avós Ana e Herculano, Nené e Joffre, pela sua imensa afectividade.

À minha querida Paula, anda cá, que te agradeço em segredo, por pintares o meu mundo com cores insuspeitáveis, porque o envolveste em melodias sussurradas, porque me ensinaste a pronunciar *unha aperta*, por teres revestido de significação a velhinha máxima de Arquimedes, “dêem-me um ponto de apoio e eu moverei o mundo”.

Preparation and characterisation of novel multifunctional chitosan-based membranes to modulate cell-material interactions

A critical scarcity of donors and the high risk of graft rejection are the two major obstacles to the wide spreading of organ transplantation as an universal therapy for the substitution of organ, which underwent disease caused failure or irreversible accidental damaging. In order to overcome some of the limitations of the current therapies, several regenerative medicine concepts have emerged in the last few decades. One of those concepts, denominated guided bone regeneration (GBR), consists on the use of barrier membranes that prevent the in-growth of connective tissue, which in critical size defects inhibits the formation of new bone through the natural healing process. The first objective of this thesis was to develop biodegradable membranes based on chitosan and soybean protein exhibiting a biphasic structure, which would originate in situ porous formation, through a two step degradation mechanism. This application features some limitations and new approaches were designed seeking to widen the impact that the developed work could have in the regenerative medicine field.

The tissue engineering field is likely to be the most paradigmatic example within the several regenerative medicine strategies born in the past decades. However, tissues and organs reconstruction have been often limited by these approaches, since tissue engineered constructs are very sensitive to a range of variables, which correlation is frequently not well understood or easily controllable. In order to overcome some of the limitations imposed by the use of supporting biodegradable materials, a new ingenious approach known as “cell sheet engineering” proved to succeed on recreating *in vitro* tissues with high therapeutic potential. Despite of the still relatively low number of the papers found in the literature about this issue, “cell sheet engineering” products are already reaching the clinical stage. This technology makes use of culture dishes grafted with thermo-responsive poly(*N*-isopropylacrylamide) (PNIPAAm) that undergo a transition at the lower critical solution temperature (LCST) from hydrophobic (above that value) to hydrophilic. At the culture temperature, grafted surfaces are slightly hydrophobic and cell adhesion and proliferation proceed as in conventional culture surfaces. Cultured confluent cell sheets spontaneously detach by merely reducing the temperature. In fact, the slightly hydrophobic surfaces are suitable for cell adhesion, while the more hydrated hydrophilic surfaces are not. The method is minimally invasive to the extracellular matrix (ECM), cell-to-cell and cell-to-ECM interactions, in opposition to the conventional enzymatic methods, which are deleterious to important biological structures such as ECM and cell membrane proteins.

Despite of the great advances that have been already done on culturing and harvesting cell sheets from varied phenotypes, much less endeavour has been devoted to the creation of multifunctional novel thermo-responsive surfaces. In this thesis, several studies have been performed towards this goal, which are described in detail in Chapters 5, 6 and 7.

First, we prepared chitosan membranes and studied the influence of crosslinking these membranes with glutaraldehyde in a range of different properties. We performed measurements of the mechanical properties with the samples immersed in an aqueous environment at 37ºC, in order to simulate physiological and cell culture conditions. Chitosan absorbs high amounts of water in aqueous solutions forming hydrogels. In this kind of systems, the determination of the mechanical properties in dry conditions has no practical meaning.

Second, a preliminary cytotoxicity screening was performed in order to check if the materials would be suitable as implantable biomaterials, as well as for cell culture purposes. The tested membranes showed to be suitable for biomedical applications.

Third, the transport properties of small molecules have been studied, showing that the membranes possess permeation properties that can be useful for the controlled delivery of bioactive agents, but also in combined strategies of growth and differentiation factors delivery and cell sheet engineering.

Finally, PNIPAAm was grafted onto chitosan membranes to render surface with thermo-responsive properties. Those modified membranes showed to be suitable for cell culture, which can reach confluence and be thermally harvested by means of lowering the temperature.

Single cell sheets can be layered in order to recreate thicker tissue-like constructs. However, the number of cell sheets that can be kept in culture is limited, because of restrictions on the delivery of nutrients and accumulation of metabolic wastes. It should be noticed that PNIPAAm grafted tissue culture polystyrene (TCPS) substrates commonly used to culture single cell sheets are impermeable. The use of chitosan membranes, which we found to be permeable to small molecules, would increase the mass transfer area for nutrients and metabolic wastes, hopefully supporting the culture of thicker layered cell sheet constructs. Furthermore, fully hydrated chitosan membranes should be easily adaptable to several anatomical shapes, owing to its flexible mechanical properties, facilitating the transfer of either single cell sheets or layered cell sheet constructs directly to the host site with minimal manipulation.

Preparação e caracterização de membranas à base de quitosano contendo simultaneamente várias funcionalidades inovadoras para modular as interacções entre células e materiais.

O elevado défice de doadores e o risco de rejeição impedem a banalização do transplante de órgãos como abordagem terapêutica. Nas últimas décadas têm sido propostas várias estratégias de investigação no campo da medicina regenerativa para tentar resolver estas limitações. A regeneração guiada de osso (GBR) é uma dessas estratégias e consiste no uso de membranas que proporcionam uma barreira à penetração de tecido conectivo no defeito ósseo, o que em lesões acima de uma determinada dimensão, impede o processo natural de regeneração. O primeiro objectivo desta tese foi desenvolver membranas biodegradáveis para este tipo de aplicações, combinando quitosano com proteína de soja, de forma a obter uma estrutura com duas fases. A diferente taxa de degradação de cada uma dessas fases originaria a formação de poros *in situ*. Ainda que bastante interessantes, estas aplicações possuem potencialidades de inovação algo limitadas, pelo que, outras estratégias foram implementadas ao longo do trabalho para alargar seu o impacto no campo da medicina regenerativa.

A engenharia de tecidos humanos é provavelmente uma das estratégias mais paradigmáticas e representativas das revoluções recentes no campo da medicina regenerativa. Contudo, a reconstrução de tecidos e órgãos é muitas vezes limitada, uma vez que os implantes produzidos por engenharia de tecidos são muito sensíveis a um conjunto de variáveis cuja correlação é frequentemente obscura ou dificilmente controlável. Mais recentemente, uma estratégia inovadora, denominada em inglês "*cell sheet engineering*", têm permitido recriar tecidos *in vitro* com elevado potencial terapêutico, evitando o uso de materiais de suporte biodegradáveis. De facto, embora seja relativamente recente, alguns produtos já foram testados clinicamente com sucesso. Esta tecnologia baseia-se no uso de superfícies modificadas com poli(*N*-isopropilacrilamida) (PNIPAAm). Este polímero possuí uma temperatura de transição em solução (LCST), conferindo à superfície carácter hidrofóbico acima da LCST e hidrofílico abaixo desse valor. Assim, superfícies modificadas com este polímero têm um carácter hidrofóbico nas condições de cultura celular, permitindo uma correcta adesão e proliferação. No entanto, diminuindo a temperatura abaixo da LCST o carácter da superfície passa a ser hidrofílico, induzindo o destacamento das células. Quando cultivadas até atingirem a confluência, ocorre uma separação espontânea de uma película de células contíguas ou "*cell sheet*", conjuntamente com a matriz extracelular entretanto produzida por essas mesmas células. Este método permite a recuperação de

estruturas biológicas importantes para o correcto funcionamento dos tecidos, em oposição aos métodos enzimáticos mais convencionais, que são bastante destrutivos. As grandes potencialidades deste método, já demonstradas para células de diversas origens e fenótipos, tornam bastante atractivo o desenvolvimento de superfícies que respondem à temperatura com outras funcionalidades inovadoras. Os diversos estudos desenvolvidos no âmbito desta tese com este objectivo estão detalhados nos capítulos 5, 6 e 7.

Em primeiro lugar, prepararam-se membranas de quitosano e estudou-se a influência da reticulação dessas membranas com glutaraldeído em várias propriedades. As propriedades mecânicas destas membranas foram estudadas submergindo as amostras em soluções aquosas a 37ºC, de forma a simular as condições fisiológicas. O quitosano absorve quantidades consideráveis de água, sendo os materiais resultantes hidrogéis. Neste tipo de sistemas, a determinação das propriedades mecânicas com as amostras secas perderia o significado prático.

Numa segunda fase foi feita uma avaliação preliminar da citotoxicidade dos materiais, o que demonstrou a sua potencial aplicabilidade como biomateriais e em culturas celulares.

No passo seguinte estudaram-se as propriedades de transporte de pequenas moléculas, demonstrando-se que as membranas possuem valores de permeabilidade que podem ser úteis para aplicações de libertação controlada de agentes bioactivos, assim como, em estratégias que combinem a libertação controlada de factores de crescimento e diferenciação com as técnicas de "*cell sheet engineering*".

Por último, a PNIPAAm foi originalmente imobilizada à superfície das membranas de quitosano, de forma a que a superfície responda a alterações de temperatura. Estas membranas demonstraram ser adequadas para a cultura de células que, uma vez atingida a confluência, puderam ser separadas da superfície apenas reduzindo a temperatura.

As "*cell sheets*" podem ser sobrepostas de forma a criar estruturas biológicas com maior espessura. No entanto, o número de "*cell sheets*" sobrepostas que se podem manter em cultura está limitado por restrições no fornecimento de nutrientes e pela acumulação de produtos metabólicos de excreção. As superfícies tipicamente usadas em "*cell sheet engineering*" consistem em PNIPAAm covalentemente imobilizado na superfície de placas de poliestireno de cultura celular. No entanto, estes materiais são impermeáveis. O uso de membranas de quitosano, permeáveis a moléculas de pequenas dimensões, aumentaria a eficiência na troca de nutrientes e produtos de excreção, permitindo eventualmente o aumento do número de "*cell sheets*" que se poderia sobrepor em cultura. Adicionalmente, as membranas de quitosano hidratadas poderão ser facilmente adaptáveis a formas anatómicas diversas, devido à sua elasticidade, facilitando a manipulação e a transferência directa de "*cell sheets*" individuais ou sobrepostas para o paciente.

Table of Contents

List of Figures

List of Tables

List of Text Boxes

List of abbreviations and nomenclature

1 Introduction. Smart thermoresponsive coatings and surfaces for tissue engineering: switching cell-material boundaries

ATP	Adenosine triphosphate
ECM	Extracellular matrix
EDTA	Ethylenediaminetetraacetic acid
LCST	Lower critical solution temperature
MBAAm	Methylenebis(acrylamide)
PEG	Polyethylene glycol
PNIPAAm	Poly(*N*-isopropylacrylamide)
SAMS	Self-assembled monolayers
SFG	Sum frequency generation
TCPS	Tissue culture polystyrene
UV	Ultraviolet

2 Materials and Methods

A	Absorbance
AE	Air-exposed surface during the drying process of a membrane
AIBN	2,2'-Azobis-isobutyronitrile
ATR	Attenuated total reflection
BA	Benzoic acid
BCA	Bicinchoninic acid
C	Concentration in g/dL
$C_{(GA)}$	Concentration of glutaraldehyde
CAE	Constant Analyser Energy mode
CTS	Chitosan
D'	Storage compliance
DA	Degree of *N*-acetylation
DD	Degree of *N*-deacetylation
DMA	Dynamic Mechanical Analysis
DMEM	Dulbecco's Modified Eagle's Medium
E'	Storage modulus

EDTA	Ethylenediaminetetraacetic acid
ESCA	Electron Spectroscopy for Chemical Analysis
ESEM	Environmental Scanning Electron Microscopy
EtO	Ethylene oxide
FBS	Foetal Bovine Serum
FTIR	Fourier transformed infrared spectroscopy
GA	Glutaraldehyde
GluN	β-(1→4)-2-amino-2-deoxy-D-glucopyranose
GluNAc	β-(1→4)-2-acetamido-2-deoxy-D-glucopyranose
IR	Infrared
ISS	Isotonic saline solution
K	Partition coefficient
K_H	Huggins coefficient
K_K	Kraemer coefficients
l	Optical pathway
$m_{(CTS)}$	Dry weight of chitosan in grams
$M_{(GluN)}$	Molecular weights of the GluN units in chitosan
$M_{(GluNAc)}$	Molecular weights of the GluNAc units in chitosan
MC	Moisture content
ME	Mould-exposed surface during the drying process of a membrane
MTT	3-(4,5-dimethylthiazol-2-yl)-2,5-diphenyltetrazolium bromide
M_v	Viscosity average molecular weight
$n_{(GluN)}$	Molar amount of amine groups in a certain chitosan
NMR	Nuclear magnetic resonance
PBS	Phosphate buffer solution
Ph	Phthalic acid
pI	Isoelectric point
S	Swelling ratio
SA	Salicylic acid
SEM	Scanning electron microscopy
S_{eq}	Equilibrium swelling ratio
SI	Soybean protein isolate
t	Flow time
t_0	Flow time for the solvent
tan δ	Loss factor
TGA	Thermogravimetric analysis

TRIS	Trishydroxymethylaminomethane
UV	Ultraviolet
$V_{(GA)}$	Volume of glutaraldehyde
W	Weight of a swelled sample
W_0	Initial weight of a sample
WAXS	Wide-angle X-ray scattering
WL	Weight loss
WU	Water uptake
x'	Crosslinking degree
XPS	X-ray photoelectron spectroscopy
η	Viscosity
η_r	Relative viscosity
η_{sp}	Specific viscosity
θ	Contact angle
σ_s	Surface tension
σ_s^d	Dispersive component of the surface tension
σ_s^p	Polar component of the surface tension

3 Straightforward determination of the degree of *N*-acetylation of chitosan by means of 1st derivative UV spectrophotometry

A	Absorbance
AcOH	Acetic acid
C	Concentration
CP/MAS	Cross Polarization Magic Angle Spinning
C_t	Molar concentration of both pyranosyl units of chitosan
$\overline{C_t}$	Concentration in g/l of both pyranosyl units of chitosan
CV	Coefficient of variation
DA	Degree of *N*-acetylation
FTIR	Fourier transformed infrared
GluN	β-(1→4)-2-amino-2-deoxy-D-glucopyranose
GluNAc	β-(1→4)-2-acetamido-2-deoxy-D-glucopyranose
HAc	Acetyl group protons
l	Optical path length
M_a	Molecular weight of the GluNAc units of chitosan
MC	Moisture content

M_g	Molecular weight of GluN units of chitosan
NMR	Nuclear magnetic resonance
TGA	Thermogravimetric analysis
UV	Ultraviolet
δ	Chemical shifts in nuclear magnetic resonance
ε	Molar absorptivity
ε_a	1st derivative of the GluNAc molar absorptivity
ε_g	1st derivative of the GluN molar absorptivity
λ	Wavelength
σ	Standard deviation

4 Influence of β-Radiation Sterilization in Properties of New Chitosan/Soybean Protein Isolate Membranes for Guided Bone Regeneration

AcOH	Acetic acid
AE	Air-exposed surface during the drying process of a membrane
BSE	Bovine Spongiform Encephalopathy
CTS	Chitosan and
ESEM	Environmental Scanning Electron Microscopy
FTIR-ATR	Fourier Transform Infrared with Attenuated Total Reflection
GBR	Guided bone regeneration
GluN	β-(1→4)-2-amino-2-deoxy-D-glucopyranose
GluNAc	β-(1→4)-2-acetamido-2-deoxy-D-glucopyranose
ME	Mould-exposed surface during the drying process of a membrane
pI	Isoelectric point
SEM	Scanning electron microscopy
SI	Soybean Protein Isolate
W	Weight of a swelled sample
W_0	Initial weight of a sample
WU	Water Uptake
θ	Contact Angle
σ_s	Surface tension
σ_s^d	Dispersive component of the surface tension
σ_s^p	Polar component of the surface tension

5 Preparation and characterisation in simulated body conditions of glutaraldehyde crosslinked chitosan membranes

BCA	Bicinchoninic acid
BSA	Bovine serum albumin
CTS	Chitosan
DD	Degree of *N*-deacetylation
DMA	Dynamic Mechanical Analysis
DMEM	Dulbecco's Modified Eagle's Medium
E'	Storage modulus
EDTA	Ethylenediaminetetraacetic acid
FBS	Fetal Bovine Serum
GluN	β-(1→4)-2-amino-2-deoxy-D-glucopyranose
GluNAc	β-(1→4)-2-acetamido-2-deoxy-D-glucopyranose
ISS	Isotonic saline solution
MTT	(3-(4,5-dimethylthiazol-2-yl)-2,5-diphenyltetrazolium bromide)
PBS	Phosphate buffer solution
tan δ	Loss factor
W	Weight of a swelled sample
W_0	Initial weight of a sample
WAXS	Wide-angle X-ray scattering
WL	Weight loss
WU	Water uptake

6 Transport of small anionic and neutral solutes through chitosan membranes: dependence on crosslinking and chelation of divalent cations

A	Membrane useful mass transfer area
BA	Benzoic acid
C	Solute concentration
$C_{(GA)}$	Concentration of glutaraldehyde solution
C_D	Concentration at donor half-cell
C_m	Solute concentration in the liquid fraction absorbed by a sample
C_R	Concentration at receptor half-cell
C_s	Solute concentration in the bulk solution
CTS	Chitosan

D	Diffusion coefficient
DD	Degree of *N*-deacetylation
FTIR-ATR	Fourier Transform Infrared with Attenuated Total Reflection
GA	Glutaraldehyde
GluN	β-(1→4)-2-amino-2-deoxy-D-glucopyranose
GluNAc	β-(1→4)-2-acetamido-2-deoxy-D-glucopyranose
J	Flux
K	Partition coefficient
l	Optical pathway
M_a	Molecular weight of the GluNAc units of chitosan
M_g	Molecular weight of the GluN units of chitosan
P	Permeability
PBS	Phosphate buffer solution
PE	2-phenylethanol
Ph	Phthalic acid
pK_a	Acidity constants
SA	Salicylic acid
TRIS	Trishydroxymethylaminomethane
UV	Ultraviolet
$V_{(GA)}$	Volume concentration of glutaraldehyde solution
V_R	Volume of the receptor half-cell
W	Weight of a swelled sample
W_0	Initial weight of a sample
WAXS	Wide-angle X-ray scattering
WU_{eq}	Equilibrium water uptake
x	Crosslinking degree
XRD	X-ray diffraction
y	Distance in the direction perpendicular to the membrane
δ	Membrane thickness
$\lambda_{máx}$	Wavelength of maximum UV absorbance

7 Poly(*N*-isopropylacrylamide) surface grafted chitosan membranes as a new substrate for cell sheet engineering and manipulation

^{1}H-NMR	Proton nuclear magnetic resonance
AIBN	2,2'-Azobis-isobutyronitrile

CAE	Constant Analyser Energy mode
DD	The degree of *N*-deacetylation
DMEM	Dulbecco's Modified Eagle's Medium
ECM	Extracelular matrix
EDTA	Ethylenediaminetetraacetic acid
FBS	Fetal bovine serum
FTIR-ATR	Fourier Transform Infrared spectroscopy
GluN	β-(1→4)-2-amino-2-deoxy-D-glucopyranose
GluNAc	β-(1→4)-2-acetamido-2-deoxy-D-glucopyranose
LCST	Lower Critical Solution Temperature
NIPAAm	*N*-isopropylacrylamide
NMR	Nuclear Magnetic Resonance
PBS	Phosphate Buffer Solution
PEG	Poly(ethylene glycol)
PNIPAAm	Poly(*N*-isopropylacrylamide)
S_{eq}	Equilibrium swelling ratio
TCPS	Tissue culture polystyrene
W	Weight of a swelled sample
W_0	Initial weight of certain sample
WU	Water uptake
WU_{eq}	Equilibrium hydration degree
XPS	X-Ray photoelectron spectroscopy
δ	Chemical shifts in nuclear magnetic resonance

Chapter 1

Introduction

Smart thermoresponsive coatings and surfaces for tissue engineering: switching cell-material boundaries

1.1 Abstract

The smart thermoresponsive coatings and surfaces that have been explicitly designed for cell culture are mostly based on poly(*N*-isopropylacrylamide) (PNIPAAm). This polymer is characterized by a sudden precipitation on heating, switching from a hydrophilic to a hydrophobic state. Mammalian cells cultured on such thermoresponsive substrates can be recovered as confluent cell sheets, while keeping the newly deposited extracellular matrix intact, simply by lowering the temperature and thereby avoiding the use of deleterious proteases. Thermoresponsive materials and surfaces are powerful tools for creating tissue-like constructs that imitate native tissue geometry and mimic its spatial cellular organization. Here we review and compare the most representative methods of producing thermoresponsive substrates for cell sheet engineering.

This chapter is based on the following publication:
Ricardo M.P. da Silva; João F. Mano; Rui L. Reis. Smart thermoresponsive coatings and surfaces for tissue engineering: switching cell-material boundaries. **Trends in Biotechnology 2007**, 25, (12), 577-583.

1.2 Tissue culture on thermoresponsive substrates

Thermoresponsive substrates designed for tissue engineering have mainly used poly(*N*-isopropylacrylamide) (PNIPAAm) as the molecular switch for cell adhesion (ON) and detachment (OFF). The first published paper reporting the inverse solubility upon heating of PNIPAAm dates from 1967 [1]. The cloud point (at around 32°C in pure water [1-3]) is also termed inverse temperature solubility or, more generally, the lower critical solution temperature (LCST). In an aqueous environment, isolated individual PNIPAAm chains undergo a reversible conformational transition from expanded coil to compact globule as the temperature is raised above the LCST [2, 3]. The solubility is affected because the amphiphilic PNIPAA chains hide the hydrophilic amide groups and expose the hydrophobic isopropyl groups in the compact globule conformation. The chemical mechanism and thermodynamic details of this phenomenon have been reviewed elsewhere [4, 5].

In their natural environment, many mammalian cells do not exist in solution but interact with immobilized components of the extracellular matrix (ECM) for the development, organization and maintenance of the tissues. Consequently, anchorage-dependent cells need to adhere to solid substrates for normal functioning. Attached cells proliferate and produce ECM, forming confluent cell monolayers. In conventional cell culture dishes, which consist of tissue culture polystyrene (TCPS), cells are harvested by disaggregating the ECM through the proteolytic action of trypsin and by chelating the Ca^{2+} and Mg^{2+} ions with ethylenediaminetetraacetic acid (EDTA). However, nonspecific proteases can damage crucial cell surface proteins, and this constitutes a major drawback of this cell harvesting method [6-10]. Moreover, from a tissue engineering perspective, the disruption of the newly formed tissue-like structures seems to be a backward step.

Thermoresponsive substrates can be created so that cells adhere and proliferate at the culture temperature, and then release the cultured cell sheets on command, by cooling below the LCST. These cell sheet engineering tools have been classified according to two distinct strategies that were demonstrated in the pioneering papers: thermoresponsive insoluble surface grafts [6] and soluble coatings [11].

The use of temperature to detach confluent cell sheets in culture, without the use of conventional enzymatic treatments, was first reported in 1990 by Takezawa *et al.* [11]. In this study, fibroblast monolayers were released at lowered temperature by dissolution of the dish coating, which consisted of a physical blend of collagen and PNIPAAm. In this method, cell sheet recovery is accomplished by disintegration of the coating.

Around the same time, Yamada *et al.* [6] reported that bovine hepatocytes, which are highly sensitive to enzymatic harvesting, could be successively subcultured on TCPS surfaces that

were covalently grafted with PNIPAAm. The rationale is that the slightly hydrophobic surfaces will support cell adhesion, whereas hydrated hydrophilic surfaces will not. At the culture temperature (37°C) insoluble grafted molecules expose their hydrophobic groups, whereas below the LCST the chains become hydrophilic and hydrated.

Here we review the thermoresponsive substrates underlying several outstanding achievements in regenerative medicine. Further sophistication of such substrates will be made possible by greater understanding of the underlying principles that govern their applicability.

1.3 Insoluble PNIPAAm surfaces: fabrication methods

A large range of different methods can be used to fabricate insoluble thermoresponsive surfaces [6, 9, 10, 12-15]. Nevertheless, only a few of these have been found to be suitable for cell sheet engineering. Some surfaces based on PNIPAAm do not support cell adhesion even above the LCST [16, 17], making them unsuitable as culture substrates. The surface fabrication methods reviewed here are limited to those that have consistently demonstrated an ability to grow cultured cells to confluence.

Electron-beam (e-beam) polymerization of NIPAAm onto TCPS is by far the most employed method for producing thermoresponsive surfaces for cell sheet engineering [6-8, 16, 18-29]. Temperature-controlled cell adhesion and detachment is achieved for grafting densities in the range of 1.4–2 μg/cm^2 (thickness 15–20 nm) [16, 19-23]. Grafted PNIPAAm layers thicker than 30 nm (2.9–3 μg/cm^2) do not support cell adhesion at any temperature [16, 17].

A second type of thermoresponsive surface that is covalently attached to a solid substrate is produced by plasma polymerization of NIPAAm [10, 30]. Plasma glow discharge power is gradually decreased to form an adhesion-promoting layer on the substrate and to deposit a functional coating at the outer surface. Plasma-deposited PNIPAAm was found to be consistent with a crosslinked structure, which largely retained the monomeric structure and preserved the PNIPAAm phase transition [31, 32]. The sum frequency generation (SFG) vibrational spectra obtained for this type of graft above the LCST suggested that the hydrophobic isopropyl side groups were oriented towards the aqueous environment. By contrast, the spectra obtained at room temperature provided evidence for a disordering of the isopropyl groups away from the surface normal (the perpendicular). Furthermore, the characteristic peaks of amide groups were not detected; this suggests that the previous hypothesis, that these groups are exposed to the aqueous environment to participate in hydrogen bonding below the LCST, is possibly not correct [32]. Finally, cell culture studies and thermal lift-off did not show obvious differences between different batches of plasma-

deposited coatings, although the thickness of deposited polymer varied from batch to batch [10, 30]. This shows that cell adhesion and proliferation do not seem to be sensitive to the grafted layer thickness of plasma-polymerized PNIPAAm substrates.

Another method of producing thermoresponsive surfaces involves the partial entrapment of a copolymer of NIPAAm and 4-(*N*-cinnamoylcarbamide)methylstyrene (CCMS) onto TCPS and irradiation with ultraviolet (UV) light to crosslink the copolymer through the dimerization of the cinnamoyl groups [9, 33]. Similarly to plasma-polymerized PNIPAAm, cell adhesion and proliferation were not sensitive to the thickness of the functional layer in the range 2.4–6.9 μg/cm^2 [33].

Another approach to functionalizing TCPS surfaces makes use of a NIPAAm copolymer derivatized with photoreactive 4-azidoaniline groups [34-37]. UV light irradiation produces a heavily crosslinked surface layer [38]. This method has been employed to produce micropatterned surfaces with thermoresponsive regions by photolithography in which the solvent cast coating is washed out from shadowed regions [34-37]. Using this approach, fibroblasts were cultured for short periods (2 h) and adhered to the micropatterned substrates. Afterwards, the cells were selectively detached from the grafted regions [34, 35]. This technique demonstrated that spatial control over detachment of adhered cells can be achieved, and might be a useful tool to control the distribution of different cell types in coculture systems.

All the methods described in this section use the hydrophobic-to-hydrophilic switch to recover cell sheets, instead of disintegration of the coating. This ensures that the coating is not harvested with the cell sheet, keeping the cell construct free of unwanted soluble polymer after detachment.

1.4 Insoluble PNIPAAm surfaces: achieving cell adhesion and proliferation

Although all thermoresponsive substrates based on PNIPAAm showed the expected hydrophilic properties below the LCST (see Tables 1.1 and 1.2), only some were able to support cell adhesion and proliferation above the LCST; in others, cells did not form contiguous monolayers. For instance, the surfaces described above as consisting of thin layers of crosslinked PNIPAAm immobilized on solid supports, do support cell adhesion and proliferation. By contrast, cells fail to adhere on e-beam-grafted PNIPAAm surfaces thicker than 30 nm [16, 17], or on PNIPAAm crosslinked with methylenebis(acrylamide) (MBAAm) [16, 17] or non-crosslinked PNIPAAm homopolymer [11]. Cell adhesion can be correlated to the adsorption of adhesive proteins, such as fibronectin. The e-beam-grafted PNIPAAm at the greatest density and the bulk crosslinked hydrogel fail to adsorb fibronectin [16, 17].

Understanding why only certain molecular architectures produce surfaces with appropriate properties could facilitate the engineering of more sophisticated thermoresponsive surfaces with increased functionalities.

The equilibrium water contact angle (measured under static conditions) of some polymer substrates has been shown to correlate with cell adhesion and proliferation, which are both optimal at an angle of around 70° [39]. Using this correlation, the unsuitability of bulk crosslinked PNIPAAm hydrogels for supporting cell adhesion can be explained by their greatly hydrophilic nature, which is revealed by a low static water contact angle, even above the LCST (see Table 1.1) [16]. However, plasma-deposited PNIPAAm, which has been shown to support reversible cell adhesion and detachment [32], gave similar values for the static water contact angle [32, 40].

Table 1.1 Temperature-induced surface free energy changes as sensed by the static water contact angle measured above and below the LCST

Surface description	T > LCST	T < LCST	Cell adhesion	Ref.
Bulk PNIPAAm hydrogel crosslinked with MBAAm (1.3%)	49.4º [(a)] (T=40ºC)	11.5º [(a)] (T=10ºC)	non-adhesive	([16])
e-beam polymerised PNIPAAm (1.4 µg/cm^2)	77.9º [(a)] (T=37ºC)	65.2º [(a)] (T=20ºC)	ok	([16])
e-beam polymerised PNIPAAm (2.9 µg/cm^2)	69.5º [(a)] (T=37ºC)	60.0º [(a)] (T=20ºC)	non-adhesive	([16])
e-beam polymerised PNIPAAm (1.6 µg/cm^2)	66º [(b)] (T=37ºC)	54º [(b)] (T=20ºC)	ok	([41])
Plasma polymerised PNIPAAm (1W)	40º [(a)] (T=40ºC)	34º [(a)] (T=20ºC)	ok	([32])
Plasma polymerised PNIPAAm (5 W, 55ºC)	42.5º [(a)] (T=45ºC)	33.5º [(a)] (T=20ºC)	NA	([40])

[(a)] Captive air bubble method; [(b)] Sessile drop method; NA = cell adhesion studies were not reported; ok = cells adhere, proliferate and detach as a confluent sheet

Also, the dependence of cell adhesion on the thickness of PNIPAAm grafted onto TCPS by e-beam irradiation cannot be clearly correlated with the differences found in the static water contact angle, because the reported values (Table 1.1) are close to what is regarded as optimal for cell adhesion. Besides, as the values in Table 1.1 show, the nonadhesive surface with the greatest grafting density (2.9 µg/cm^2) showed a contact angle between the values

found for lower densities (1.4 and 1.6 μg/cm^2), which are in turn appropriate for cell adhesion and proliferation [16, 41]. These findings suggest that an additional effect other than the surface wettability, but nevertheless strongly related to the grafting density or thickness, is responsible for inhibiting protein adsorption onto e-beam-grafted surfaces at the greatest density and, consequently, hindering cell adhesion.

The performance of the surfaces can also be affected by the swelling ability. Akiyama *et al.* reported that swelling was significantly reduced for crosslinked gels immobilized on a rigid surface and that the swelling ratio was further lowered for the thinner crosslinked gels. Consequently, they suggested that the surface immobilization of the crosslinked chains dramatically restricted the molecular motion, and extrapolated that those restrictions on molecular mobility would be more significant in the vicinity of the rigid support surface, as in the case of the e-beam-grafted PNIPAAm on TCPS [16], enabling cell adhesion below a suitable thickness limit.

It is well established that, under suitable grafting densities and sufficient molecular mobility [42-44], immobilized nonionic and greatly hydrated macromolecules such as polyethylene glycol (PEG) can prevent (or minimize) protein adsorption and, consequently, render surfaces resistant to cell adhesion. The nonfouling nature of those surfaces is often interpreted in terms of the 'steric repulsion' model. It is considered that the solvation of the PEG chains together with their great conformational freedom and hence entropy prevents the protein adsorption that, otherwise, would restrict the conformational mobility of the hydrated free polymer molecules [42, 45, 46]. The nonfouling property of PEG chains has been used to explain the nonadhesive property of hydrated PNIPAAm surfaces below the LCST [15, 17, 47].

However, the same 'steric repulsion' model is less successful at explaining the nonfouling nature of the thicker e-beam PNIPAAm-grafted surfaces (2.9 μg/cm^2) above the LCST. In fact, during the volume transition it is expected that the PNIPAAm molecules dehydrate, at least partially, and expose their hydrophobic isopropyl groups, as was reported for plasma-polymerized NIPAAm NIPAAm [32]. In Figure 1.1, crosslinked PNIPAAm chains are schematically represented above the LCST. The isopropyl groups are oriented towards the interface with the water, and the dependence of protein adsorption on the grafting thickness and chain mobility is illustrated. The decrease of the PNIPAAm chain density with increasing grafting thickness is based on the model proposed by Kikuchi and Okano [48]. Similarly, surfaces containing methoxy-terminated oligo(ethylene glycol) self-assembled monolayers (SAMs) on gold resist protein adsorption, despite the hydrophobic group pointing to the water interface [43, 46]. By contrast, protein adsorption is detected for the same SAMs on silver, which form a denser SAM phase, thereby restricting access to water molecules and molecular mobility of the oligo(ethylene glycol) tails [46]. The 'steric repulsion' model does not explain the nonfouling nature of some short oligomers, but this nature can be interpreted based on the

'water barrier' theory, that is, protein cannot adsorb because of a tightly bound water layer [42, 46].

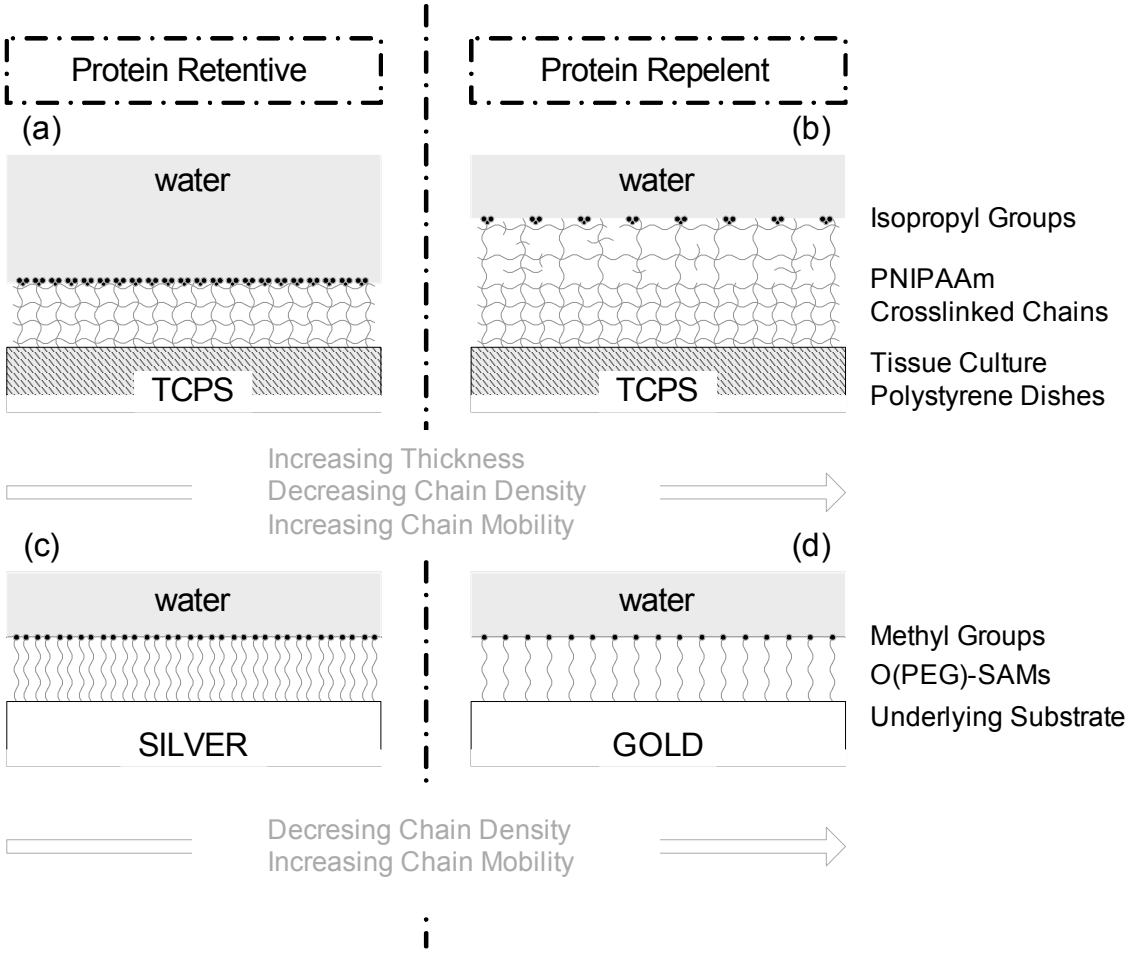

Figure 1.1 (a) Schematic representation of the e-beam-grafted insoluble PNIPAAm surfaces. At culture temperatures above the LCST, the isopropyl groups point to the interface with the water, conferring hydrophobic properties on the surface. At low graft thicknesses, adhesive proteins will adsorb and cells can adhere to the surface. **(b)** As the graft thickness increases, the PNIPAAm chain density decreases (lower surface concentration of isopropyl groups) and the surface becomes unsuitable for cell culture. **(c)** Methoxy-terminated oligo(ethylene glycol) self-assembled monolayers (SAMs) behave in a similar way to (a) and (b). These SAMs expose the hydrophobic methyl groups to the water interface. The SAMs on silver form greatly compacted structures that were found to adsorb proteins. **(d)** The same molecules form less compacted SAMs on gold producing nonfouling properties typical of other oligo(ethylene glycol) molecules. The black dots represent the hydrophobic isopropyl and methyl groups of PNIPAAm and O(PEG)-SAMs, respectively.

The similarity between the results on the methoxy-terminated oligo(ethylene glycol)-SAMs and the dependence of protein adsorption on the thickness of the e-beam-grafted PNIPAAm layer, and its consequences for cell adhesion behaviour (see Figure 1.1), is remarkable. Greater restrictions to the molecular mobility and lower hydration, which have been associated with the lower thicknesses of e-beam-grafted PNIPAAm, are in turn correlated with the denser molecular packing of SAMs on the model surfaces.

Table 1.2 Temperature-induced surface free energy changes associated with the dispersive component as sensed by the advancing water contact angle measured above and below the LCST

Surface description	T > LCST	T < LCST	Cell adhesion	Ref.
UV crosslinked P(NIPAAm-co-CCMS) (0.7%)	87.8º [(a)] (T=37ºC)	37.2º [(a)] (T=19ºC)	ok	([33])
UV crosslinked P(NIPAAm-co-CCMS) (1.2%)	92.6º [(a)] (T=37ºC)	40.5º [(a)] (T=19ºC)	ok	([33])
Bulk PNIPAAm hydrogel crosslinked with MBAAm (1%)	90º [(b)] (T=36ºC)	42º [(b)] (T=25ºC)	NA	([49])
Bulk PNIPAAm hydrogel crosslinked with MBAAm (1.8%)	90º [(b)] (T=36ºC)	42º [(b)] (T=25ºC)	NA	([50])
Bulk PNIPAAm hydrogel crosslinked with MBAAm (2.2%)	60º [(a)] [(c)] (T=37ºC)	25º [(a)] [(c)] (T=20ºC)	NA	([51])
Bulk PNIPAAm hydrogel crosslinked with MBAAm (10%)	90º [(a)] [(c)] (T=37ºC)	30º [(a)] [(c)] (T=20ºC)	NA	([51])

[(a)] Dynamic Wilhelmy plate method; [(b)] Sessile drop method; [(c)]Estimated from a chart; NA = cell adhesion studies were not reported in these articles, but it has been reported that cells do not adhere on bulk PNIPAAm hydrogel crosslinked with MBAAm[16, 17]; ok = cells adhere, proliferate and detached as confluent sheet

The dynamic contact angle, that is, the measurement of the 'advancing' and 'receding' contact angles at the moving three phase boundary (solid–liquid–air), was also used to study the properties of insoluble PNIPAAm surfaces. Johnson and Dettre proposed a model for dynamic contact angle hysteresis caused by surface chemical heterogeneity; they predicted that the advancing contact angle would be associated with the surface concentration of hydrophobic regions [52, 53]. They also found that the advancing contact angle does not vary greatly for elevated concentrations of the hydrophobic regions, but decreases sharply when the concentration of the latter is reduced to a low coverage ratio [52, 53]. When analysing the

values of the advancing water contact angle reported by several authors (Table 1.2), and considering the nonadhesive nature of bulk PNIPAAm hydrogels crosslinked with MBAAm, no clear tendency can be seen correlating these values with the suitability of the surface to support cell growth. However, similar elevated values for advancing contact angle of the surfaces above the LCST confirm the raised concentration of hydrophobic regions, but can still hide considerable differences in the concentration of isopropyl groups. Moreover, a low advancing contact angle (Table 1.2) below the LCST should mean that most of the isopropyl groups are no longer oriented to the interface. This is corroborated by SFG vibrational spectra, which provide evidence for the orientation of the isopropyl groups towards the aqueous environment above the LCST, and their disordering away from the surface normal at lower temperatures [32].

In conclusion, cell adhesion and proliferation on insoluble PNIPAAm surfaces cannot be described only in terms of surface wettability, because above the LCST the surfaces are only partially dehydrated. Interdependent variables such as swelling ratio, molecular mobility, chain density and concentration of the hydrophobic groups must be simultaneously addressed.

1.5 Insoluble PNIPAAm surfaces: mechanisms underlying cell sheet detachment

Spontaneous cell sheet detachment is driven by physical events, such as an increased hydrophilicity, that are induced by lowering the temperature below the LCST. Nevertheless, detachment seems also to be mediated by active cellular metabolic processes, given that cell detachment can be suppressed by adding an ATP synthesis inhibitor [54]. Selective inhibition of actin filaments, by means of either an actin stabilizer or an actin depolymerizer, strongly indicates that forces exerted by the cytoskeleton are important in the detachment process [54]. Moreover, cells of different phenotypes require varying optimum temperatures for detachment, depending on their differing temperature sensitivities for cellular metabolic processes [55]. Furthermore, each specific cell phenotype creates different ECM structures, and it is expected that deposited basal structures could also be different. This could also have implications for the response to the thermoresponsive switch of cell sheets created from different cell sources. For example, fibronectin, which was deposited as a matrix composed of thin fibrils on the thermoresponsive surface, could be recovered together with the confluent monolayer of bovine aortic endothelial cells by low-temperature lift-off [56]. This is in good agreement with the resistance exhibited by e-beam PNIPAAm-grafted surfaces to adsorb the soluble form of fibronectin below the LCST [16]. In addition, bovine aortic

endothelial cell sheets grown on plasma-polymerized NIPAAm surfaces left behind little (if any) laminin or fibronectin after thermal harvesting. However, a detailed analysis of the thermoresponsive surface after cell sheet detachment showed evidence of a protein film consistent with collagen types I and IV [10, 30], indicating that a fraction of some of the ECM proteins that cells deposit in the culture surfaces remains in that substrate after thermal lift-off. Canavan *et al.* suggested that, because cells mainly interact with the ECM at focal points, the ECM proteins that do not have strong interactions with cells could be retained in the substrate after thermal recovery of the cell sheet [10]. Finally, it is also reasonable to consider that thermoresponsive surfaces below the LCST have a different adhesiveness towards ECM proteins. Cell sheets could resist detachment because of proteins that function as anchoring points and therefore remain attached to the surface after detachment. This might explain why cell sheets do not detach when the cytoskeletal contractile forces are selectively inhibited.

1.6 Cell sheet engineering and manipulation

When confluent cell sheets are harvested from thermoresponsive dishes, the cellular contractile forces exerted by the cytoskeleton are no longer supported by the forces of adhesion to the solid surface. As a result, the cell sheet starts to shrink [21] and to aggregate resulting in multicellular spheroids [11]. Hydrophilic membranes placed on top of the cell sheets adhere to their apical surface upon removing the culture medium, possibly because of capillary forces. When the temperature is lowered, the cell sheet is released but still stuck to the supporting membranes, which provide a physical support for the manipulation of the delicate cell sheets and enable their transfer from the thermoresponsive surface to the desired substrate [19, 21-23, 25, 28]. The basal surface of the cell sheet will adhere to the new substrate, possibly through the remaining adhesive proteins that were present at the interface with the previous thermoresponsive surface and harvested with the cell sheet [56]. In a final step, the supporting membrane will spontaneously detach by adding culture medium. Cell sheet manipulation techniques have been established notably by the group led by Dr T. Okano; after their pioneering paper [6], this team systematically investigated insoluble PNIPAAm-grafted substrates to produce different cell sheets from several cell phenotypes [48, 57, 58].

The advantages of cell sheet engineering over more conventional tissue engineering strategies are described in Box 1.1. Single cell sheets have been produced for regeneration of cornea [7, 18, 24, 29] and epidermis [19] . When directly transplanted to human patients for corneal regeneration, cell sheets adhered rapidly, avoiding the need for sutures [18]. In

comparison, conventional corneal and epidermal tissue engineering approaches use dispase to harvest corneal epithelial cell sheets and multilayered keratinocyte sheets from the culture dishes. These nonspecific proteases damage the formed ECM and other proteins, leading to fragility of the cell sheets and disrupting differentiated structures and functions [7, 19, 20]. Residual dispases can also be harmful to the transplantation site and jeopardize the treatment.

Box 1.1 Advantages of cell sheet engineering compared with more conventional approaches

- Cell sheets harvested from thermoresponsive substrates adhere to the host tissues without the need for sutures [18].
- Tissue engineering strategies require the scaffold material to be surgically placed between cultured cells and the injury site, which can complicate or delay integration of the tissue implant [58].
- Cell sheet engineering avoids the use of scaffold materials, which can have potential for inflammatory or foreign body reactions or other complications arising from the by-products of scaffold biodegradation.
- Thermoresponsive substrates avoid the use of deleterious enzymes that typically are used to remove cell monolayers from conventional culture dishes [7, 19, 20].
- Control over the spatial distribution of cells within three-dimensional stratified tissues can be achieved by layering cell sheets created from different cell types [22].
- Cell sheet engineering offers better control over cell seeding; that is, when cells are seeded at a cell concentration similar to that observed on a confluent monolayer, final tissue-like constructs have greater cell densities and less ECM, reflecting the varying cell densities of the different native tissues [21, 26].

An alternative tissue engineering approach makes use of biodegradable scaffolds, such as collagen [59]. However, this technique requires that scaffold material is surgically placed between the cultured cells and the host tissue at the injured (or diseased) site. Unless the use of scaffolds is crucial for treatment, such as to provide short-term mechanical support, cell sheet engineering can be an appealing alternative. For example, if a scaffold is used only to recover and manipulate cultured tissue, replacing it with engineered cell sheets has great advantages – in avoiding a possible inflammatory or foreign body reaction or other complications arising from the by-products of scaffold biodegradation.

Moreover, from the tissue organization point of view, it might be desirable to avoid the use of scaffolds, whose supramolecular organization does not match that of the ECM deposited by

the cells. For instance, in native cardiac muscle, cells are densely packed with diffuse gap junctions, important for electrical transmission. Layered cardiomyocyte cell sheets showed a greater cell density with diffuse gap junctions and less ECM deposition, than constructs that were created using biodegradable scaffolds [21, 26]. Further, cell sheet engineered cardiac grafts showed synchronized pulsation [26].

This method was also used to create cell sheets of hepatocytes and endothelial cells that were subsequently layered to mimic the three-dimensional cellular organization in liver lobules. It was found that the hepatocytes cocultured in the layered system maintained differentiated functions for over 41 days, whereas these functions disappeared within 10 days in hepatocyte monoculture controls [22].

It should be emphasized that in all the examples given above of applications for cell sheet engineering, the cell sheets were obtained using insoluble thermoresponsive surfaces. In fact, the majority of the cell sheet engineering applications were developed for insoluble thermoresponsive surfaces. It was only recently that the attention of cell sheet engineers turned again toward the approach based on thermoresponsive substrates that become soluble below the LCST. Endothelial cells were cultured until confluency on coatings of PNIPAAm-grafted gelatin produced by living radical photopolymerization [60-66]. Gelatin, the denaturated form of collagen, was used to address the nonadhesive nature of soluble PNIPAAm. These cells were shown to detach successfully when the temperature was lowered to 20 °C [61]. Moreover, a tubular monolayer of endothelial cells was created by coating a glass capillary tube with the same PNIPAAm-grafted gelatin. An engineered vascular graft could be recovered that consisted of the endothelial cells and secreted ECM. The resulting tubular endothelium resembled the intimal layer of a native blood vessel [60].

The disintegration of the coating could be a potential drawback of this method, because it poses the risk that the harvested cell sheet will be contaminated with soluble polymer after detachment. Nevertheless, the method gives the cell sheet engineer the ability to release biological structures from intricate supportive moulds, enabling the design and one-step fabrication of ‘cell sheets’ with complex geometries resembling the native tissue shapes.

1.7 Concluding remarks

Thermoresponsive surfaces that consist of thin layers of crosslinked PNIPAAm on a nonthermoresponsive solid support were initially proposed as new technologies for cell proliferation. However, since then thermoresponsive surfaces have been developed into valuable tools for engineering cell sheets and used successfully to produce tissue-like structures with interesting and important applications in regenerative medicine. So far, this

technology is being applied for the regeneration of cornea [7, 18, 24, 29], skin [19], liver [22], heart [21, 26] and blood vessels [60].

The insoluble PNIPAAm surfaces are suitable for producing cell sheets that seem to be ideal for applications where the native tissues show stratified structures. Cell sheets can be layered to obtain thicker tissue-like constructs composed of single [26] or multiple cell phenotypes [22]. Moreover, the low-temperature soluble coatings that can support cell adhesion and proliferation above the LCST have great potential for engineering 'cell sheets' with more complex geometries resembling tissue shapes, which can only be obtained after complete removal of supporting materials.

Despite the advances that thermoresponsive coatings and surfaces have already made for the regeneration of injured tissues, cell sheet engineering is still in its infancy and has enormous research potential. The scarcity of suitable cell sources is an important obstacle to developing clinically relevant applications, a common issue in the field of regenerative medicine. Future developments in stem cell technologies combined with a full toolbox of thermoresponsive technologies promise great benefits for human health and welfare.

1.8 Acknowledgements

This work was partially supported by the Portuguese Foundation for Science and Technology (FCT), funds from the POCTI and FEDER programmes, the scholarship SFRH/BD/6862/2001 granted to R.M.P.S. and the project PTDC/QUI/68804/2006. This work was carried out under the scope of the European NoE EXPERTISSUES (NMP3-CT-2004–500283).

1.9 References

1. Scarpa, J. S.; Mueller, D. D.; Klotz, I. M., Slow hydrogen-deuterium exchange in a non-alfa-helical polyamide. *Journal of the American Chemical Society* **1967,** 89, (24), 6024-6030.

2. Fujishige, S.; Kubota, K.; Ando, I., Phase-transition of aqueous-solutions of poly(*N*-isopropylacrylamide) and poly(*N*-isopropylmethacrylamide). *Journal of Physical Chemistry* **1989,** 93, (8), 3311-3313.

3. Kubota, K.; Fujishige, S.; Ando, I., Single-chain transition of poly(*N*-isopropylacrylamide) in water. *Journal of Physical Chemistry* **1990,** 94, (12), 5154-5158.

4. Graziano, G., On the temperature-induced coil to globule transition of poly-*N*-isopropylacrylamide in dilute aqueous solutions. *International Journal of Biological Macromolecules* **2000,** 27, (1), 89-97.

5. Baysal, B. M.; Karasz, F. E., Coil-globule collapse in flexible macromolecules. *Macromolecular Theory and Simulations* **2003,** 12, (9), 627-646.

6. Yamada, N.; Okano, T.; Sakai, H.; Karikusa, F.; Sawasaki, Y.; Sakurai, Y., Thermoresponsive polymeric surfaces - control of attachment and detachment of cultured-cells. *Makromolekulare Chemie-Rapid Communications* **1990,** 11, (11), 571-576.

7. Ide, T.; Nishida, K.; Yamato, M.; Sumide, T.; Utsumi, M.; Nozaki, T.; Kikuchi, A.; Okano, T.; Tano, Y., Structural characterization of bioengineered human corneal endothelial cell sheets fabricated on temperature-responsive culture dishes. *Biomaterials* **2006,** 27, (4), 607-614.

8. Nakajima, K.; Honda, S.; Nakamura, Y.; Lopez-Redondo, F.; Kohsaka, S.; Yamato, M.; Kikuchi, A.; Okano, T., Intact microglia are cultured and non-invasively harvested without pathological activation using a novel cultured cell recovery method. *Biomaterials* **2001,** 22, (11), 1213-1223.

9. Von Recum, H. A.; Okano, T.; Kim, S. W.; Bernstein, P. S., Maintenance of retinoid metabolism in human retinal pigment epithelium cell culture. *Experimental Eye Research* **1999,** 69, (1), 97-107.

10. Canavan, H. E.; Cheng, X. H.; Graham, D. J.; Ratner, B. D.; Castner, D. G., Cell sheet detachment affects the extracellular matrix: a surface science study comparing thermal liftoff, enzymatic, and mechanical methods. *Journal of Biomedical Materials Research Part A* **2005,** 75A, (1), 1-13.

11. Takezawa, T.; Mori, Y.; Yoshizato, K., Cell-culture on a thermoresponsive polymer surface. *Bio-Technology* **1990,** 8, (9), 854-856.

12. Ista, L. K.; Mendez, S.; Perez-Luna, V. H.; Lopez, G. P., Synthesis of poly(*N*-isopropylacrylamide) on initiator-modified self-assembled monolayers. *Langmuir* **2001,** 17, (9), 2552-2555.

13. Taniguchi, T.; Duracher, D.; Delair, T.; Elaissari, A.; Pichot, C., Adsorption/desorption behavior and covalent grafting of an antibody onto cationic amino-functionalized poly(styrene-*N*-isopropylacrylamide) core-shell latex particles. *Colloids and Surfaces B-Biointerfaces* **2003,** 29, (1), 53-65.

14. Sakamoto, C.; Okada, Y.; Kanazawa, H.; Ayano, E.; Nishimura, T.; Ando, M.; Kikuchi, A.; Okano, T., Temperature- and pH-responsive aminopropyl-silica ion-exchange columns grafted with copolymers of *N*-isopropylacrylamide. *Journal of Chromatography* **2004,** 1030, (1-2), 247-253.

15. Huber, D. L.; Manginell, R. P.; Samara, M. A.; Kim, B. I.; Bunker, B. C., Programmed adsorption and release of proteins in a microfluidic device. *Science* **2003,** 301, (5631), 352-354.

16. Akiyama, Y.; Kikuchi, A.; Yamato, M.; Okano, T., Ultrathin poly(*N*-isopropylacrylamide) grafted layer on polystyrene surfaces for cell adhesion/detachment control. *Langmuir* **2004,** 20, (13), 5506-5511.

17. Yamato, M.; Konno, C.; Koike, S.; Isoi, Y.; Shimizu, T.; Kikuchi, A.; Makino, K.; Okano, T., Nanofabrication for micropatterned cell arrays by combining electron beam-irradiated polymer grafting and localized laser ablation. *Journal of Biomedical Materials Research Part A* **2003,** 67A, (4), 1065-1071.

18. Nishida, K.; Yamato, M.; Hayashida, Y.; Watanabe, K.; Yamamoto, K.; Adachi, E.; Nagai, S.; Kikuchi, A.; Maeda, N.; Watanabe, H.; Okano, T.; Tano, Y., Corneal reconstruction with tissue-engineered cell sheets composed of autologous oral mucosal epithelium. *New England Journal Of Medicine* **2004,** 351, (12), 1187-1196.

19. Yamato, M.; Utsumi, M.; Kushida, A.; Konno, C.; Kikuchi, A.; Okano, T., Thermo-responsive culture dishes allow the intact harvest of multilayered keratinocyte sheets without dispase by reducing temperature. *Tissue Engineering* **2001,** 7, (4), 473-480.

20. Shiroyanagi, Y.; Yamato, M.; Yamazaki, Y.; Toma, H.; Okano, T., Transplantable urothelial cell sheets harvested noninvasively from temperature-responsive culture surfaces by reducing temperature. *Tissue Engineering* **2003,** 9, (5), 1005-1012.

21. Shimizu, T.; Yamato, M.; Kikuchi, A.; Okano, T., Two-dimensional manipulation of cardiac myocyte sheets utilizing temperature-responsive culture dishes augments the pulsatile amplitude. *Tissue Engineering* **2001,** 7, (2), 141-151.

22. Harimoto, M.; Yamato, M.; Hirose, M.; Takahashi, C.; Isoi, Y.; Kikuchi, A.; Okano, T., Novel approach for achieving double-layered cell sheets co-culture: overlaying endothelial cell sheets onto monolayer hepatocytes utilizing temperature-responsive culture dishes. *Journal of Biomedical Materials Research* **2002,** 62, (3), 464-470.

23. Nandkumar, M. A.; Yamato, M.; Kushida, A.; Konno, C.; Hirose, M.; Kikuchi, A.; Okano, T., Two-dimensional cell sheet manipulation of heterotypically co-cultured lung cells utilizing temperature-responsive culture dishes results in long-term maintenance of differentiated epithelial cell functions. *Biomaterials* **2002,** 23, (4), 1121-1130.

24. Sumide, T.; Nishida, K.; Yamato, M.; Ide, T.; Hayashida, Y.; Watanabe, K.; Yang, J.; Kohno, C.; Kikuchi, A.; Maeda, N.; Watanabe, H.; Okano, T.; Tano, Y., Functional human corneal endothelial cell sheets harvested from temperature-responsive culture surfaces. *Faseb Journal* **2005**.

25. Shimizu, T.; Yamato, M.; Akutsu, T.; Shibata, T.; Isoi, Y.; Kikuchi, A.; Umezu, M.; Okano, T., Electrically communicating three-dimensional cardiac tissue mimic fabricated by

layered cultured cardiomyocyte sheets. *Journal of Biomedical Materials Research* **2002,** 60, (1), 110-117.

26. Shimizu, T.; Yamato, M.; Isoi, Y.; Akutsu, T.; Setomaru, T.; Abe, K.; Kikuchi, A.; Umezu, M.; Okano, T., Fabrication of pulsatile cardiac tissue grafts using a novel 3-dimensional cell sheet manipulation technique and temperature-responsive cell culture surfaces. *Circulation Research* **2002,** 90, (3), E40-E48.

27. Memon, I. A.; Sawa, Y.; Fukushima, N.; Matsumiya, G.; Miyagawa, S.; Taketani, S.; Sakakida, S. K.; Kondoh, H.; Aleshin, A. N.; Shimizu, T.; Okano, T.; Matsuda, H., Repair of impaired myocardium by means of implantation of engineered autologous myoblast sheets. *Journal of Thoracic and Cardiovascular Surgery* **2005,** 130, (5), 1333-1341.

28. Kushida, A.; Yamato, M.; Kikuchi, A.; Okano, T., Two-dimensional manipulation of differentiated Madin-Darby canine kidney (MDCK) cell sheets: The noninvasive harvest from temperature-responsive culture dishes and transfer to other surfaces. *Journal of Biomedical Materials Research* **2001,** 54, (1), 37-46.

29. Nishida, K.; Yamato, M.; Hayashida, Y.; Watanabe, K.; Maeda, N.; Watanabe, H.; Yamamoto, K.; Nagai, S.; Kikuchi, A.; Tano, Y.; Okano, T., Functional bioengineered corneal epithelial sheet grafts from corneal stem cells expanded *ex vivo* on a temperature-responsive cell culture surface. *Transplantation* **2004,** 77, (3), 379-385.

30. Canavan, H. E.; Cheng, X. H.; Graham, D. J.; Ratner, B. D.; Castner, D. G., Surface characterization of the extracellular matrix remaining after cell detachment from a thermoresponsive polymer. *Langmuir* **2005,** 21, (5), 1949-1955.

31. Pan, Y. V.; Wesley, R. A.; Luginbuhl, R.; Denton, D. D.; Ratner, B. D., Plasma polymerized *N*-isopropylacrylamide: Synthesis and characterization of a smart thermally responsive coating. *Biomacromolecules* **2001,** 2, (1), 32-36.

32. Cheng, X. H.; Canavan, H. E.; Stein, M. J.; Hull, J. R.; Kweskin, S. J.; Wagner, M. S.; Somorjai, G. A.; Castner, D. G.; Ratner, B. D., Surface chemical and mechanical properties of plasma-polymerized *N*-isopropylacrylamide. *Langmuir* **2005,** 21, (17), 7833-7841.

33. von Recum, H. A.; Kim, S. W.; Kikuchi, A.; Okuhara, M.; Sakurai, Y.; Okano, T., Novel thermally reversible hydrogel as detachable cell culture substrate. *Journal of Biomedical Materials Research* **1998,** 40, (4), 631-639.

34. Ito, Y.; Chen, G. P.; Guan, Y. Q.; Imanishi, Y., Patterned immobilization of thermoresponsive polymer. *Langmuir* **1997,** 13, (10), 2756-2759.

35. Chen, G. P.; Imanishi, Y.; Ito, Y., Effect of protein and cell behavior on pattern-grafted thermoresponsive polymer. *Journal of Biomedical Materials Research* **1998,** 42, (1), 38-44.

36. Liu, H. C.; Ito, Y., Cell attachment and detachment on micropattern-immobilized poly(*N*-isopropylacrylamide) with gelatin. *Lab on a Chip* **2002,** 2, (3), 175-178.

37. Liu, H. C.; Ito, Y., Gradient micropattern immobilization of a thermo-responsive polymer to investigate its effect on cell behavior. *Journal of Biomedical Materials Research Part A* **2003,** 67A, (4), 1424-1429.

38. Sugawara, T.; Matsuda, T., Novel surface graft-copolymerization method with micron-order regional precision. *Macromolecules* **1994,** 27, (26), 7809-7814.

39. Tamada, Y.; Ikada, Y., Fibroblast growth on polymer surfaces and biosynthesis of collagen. *Journal of Biomedical Materials Research* **1994,** 28, (7), 783-789.

40. Bullett, N. A.; Talib, R. A.; Short, R. D.; McArthur, S. L.; Shard, A. G., Chemical and thermo-responsive characterisation of surfaces formed by plasma polymerisation of *N*-isopropylacrylamide. *Surface and Interface Analysis* **2006,** 38, (7), 1109-1116.

41. Kwon, O. H.; Kikuchi, A.; Yamato, M.; Sakurai, Y.; Okano, T., Rapid cell sheet detachment from poly(*N*-isopropylacrylamide)-grafted porous cell culture membranes. *Journal of Biomedical Materials Research* **2000,** 50, (1), 82-89.

42. Li, L. Y.; Chen, S. F.; Zheng, J.; Ratner, B. D.; Jiang, S. Y., Protein adsorption on oligo(ethylene glycol)-terminated alkanethiolate self-assembled monolayers: the molecular basis for nonfouling behavior. *Journal Of Physical Chemistry B* **2005,** 109, (7), 2934-2941.

43. Prime, K. L.; Whitesides, G. M., Adsorption of proteins onto surfaces containing end-attached oligo(ethylene oxide) - a model system using self-assembled monolayers. *Journal of the American Chemical Society* **1993,** 115, (23), 10714-10721.

44. Michel, R.; Pasche, S.; Textor, M.; Castner, D. G., Influence of PEG architecture on protein adsorption and conformation. *Langmuir* **2005,** 21, (26), 12327-12332.

45. Menz, B.; Knerr, R.; Gopferich, A.; Steinem, C., Impedance and QCM analysis of the protein resistance of self-assembled PEGylated alkanethiol layers on gold. *Biomaterials* **2005,** 26, (20), 4237-4243.

46. Feldman, K.; Hahner, G.; Spencer, N. D.; Harder, P.; Grunze, M., Probing resistance to protein adsorption of oligo(ethylene glycol)-terminated self-assembled monolayers by scanning force microscopy. *Journal of the American Chemical Society* **1999,** 121, (43), 10134-10141.

47. Kidoaki, S.; Ohya, S.; Nakayama, Y.; Matsuda, T., Thermoresponsive structural change of a poly(*N*-isopropylacrylamide) graft layer measured with an atomic force microscope. *Langmuir* **2001,** 17, (8), 2402-2407.

48. Kikuchi, A.; Okano, T., Nanostructured designs of biomedical materials: applications of cell sheet engineering to functional regenerative tissues and organs. *Journal of Controlled Release* **2005,** 101, (1-3), 69-84.

49. Liang, L.; Rieke, P. C.; Liu, J.; Fryxell, G. E.; Young, J. S.; Engelhard, M. H.; Alford, K. L., Surfaces with reversible hydrophilic/hydrophobic characteristics on cross-linked poly(*N*-isopropylacrylamide) hydrogels. *Langmuir* **2000,** 16, (21), 8016-8023.

50. Zhang, J.; Pelton, R.; Deng, Y., Temperature-dependent contact angles of water on poly(*N*-isopropylacrylamide) gels. *Langmuir* **1995,** 11, 2301-2302.

51. Liang, L.; Feng, X. D.; Liu, J.; Rieke, P. C., Preparation of composite-crosslinked poly(*N*-isopropylacrylamide) gel layer and characteristics of reverse hydrophilic-hydrophobic surface. *Journal of Applied Polymer Science* **1999,** 72, (1), 1-11.

52. Johnson, R. E.; Dettre, R. H., Contact angle hysteresis. III. Study of an idealized heterogeneous surface. *Journal of Physical Chemistry* **1964,** 68, (7), 1744-1750.

53. Dettre, R. H.; Johnson, R. E., Contact angle hysteresis. IV. Contact angle measurements on heterogeneous surfaces. *Journal of Physical Chemistry* **1965,** 69, (5), 1507-1515.

54. Yamato, M.; Okuhara, M.; Karikusa, F.; Kikuchi, A.; Sakurai, Y.; Okano, T., Signal transduction and cytoskeletal reorganization are required for cell detachment from cell culture surfaces grafted with a temperature-responsive polymer. *Journal of Biomedical Materials Research* **1999,** 44, (1), 44-52.

55. Okano, T.; Yamada, N.; Okuhara, M.; Sakai, H.; Sakurai, Y., Mechanism of cell detachment from temperature-modulated, hydrophilic-hydrophobic polymer surfaces. *Biomaterials* **1995,** 16, (4), 297-303.

56. Kushida, A.; Yamato, M.; Konno, C.; Kikuchi, A.; Sakurai, Y.; Okano, T., Decrease in culture temperature releases monolayer endothelial cell sheets together with deposited fibronectin matrix from temperature-responsive culture surfaces. *Journal of Biomedical Materials Research* **1999,** 45, (4), 355-362.

57. Shimizu, T.; Yamato, M.; Kikuchi, A.; Okano, T., Cell sheet engineering for myocardial tissue reconstruction. *Biomaterials* **2003,** 24, (13), 2309-2316.

58. Yang, J.; Yamato, M.; Kohno, C.; Nishimoto, A.; Sekine, H.; Fukai, F.; Okano, T., Cell sheet engineering: Recreating tissues without biodegradable scaffolds. *Biomaterials* **2005,** 26, (33), 6415-6422.

59. Duan, X.; Sheardown, H., Dendrimer crosslinked collagen as a corneal tissue engineering scaffold: Mechanical properties and corneal epithelial cell interactions. *Biomaterials* **2006,** 27, (26), 4608.

60. Matsuda, T., Poly(*N*-isopropylacrylamide)-grafted gelatin as a thermoresponsive cell-adhesive, mold-releasable material for shape-engineered tissues. *Journal of Biomaterials Science-Polymer Edition* **2004,** 15, (7), 947-955.

61. Morikawa, N.; Matsuda, T., Thermoresponsive artificial extracellular matrix: *N*-isopropylacrylamide-graft-copolymerized gelatin. *Journal of Biomaterials Science-Polymer Edition* **2002,** 13, (2), 167-183.

62. Ohya, S.; Kidoaki, S.; Matsuda, T., Poly(*N*-isopropylacrylamide) (PNIPAM)-grafted gelatin hydrogel surfaces: interrelationship between microscopic structure and mechanical property of surface regions and cell adhesiveness. *Biomaterials* **2005,** 26, (16), 3105-3111.

63. Ohya, S.; Matsuda, T., Poly(*N*-isopropylacrylamide) (PNIPAM)-grafted gelatin as thermoresponsive three-dimensional artificial extracellular matrix: molecular and formulation parameters *vs* cell proliferation potential. *Journal of Biomaterials Science-Polymer Edition* **2005,** 16, (7), 809-827.

64. Ibusuki, S.; Fujii, Y.; Iwamoto, Y.; Matsuda, T., Tissue-engineered cartilage using an injectable and *in situ* gelable thermoresponsive gelatin: fabrication and *in vitro* performance. *Tissue Engineering* **2003,** 9, (2), 371-384.

65. Ibusuki, S.; Iwamoto, Y.; Matsuda, T., System-engineered cartilage using poly(*N*-isopropylacrylamide)-grafted gelatin as *in situ*-formable scaffold: *in vivo* performance. *Tissue Engineering* **2003,** 9, (6), 1133-1142.

66. Ibusuki, S.; Matsuda, T.; Iwamoto, Y., Tissue-engineered cartilage using thermoresponsive gelatin as an *in situ* forming and moldable scaffold with chondrocytes: *in vitro* and *in vivo* performances. *Arthritis Research & Therapy* **2003,** 5, S19-S20.

Chapter 2

Materials and methods

Scientific knowledge is a constant evolution process. Testing the formulated hypotheses often requires the adjustment of methods or even major changes to meet specific requirements. This is even more significant when trying to simulate real and complicated systems such as the human one through simplifications, in order to isolate factors and understand how different variables correlate. In the scientific dynamic process, methods are also constantly being perfected for higher accuracy and to obtain more relevant information.

This thesis, as a scientific endeavour, comprises the use of different techniques, which in some cases evolved along its time span in order to test different hypotheses or to better simulate the aimed application environment. On the other hand, procedures and methods as described in the different papers are often lacking less relevant details, that are however still important to permit a faster replication. Furthermore, each one of these papers alone is not able either to transmit that evolution process, or to explain the reason behind some decisions on the experimental design.

This section is a comprehensive effort to condensate, to contextualise and to explain the methods used throughout the thesis, as well as to provide further details, thereby shortening the way of future scientific works built over the foundations of this scientific enterprise.

2.1 Materials

2.1.1 Chitosan

Chitosan with origin from crab shells was purchased from Sigma-Aldrich (see Figure 3.5 for chemical structure). The early experiments that we have performed to determine important properties of chitosan, such as the degree of *N*-acetylation (DA)[1] and the molecular weight, revealed a substantial variability between batches. Moreover, chitosan raw-materials sometimes possess an insoluble fraction that could be remaining chitin or other type of impurities. For that reason, a purification procedure was set up. The products obtained from

[1] The degree of *N*-acetylation (DA) and the degree of *N*-deacetylation (DD) refer to the same property, but are defined as the molar fraction of the different monosaccharide units (DA = 1 - DD).

independent purifications were thoroughly mixed to obtain a final homogeneous batch of purified chitosan. Each homogeneous batch was characterised independently and no further chitosan was added, even if obtained using similar purification procedures and belonging to the same raw-material. These careful measures were taken to prevent concerns about the influence of the purification in the DA or in the molecular weight. It was not possible to keep the same batch along the entire experimental work, but each chapter refers only to a single batch, with a well defined DA (or DD) and viscosity molecular weight (Mv).

Purification of chitosan

A suitable amount of chitosan was dissolved in an aqueous acetic acid solution (1%) at ~1% (w/v). The insoluble material was removed by filtration with Whatman® ashless filter paper (20-25 µm). The obtained clear solution was precipitated adding a NaOH solution (final pH ~ 8). The formed white gel was sieved to remove the exuded liquid and thoroughly rinsed with distilled water, until no changes in the pH were detected. The chitosan gel was further washed with ethanol, freeze-dried, ground to powder and dried at 60ºC overnight.

Determination of the viscosity molecular weight

Viscosity is empirically related to molecular weight, because the measurement depends upon the hydrodynamic volume of the macromolecule, which is a function of the molecular weight, conformational properties and polymer-solvent interactions[1-3]. Measurements of solution viscosity are made by comparing the flow time *t* required for a specific volume of polymer solution to flow through a capillary tube with the correspondent flow time t_0 for the solvent. Relative viscosity (η_r) and specific viscosity (η_{sp}) are calculated from *t and* t_0, according to the following equations:

$$\eta_r = \eta/\eta_0 \cong t/t_0 \qquad (2.1)$$

$$\eta_{sp} = \frac{\eta - \eta_0}{\eta_0} = \eta_r - 1 \qquad (2.2)$$

Several mathematical equations are available for determining the intrinsic viscosity [η] of a polymer. These equations are found to be valid at sufficiently low concentrations, assuring that the polymer chains are free to move individually in the solvent, i.e., the kinetic units are not aggregates but single polymer molecules. The equations derived by Huggins[2] (equation

2.3) and Kraemer[3] (equation 2.4) relate η_r and η_{sp}, respectively, with the polymer concentration in the solvent (*C in* g/dL or any other units proportional to this), according to the following expressions:

$$\frac{\eta_{sp}}{C} = [\eta] + K_H[\eta]^2 C \quad (2.3)$$

$$\frac{\ln \eta_r}{C} = [\eta] - K_K[\eta]^2 C \quad (2.4)$$

The Huggins (K_H) and the Kraemer (K_K) coefficients give information on the polymer-solvent interactions, being the K_H lower values (ranging from 0.25 to 0.5) and the K_K negative values related to a better solvation of the polymer chains[4]. Theoretically, $K_H + K_K$ should be equal to 0.5. The intrinsic viscosity [η] is a theoretical value calculated at the limit of infinite dilution using those equations:

$$[\eta] = (\eta_{sp}/C)_{c=0} \quad \text{(Huggins)} \quad (2.5)$$

$$[\eta] = (\ln \eta_r/C)_{c=0} \quad \text{(Kraemer)} \quad (2.6)$$

The graphical extrapolation (C=0) using both equations is expected to produce more or less the same values of [η] for a particular polymer-solvent system. The quality of the results was assessed by comparing the values of [η] and evaluating K_H and K_K. Chitosan fresh solutions were prepared with five different concentrations in the range that gives η_r between 1.1 and 1.9. The flow time was obtained from five reproducible measurements for each solution, using an Ubbelohde viscometer (T = 25.0 ± 0.1ºC). The intrinsic viscosity [η] was calculated by linear regression plotting η_{sp}/C and $\ln(\eta_r)/C$ against C(g/dL) (see Figure 2.1). The solutions were carefully prepared since the method is very sensitive to small errors in the concentration, solutions ageing and the presence of dust particles, which due to the small diameter of the capillary can decrease significantly the flow section area. The purified chitosan samples were oven dried overnight and accurately weighted in an analytical balance (± 0.1 mg). In any case the amount of weighted chitosan was inferior to 20.0 mg in other to minimise weighting errors. The residual water was determined thermo-gravimetrically (TGA) and the concentration was corrected accordingly. First, the chitosan powder was completely dissolved in acetic acid (AcOH) 0.5 M. Then, a suitable amount of sodium acetate (AcONa) was added to give a final concentration of 0.2 M. This solution was filtered and transferred to a volumetric flask. The filter and glassware was rinsed with the same 0.5 M AcOH solution to assure that chitosan is completely transferred. The volumetric

flask was filled up to the mark with the same 0.5 M AcOH solution. The blank solution was prepared in the same way, but without adding chitosan. Finally, the pH was checked (it should be around 4.3-4.4) and the flow time was analysed immediately to avoid chitosan depolymerisation.

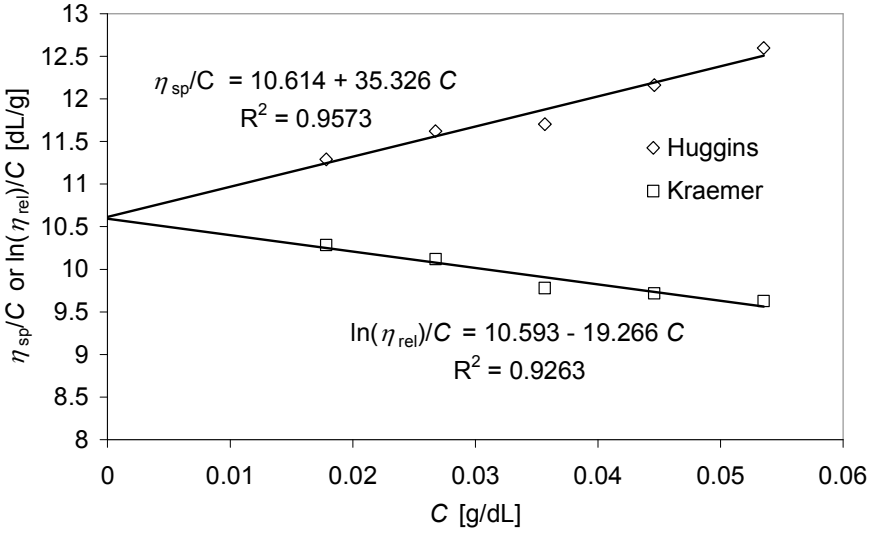

Figure 2.1 Example of linear regressions obtained by plotting η_{sp}/C (Huggins) or $\ln(\eta_{rel}/C)$ (Kraemer) against C (M_v = 790 kDa, K_H = 0.31;K_K = 0.17)

The viscosity average molecular weight (M_v) was calculated based on the Mark-Houwink equation:

$$[\eta] = k(M_v)^a \qquad (2.7)$$

with, [η] in dL/g, M_v in Da, k = 3.5 x 10^{-4} and a = 0.76 for 0.5 M AcOH/0.2 M NaOAc aqueous solution as solvent at 25ºC (independent of the DA at these conditions)[1, 5].

Determination of the degree of *N*-acetylation

Chitosan is the most deacetylated part (DA < 60) of a series of copolymers of β-(1→4)-2-acetamido-2-deoxy-D-glucopyranose (GluNAc) and β-(1→4)-2-amino-2-deoxy-D-glucopyranose units (GluN). The properties of chitosan vary considerably with the DA; therefore it can only be correctly defined once its DA is known. Although apparently a simple analytical problem, the DA determination has revealed to be a complicate issue. A huge number of methods have been proposed in the literature[6-22], which include Fourier

transformed infrared spectroscopy (FTIR)[6-9], potentiometric[10] and metachromatic[11] titrations, elemental analysis[10,12], ultraviolet (UV) spectrophotometry[12-14], ninhydrin assay[15], conductometric titration[16] and nuclear magnetic resonance (NMR) spectroscopy[17-22], just to refer to most common. The great number of methods described in the literature may be regarded as an advantage, but can pose some difficulties to the untrained researchers at the time of deciding which method to use. In fact, these methods differ in reliability, robustness, precision and accuracy over the entire DA range.

In a first approach, we used several methods and compared them in terms of precision and accuracy of the obtained values, but we also evaluated practical issues such as the amount and harmfulness of the produced residues or if the methods encompass time-spending and laborious procedures. The DA value determined by metachromatic titration[11] for highly deacetylated samples (DA = 6.7 %) was abnormally high, with no practical meaning since greater than 100%. We hypothesised that the methachromatic effect is no longer stoichiometric for high DD. This anomalous result, together with the poor accuracy for lower DA values (considering the ^{1}H-RMN as the reference technique), as well as with the fact of being highly time-spending, made this method one of the most inappropriate that we tested in this first screening. FTIR methods are widely used to determine the DA of chitosan and, since the determination is performed in the solid state, they are also suitable to determine the DA of chitin (DA > 60). If the materials are in the salt form they should be previously converted to the free amine form. The FTIR methods involve the comparison between the absorbance of a band assigned exclusively to one of the monosaccharides and a suitable internal reference band to correct for film thickness or sample concentration (KBr disks). A big effort has been devoted to identity the right combination of bands and respective baselines, which led to a large number of proposed methods found in the literature[6-9]. In our first attempt to determine the DA by FTIR we used the method proposed by Baxter *et al*.[6] and the bands proposed by Brugnerotto *et al*.[8] that are depicted in Table 2.1.

Table 2.1 Calibration curves to determine the DA using the FTIR spectrum of chitosan that make use of different combinations of bands and baselines. The absorbance (*A*) is the height at the band maximum corrected by the intercept with the respective baseline

Band (cm^{-1})	Baseline (cm^{-1})	DA (%)	Ref.
1655	1800 - 1600	DA = (A_{1655}/A_{3450}) x 115	[6]
3450	4000 - 2500		
1320	1355 - 1270	A_{1320}/A_{1420} = 0.3822 + 0.03133 x DA	[8]
1420	1495 - 1405		
1320	1355 - 1270	A_{1320}/A_{3450} = 0.03146 + 0.00226 x DA	[8]
3450	4000 - 2500		

The methods that used the –OH stretching band at 3450 cm^{-1} gave in general lower values than the ones obtained by using the band at 1420 cm^{-1}. This is likely due to the fast uptake of moisture from the atmosphere that oven-dried chitosan materials present (see Chapter 3), which interfere with the band at 3450 cm^{-1} leading to an overestimation of its intensity.
Moreover, we found that the values achieved making use of the reference band at 1420 cm^{-1} did not consistently match the DA obtained using ^{1}H-NMR. The discrepancy between the results obtained using different calibration curves and also with respect to reference methods has been described in the literature[7]. The use of FTIR for quantification purposes have drawbacks intrinsic to the fact that some bands depend on intricate associations with the typical hydrogen-bonding networks different for each chitin polymorphic form[7]. This fact makes the selection of suitable bands and baselines quite problematic. More recently, statistical studies comparing the vast number of proposed bands and baselines combinations have been employed to assist in that selection based on robust criteria[9]. Despite its drawbacks, FTIR has been often preferred because it is a quick, user-friendly and low-cost method, but mostly because it can also be applied to the insoluble chitin. Nevertheless, the construction of a specific calibration line for each particular isolation and deacetylation procedure may be necessary to obtain reliable values of DA[9]. The calibration requires the use of standards previously assessed for the DA, which, in the case of insoluble samples, is normally done using solid state ^{13}C-NMR as a reference method[7-9]. For these reasons, we did not consider the FTIR technique to report the DA of the chitosan raw-materials used in this thesis and focused on two methods, which results were consistently similar all over the entire range of the DA of chitosan, by means of ^{1}H-NMR and 1st derivative UV spectrophotometry. One entire chapter (Chapter 3) is dedicated to this issue, in which 1st derivative UV spectrophotometry first proposed by Muzzarelli and Rocchetti[13] is improved. A mathematical expression is derived to avoid the use of empiric correction curves for highly deacetylated samples. The DA is determined directly from the mass concentration of chitosan solutions and the first derivative value of its UV spectra at 202 nm (the acetic acid solutions zero crossing point), over the entire range of the DA of chitosan.

Preparation of chitosan samples with several DA by selective *N*-acetylation

The selective *N*-acetylation of chitosan can be performed under mild conditions at which the molecular weight was reported to not vary considerably[23]. This is a valuable route to obtain chitosan materials with similar molecular weight, but different DA. The chitosan sample (5 g) was dissolved in 1% (w/v) of aqueous acetic acid (50 ml). A variable volume of acetic anhydride was mixed with 50 ml of ethanol, added slowly to the chitosan solution and stirred

overnight. The ratio of the acetic anhydride to the chitosan GluN units was adjusted to obtain samples with different DA. The solutions were precipitated with acetone, followed by diethyl ether and dried under vacuum. The acetylated samples were then neutralised in 1N NH_4OH aqueous solution, thoroughly washed with distilled water and freeze-dried. The resultant sponges were milled with liquid nitrogen and the obtained flakes were dried at 80ºC under reduced pressure.

Determination of the moisture content by thermogravimetric analysis (TGA)

Chitosan usually contains residual moisture irrespective to the drying procedure[24]. The hypothesis that this residual moisture could be caused by a fast water uptake from the atmosphere would make the accurate determination of the chitosan weight a tricky procedure. The water content of the chitosan samples was estimated by TGA (TA Instruments, model TGA Q500), immediately after being weighted for the UV determination of the DA. The thermograms were obtained under an atmosphere of flowing nitrogen. The chitosan powder (4-10 mg) was first heated at a 10ºC/min ramp, which was followed by an isothermal step of 20 min at 110ºC to assure complete dryness of the samples. Moisture content (MC(%)) was considered to be the weight loss at that time point. The temperature programme also included a cooling down period, under the same nitrogen stream. Then, the dried sample was exposed to the air atmosphere and weighted again at preset time periods, by closing temporarily the TGA apparatus furnace. This procedure allowed us to estimate the time necessary for the dried chitosan materials to recover the initial water content when exposed to the atmospheric moisture.

2.1.2 Soybean protein Isolate

Soybean protein isolate (SI) was provided by Loders Crocklaan BV (Netherlands). SI is a mixture of globulin proteins on which Glycinin is present at about 40% (isoelectric point - pI 6.4) and β-conglycinin at about 28% (pI 4.8)[25]. The same material has been used in different works in our group[26-30]. SI is not totally soluble in water, but about 90% of the proteins present in soybean are soluble at some pH (water extractable)[31].

2.1.3 *N*-Isopropylacrylamide

N-isopropylacrylamide (NIPAAm) (see Figure 2.2) from Acros-Organics was purified by recrystallisation. The monomer was dissolved in a boiling mixture of n-hexane/diethyl ether (5:1), filtrated and left at room temperature overnight to obtain a greater amount of crystallised monomer. After solvent removal by decantation the purified monomer was dried over vacuum for 24h to remove the residual solvent.

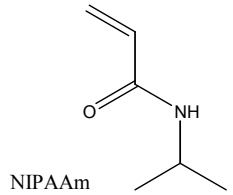

Figure 2.2 Chemical structure of *N*-isopropylacrylamide

2.2 Processing of multifunctional chitosan-based membranes

2.2.1 Chitosan/Soybean protein isolate membranes

Chitosan was dissolved at a concentration of 1 wt.% in an acetic acid 1 wt.% solution (AcOH). SI was suspended in distilled water at room temperature under gentle stirring in order to avoid protein denaturation and consequently, foam formation. SI suspensions were added dropwise to chitosan solutions under constant stirring at different ratios (designated cts100%, cts75%, cts50%, cts25%, related to chitosan percentage), and pH was corrected to 4.0 with AcOH (equal to chitosan solution). Mixtures were poured into the moulds directly in the drying place and moulds were no longer moved or removed until complete drying, in order assure that the insoluble part of SI was uniformly distributed. Drying was performed at room temperature (c.a. 20ºC) and relative humidity (c.a. 55%). The air-exposed (AE) surface during the drying process presented some roughness at the macroscopic level, whereas the mould-exposed (ME) surface presented a very smooth appearance. In this way, the surface characterization was carried on taking in consideration this feature. β-radiation sterilization was preformed by *Ionmed Esterilizatión*, SA (Cuenca, Spain) at different radiation doses (25, 50 and 100 kGy) using the electron accelerator Rhodotron TT2 (10 MeV).

2.2.2 Chitosan membranes

The chitosan solution was prepared by dissolving chitosan (1% wt.) in acetic acid solution (1% wt.). The solutions were carefully stirred in order to avoid the formation of any air bubble, poured on Petri Dishes and dried at room temperature in a dust free environment. The resultant membranes (thickness approx. 50 μm for 5 mg of chitosan/cm^2) were neutralised in NaOH 0.1M solution for 10 min and washed thoroughly with distilled water. The obtained membranes (CTS) were hold in a frame and dried again, presenting a smooth surface without the typical wrinkles derived from the material shrinking during the drying process.

2.2.3 Crosslinking with glutaraldehyde

The chitosan solution was prepared by dissolving chitosan (1% wt.) in acetic acid solution (1% wt.). Glutaraldehyde (GA) solutions were prepared at concentrations ranging from 0.1 M to 5 x 10^{-4} M. The amount of chitosan amine groups (NH_2) (GluN units) can be determined using the following expression:

$$n_{(\mathrm{GluN})} = \frac{m_{(\mathrm{CTS})}}{\left[M_{(\mathrm{GluN})} + \frac{1-\mathrm{DD}}{\mathrm{DD}} M_{(\mathrm{GluNAc})} \right]} \tag{2.8}$$

where $M_{(\mathrm{GluNAc})}$ = 203 and $M_{(\mathrm{GluN})}$ = 161 are the molecular weights of the GluNAc and GluN units within the copolymer, $m_{(\mathrm{CTS})}$ is dry weight of chitosan in grams, $n_{(\mathrm{GluN})}$ is the molar amount of amine groups in that weight of chitosan and DD the degree of *N*-deacetylation.
Then, defining the crosslinking degree (x) as the percentage of aldehyde (CHO) groups with respect to the initial free NH_2 groups (CHO/NH_2 ratio), we can write:

$$x(\%) = \frac{n_{(\mathrm{CHO})}}{n_{\mathrm{NH_2}}} \times 100 = \frac{2n_{(\mathrm{GA})}}{n_{(\mathrm{GluN})}} \times 100 \tag{2.9}$$

and it follows that:

$$x(\%) = \frac{2V_{(\mathrm{GA})}C_{(\mathrm{GA})} \times \left(M_{(\mathrm{GluN})} + \frac{1-\mathrm{DD}}{\mathrm{DD}} M_{(\mathrm{GluNAc})} \right)}{m_{(\mathrm{CTS})}} \times 100 \tag{2.10}$$

where $V_{(\mathrm{GA})}$ and $C_{(\mathrm{GA})}$ are respectively the volume and concentration of the glutaraldehyde solutions. Actually, the crosslinking degree defined by equation 2.10 is the reagents feed ratio, since the real crosslinking efficiency depends upon the chemical conversion and on the occurrence of other parallel reactions, which can form either any or longer crosslinks.

The glutaraldehyde solution volume added to a certain amount of the previous chitosan solution was kept constant. The several crosslinking degrees were obtained by only changing the concentration of glutaraldehyde, according to equation 2.10. In this way, the reaction volume and polymer concentration was kept constant for all the samples, varying only the molar amount of glutaraldehyde added, which determines the crosslinking degree.

Glutaraldehyde solution was added dropwise during 5 min under gentle stirring and the resultant solutions were let quiescent for about 1 h to remove any air bubble formed. Solutions were poured into Petri dishes and dried at room conditions. The resultant membranes were neutralised in NaOH 0.1M solution for 10 min, washed thoroughly with distilled water and dried again. Samples were labelled according to their crosslinking degree as CTS[*x*(%)]. For instance, samples with *x* = 0.1%, 1% and 20% were labelled as CTS0.1, CTS01 and CTS20, respectively.

It should be noticed that in Chapter 5, the crosslinking degree (*x*') is defined in a slightly different way. It is defined as the molar ratio between the added glutaraldehyde and the chitosan amine groups, which can be written as:

$$x'(\%) = \frac{n_{(GA)}}{n_{(GluN)}} \times 100 = \frac{x(\%)}{2} \qquad (2.11)$$

Although both values are interconvertible, the equation 2.11 cannot be used to make an exact comparison between the crosslinked samples referred in Chapters 5 and 6. In fact, since the chitosan raw-materials used in each one of these chapters possess different DA, the same *x* or *x*' value should correspond to a similar chemical efficiency, but it probably gives a different average molecular weight between crosslinks. As we already referred previously, it was not possible to keep the same batch along the entire experimental work, but each chapter refers only to a single batch, with a well defined DA and molecular weight.

2.2.4 Oxygen plasma treatment

The surface of chitosan membranes was modified by plasma treatment according to a procedure described elsewhere [32]. Briefly, the plasma treatment was performed using radio frequency (13.56 MHz) Plasma Prep5 equipment from GaLa Instrumente (Bad Schwalbach, Germany). Samples were exposed to O_2 plasma at 30 W of power during 15 min. The pressure in the reactor was maintained under 20 Pa by regulating the gas flow. The samples were only further processed after 48 h in order to assure that free radicals formed during the plasma treatment have been quenched.

2.2.5 Modification of chitosan membranes with PNIPAAm

The monomer (NIPAAm) was dissolved in several compositions of isopropanol/water mixtures varying in the volume ratio from (50:50) to pure isopropanol (100:0). The initiator, 2,2'-Azobis-isobutyronitrile (AIBN), was dissolved in each solvent mixture used in the respective monomer solution. Chitosan membranes were immersed in the monomer solutions. Both monomer and initiator solutions were deoxygenated under slow nitrogen flow for 10 min. The polymerisation was initiated adding the AIBN solution to the monomer solutions and the reaction was performed at 60ºC under N_2 atmosphere for 18h. The volumes of NIPAAM and AIBN solutions give a final monomer concentration of 0.25 g/mL and AIBN to NIPAAm molar ratio of 1%. The grafted membranes were washed thoroughly with acetone/water (75:25) to remove unbound polymer. Samples were labelled as iPrOH100, iPrOH90, iPrOH75 and iPrOH50, according to the volume of isopropanol used in the non-solvent/solvent mixture composition. The same PNIPAAm grafting procedure was also applied to plasma treated chitosan membranes at an isopropanol/water composition of 75:25 (P-iPrOH75).

2.3 Surface characterisation of the chitosan-based membranes

In biomaterials science the surface analysis has a central role, because the surface is the first contact between the living body and the biomaterial when a certain device is implanted into the body. It is well known[33] that the surface properties of biomaterials, namely chemistry, topography and/or surface energy, are essential factors for cell adhesion and proliferation and consequently for the performance (rejection or acceptance) of a potential device.

2.3.1 Contact angle measurements

The contact angle of a liquid drop with a solid surface is a consequence of the force balance between the liquid-vapour surface tension of the drop and the interfacial tension between the solid and the drop. The surface energy can be calculated with data from liquids of different surface tensions. The contact angle methods are very surface-sensitive, being the analysed depth of around 3-20 Å [34]. The equilibrium water contact angle (measured under static conditions) of some polymer substrates has been shown to correlate with the cell adhesion and proliferation, which are both optimal at around 70º [35].

In Chapter 4, contact angle (θ) measurements were undertaken by means of sessile drop method with contact angle measurement system G10 from Krűss (Hamburg, Germany) at room temperature (c.a. 20ºC). At least five measurements were performed for each solvent. Surface tension (σ_s), as well as its polar (σ_s^p) and dispersive (σ_s^d) components were determined by Owens and Wendt method[36], using the equipment software G402 (Krűss, Hamburg, Germany). Glycerol and methylene iodide were respectively used as polar and non-polar test liquids.

In Chapter 6, the influence of the glutaraldehyde crosslinking on the hydrophilicity of the materials was assessed by means of evaluating the surface wettability using water contact angle measurements. Static contact angle measurements were carried out by the sessile drop method using a contact angle meter OCA 15+ with high-performance image processing system from DataPhysics Instruments (Filderstadt, Germany). A drop (1 µL) of water was added by a motor driven syringe at room temperature and the contact angle was measured after the contact between the drop and the surface. Two different samples of each material were used and at least three measurements were carried out for each sample.

2.3.2 X-ray photoelectron spectroscopy (XPS)

The X-ray photoelectron spectroscopy (XPS) method (also called Electron Spectroscopy for Chemical Analysis, ESCA) is based on the photoelectric effect. The interaction of the X-rays focused on the sample with its atoms causes the emission of a core level (inner shell) electron. The energy of this electron is measured and its value provides information about the nature (survey spectrum) and environment (high resolution spectrum) of the atom from which it came. Being so, information about the elemental composition and chemistry can be obtained at the surface level of the sample within a depth of 10-250 Å [34].

Possible chemical changes occurred on the surfaces after the modifications performed in Chapter 7 were evaluated by XPS. The spectra were obtained using an ESCALAB 200A instrument from VG Scientific (East Grinstead, UK) with PISCES software for data acquisition and analysis. A monochromatic Al-Kα radiation (hv = 1486.60 eV) operating at 15 kV (300 W) was used. The measurements were performed in a constant Analyser Energy mode (CAE) and take off angle of 90º relative to the sample surfaces. Survey spectra were acquire using a pass energy of 50 eV, over a binding energy range of 0 to 1100 eV, and were used to calculate the elemental composition of the surfaces. Element atomic percentages were calculated from the integrated intensities of the survey spectra using the sensitivity factor of the instrument data system. High resolution spectra for different regions (C1s, O1s and N1s) were obtained using a pass energy of 20 eV and were peak-fitted using a least-squares peak

analysis software, XPSPEAK version 4.1, using the Gaussian/Lorenzian sum function. Background counts were subtracted using a linear baseline and the sample charging was corrected assigning a binding energy of 285.0 eV to the saturated hydrocarbons C1s peak.

2.3.3 Morphological characterisation by scanning electron microscopy (SEM)

Scanning electron microscopy (SEM) images are obtained from the low-energy secondary electrons emitted from each spot of the sample where the focused electron beam impacts. It possess a penetration depth of 5 Å [34]. The samples should be previously dehydrated. Non-conductive samples are typically coated with a thin, electrically deposited metal layer, to minimise charge accumulation. In turn, although based on the same principal, environmental SEM (ESEM) allows observing wet and uncoated samples, due to small changes introduced in the apparatus configuration [34]. The main disadvantage of ESEM relies on its lower resolution when compared with SEM. Uncoated surfaces of chitosan and chitosan/soybean protein isolate (Chapter 4) membranes were characterized morphologically by Scanning Electron Microscopy (SEM, Philips XL30) and Environmental Scanning Electron Microscopy (ESEM, Philips XL30).

2.4 Solvent induced swelling and degradation experiments

Many polymeric systems can uptake limited amounts of solvents and swell to accommodate the absorbed liquid without dissolving. When the solvent is water, the network of polymer chains that are water-insoluble is called a hydrogel. The chitosan membranes developed in this thesis fit well the hydrogel definition. The properties of chitosan are highly dependent on the swelling ratio. For instance, the mechanical properties were found to vary dramatically when determined with the samples immersed in aqueous solutions (Chapter 5) and the permeability correlated well with the crosslinked membranes water uptake (swelling ratio) (Chapter 6). In this sense, the determination of the swelling ratio in aqueous solutions that simulate the physiological environment was very important for a better understanding of the physico-chemical and biological behaviour of the membranes.

Moreover, the water uptake ability of chitosan membranes and the non-solvent properties of isopropanol were used to control the grafting of PNIPAAm. This control was based on the different swelling ratios that chitosan membranes possess towards mixtures of both solvents. In this sense, the relevance of measuring the solvent induced swelling or solvent uptake was

not limited to aqueous solutions. In section 2.4.1, it is given a general overview of these experiments procedure. More detailed information is given in the respective chapters.
Finally, the aqueous environment can also induce materials degradation by leaching out small molecular weight polymer chains or other additives or through hydrolytic degradation. The determination of the degradation in aqueous solutions was also performed.

2.4.1 Swelling (solvent uptake) experiments

The swelling behaviour of chitosan membranes in different solvents and aqueous solutions was determined by immersing previously weighted chitosan membranes. Containers were sealed and placed in a controlled temperature environment. After a certain time period, swelled samples were blotted with filter paper to remove the adsorbed solvent and weighted immediately. The swelling ratio (*S*) was calculated using the following equation:

$$S(\%) = \frac{W - W_0}{W_0} \times 100 \qquad (2.12)$$

where W_0 is the initial weight of the sample and W is the weight of the swelled sample. The equilibrium swelling ratio (S_{eq}) was considered to be the last point of a swelling kinetics curve, where no further swelling is observed with time. In the case of aqueous solutions the swelling ratio was denoted water uptake (*WU*).

2.4.2. *In vitro* degradation

In vitro degradation of chitosan membranes was assessed in isotonic saline solution (ISS) (NaCl 0.154 M and pH = 7.4 $\pm$ 0.02). Samples were previously weighted and then fully immersed in solution. Containers were sealed and placed in a thermostatic bath at 37 $\pm$ 1 ºC. After each test period (7, 14, 30 and 60 days) samples were dried until constant weight (W_1). The weight loss (*WL*) was calculated using the following equation:

$$WL = \frac{W_0 - W_1}{W_0} = 1 - \frac{W_1}{W_0} \qquad (2.13)$$

where W_0 is the initial weight of the sample.

2.5. Chemical characterisation

2.5.1 Fourier Transform infrared spectroscopy (FTIR)

Fourier transform infrared spectroscopy (FTIR) is a standard analytical method that can reveal information about the sample chemical structure, since the absorption of infrared (IR) light is related to discrete energy transitions of the vibrational states of atomic and molecular units within a molecule. In transmission mode, the FTIR spectra give information related to the bulk material. The attenuated total reflection (ATR) sampling mode can be used to increase the intensity of the surface signal, because it observes the region near the surface. However, FTIR-ATR is not truly surface sensitive due to the high penetration depth of the analysis (1 – 5 μm) [34]. Nevertheless, the rich structural information that the IR spectra provide makes the FITR-ATR an interesting technique to evaluate greater chemical changes, such as the grafting of polymers both at the surface and also at a broader region nearby the surface (Chapter 7). If thick enough, deposited layers of materials onto the original surface can also be observed. Finally, FTIR-ATR can be also used to evaluate homogeneous materials, in which the surface composition does not differ significantly from the bulk. Different FTIR spectrophotometers have been used based on the availability of the equipments or ATR accessory at the place and moment the work has been performed. For this reason, there is an unusual heterogeneity of equipment models/trademarks in the different chapters. See each chapter for further details on the equipments and experimental procedures.

2.5.2 Proton nuclear magnetic resonance (^{1}H-NMR)

Chitosan is soluble in moderately acid conditions. In this way, chitosan materials (10 mg) were dissolved in 1 ml of 0.4% (w/v) of deuterium chloride (DCl) in D_2O solution at room temperature. On the other hand, since chitosan easily absorb water from the atmosphere the signal arose from this residual water (HDO) may be too intense. If this is the case, samples can be lyophilised and dissolved again in D_2O or, alternatively, dried thoroughly. Proton nuclear magnetic resonance (^{1}H-NMR) was used to estimate the total amount of grafted PNIPAAm, which were thought to be detectable for samples in which grafting reaction was performed in solvents with higher water content. The ^{1}H-NMR spectra were acquired in a Varian Inova-300 (300 MHz) spectrometer (Palo Alto, USA).

The determination of the degree of *N*-deacetylation by ^{1}H-NMR required additional care in the adjustment of the experimental conditions. In order to minimise the deacetylation catalysed by the presence of deuterium chloride, only freshly prepared solutions were used. The ^{1}H-NMR spectra were acquired in a Varian Unity Plus (300 MHz) spectrometer (Palo Alto, USA) at 70ºC, temperature at which the solvent signal (HOD) does not interfere with the chitosan peaks. The acquisition (64 transients) started after 10 min, considered to be enough to reach the thermal equilibrium. The pulse repetition delay, 6 s, and the acquisition time, 2 s, were set to assure complete relaxation of the nuclei before each pulse application. This procedure (repetition time of 8 s) guarantees that the relative intensities of the resonances correlate with the exact number of nuclei originating that signal[19].

2.6 Crystallinity

Chitosan is a semi-crystalline polymer from which several polymorphs have been mentioned in the literature [37-39]. Chitosan molecular weight [38], DD [40] and different membrane processing methods gave origin to substantial variations in the presence and amounts of the different polymorphs [38, 39]. Several properties of chitosan membranes should depend on the type and the degree of crystallinity. In this sense, the samples used in Chapters 5 and 6 were analysed by X-ray diffraction since the properties been analysed could be affected by the crystallinity.

In Chapter 5, the morphology of the studied membranes was analysed by X-ray diffraction using synchrotron radiation at the A2 Soft Condensed Matter Beamline of HASYLAB, DESY (Hamburg, Germany). 2D wide-angle X-ray scattering (WAXS) patterns were obtained employing an image plate, separated 22 cm from the sample.

In Chapter 6, the morphology of the membranes was analysed recording the wide-angle X-ray scattering (WAXS) patterns in a Philips PW1710 reflection diffractometer (Almelo, The Netherlands), with a step ($2\theta = 0.02º$) scanning time of 2 s and Cu-Kα-radiation generated at 40 kV and 30 mA.

2.7 Mechanical properties

The mechanical properties of a material are usually an important criterion in the appropriate selection of a material for a particular biomedical application, mainly for implants that will withstand mechanical stresses in a clinical situation. Thus, a proper mechanical characterisation is one of the critical physical tests, which must be undertaken in order to get

a reliable prediction of the implant geometrical integrity under service conditions, both at short-term (determined by means of quasi-static mechanical tests) and long-term (obtained from extrapolated creap/stress relaxation tests or fatigue).

Besides the information that can be obtained about the mechanical performance in a wide temperature and timescale range, dynamic mechanical analysis (DMA) also reveals the existence of relaxation processes. These processes are evidenced by great changes in the level of the storage modulus (*E*') and storage compliance (*D*') and by peaks in the corresponding imaginary components or in the loss factor (tan δ) in the log frequency or temperature axis. Interpretation of the relaxation phenomena (e.g. glass transition) gives a better understanding of the relationship between structure and properties. The relaxation processes may alter the viscoelastic behaviour of the material in a given temperature or frequency range in such a way that it would hamper the device general performance.

In the other hand, novel materials to be used in biomedical applications should have compatible time-dependent mechanical (viscoelastic) features with the organ or tissues that they will contact with. For this reason it is also important to know the mechanical behaviour of the tissues that they will contact[41]. It should be noticed that most of the biological tissues have viscoelastic properties with excellent damping capabilities, allowing for an efficient dissipation of external loads caused by daily life[42, 43]. For instance, in cardiovascular or skin applications, one should have materials that are relatively compliant at low strains but with high strengths, as it happens with the corresponding biological materials, in order to integrate well within the living tissues[41].

If the material swells easily in aqueous solutions, as it is the case of chitosan materials, the evaluation of the mechanical performance both under static and dynamic solicitations with the samples at an air atmosphere is worthless. Actually, these test conditions do not represent the physiological environments in which the materials will have a completely different mechanical behaviour. The tests should be performed while immersing the specimen in physiological simulated aqueous solutions and ideally at 37ºC. In fact, water content of hydrogel materials can affect drastically its mechanical properties, as we will see later in this thesis (Chapter 5). In this sense, materials were tested in a water bath designed to fit the DMA equipment and described below.

2.7.1 Quasi-static mechanical properties

Neutralised chitosan membranes were cut into strips with around 15 x 2 x 0.02 mm after conditioning in isotonic saline solutions (ISS) for 15 min. Thickness was taken as a mean of ten values at different points measured with a low-pressure micrometer. Their resistance to

stretching was evaluated with a Perkin-Elmer DMA7e at a constant stress rate of 5 MPa/min using the tensile mode. In such experiments, the strain was monitored as a function of stress. Please note that such procedure is different from conventional mechanical tests where the stress is monitored as a function of strain, which varies at constant rate. However, one can also build stress-strain curves and obtain a measure of the stiffness (by looking at the slope of the curve at early stages) and the strength (measured by the stress at break) of the sample, when experiments at constant stress rate are performed. The assays with samples immersed in solution were preformed using a liquid bath built in stainless steel. This bath can be fitted into the furnace of the DMA equipment. A schematic representation is shown in Figure 5.1. Mechanical tests in immersed conditions were carried out in an ISS (NaCl 0.154 M and pH = 7.4 $\pm$ 0.02) at body temperature (37 ºC). Samples were kept immersed for 15 min in order to reach the hydration and thermal equilibrium, after holding it in the test probe. Mechanical tests in a dry environment and in solution at room temperature (c.a. 20ºC) were undertaken for comparison purposes. Non-neutralised chitosan membranes were only tested in a dry environment. Temperature was checked with an external temperature sensor after and before each test. The temperature read by the sensor fluctuated less then 0.1ºC during the experiments. Secant modulus was calculated at 2% of elongation. Stress and strain at break were also estimated.

2.7.2 Dynamic mechanical analysis

Dynamical mechanical measurements were carried out on chitosan membranes with a Perkin-Elmer DMA7e analyser (Waltham, USA) at 1 Hz and heat rate of 2ºC/min. The tests were preformed with samples immersed in ISS, using the same system described above. In these measurements, sample and solution was carefully cooled down to near 0ºC, in order to avoid solution freezing and consequent sample damage. Experiments were stopped at about 80ºC. The dimensions were the same of those for quasi-static mechanical tests and thickness was also taken using the same procedure. It was considered that the cross-section area of the samples do not vary during the experiment.

During each DMA experiment, both the storage modulus, E', and the loss factor, tan δ, were measured as a function of temperature. The first corresponds to the real component of the complex modulus ($E^* = E' + iE''$), being a measure of the sample's stiffness, whereas the later gives the ratio between the amount of mechanical energy lost and stored during a cycle ($\tan \delta = E'' / E'$), measuring the damping capability of the sample.

A control sample of polybutadiene was tested both into solution and in the conventional dry state. This rubber material was found to not absorb any water by a simple gravimetric assay

and so mechanical dynamic performance in wet conditions should not differ from conventional assay. In fact, it was found that both *E*' and tan δ are similar when measuring in both dry and wet conditions, indicating that immersion into the solution does not influence significantly the measurements.

2.8 Determination of the polymer density

The chitosan and chitosan/SI membranes density measurements were undertaken making use of the miscible solvents system n-heptane/dibromoethane. The rational for the solvents choice was based on their density (polymer density limited by solvents density) and the fact that samples did not absorb any measurable quantity of both. Membranes were cut in at least 3 strips (c.a. 1 x 20 mm). A test tube was filled with n-heptane and placed in a ultrasound bath for 5 min to eliminate air bubbles (at this stage membrane strips should be settled down at the bottom). Then, dibromoethane was added drop by drop until all polymer strips start to go up and tend to float. At this stage the liquid density, determined by pycnometry, should be an approximation of the polymer density. The procedure was repeated 3 times giving results with a good precision (maximum standard deviation of 0.0058). In general, measures revealed to be accurate since near the polymer density the addition of a few drops did not change significantly the liquid density.

2.9 Study of the diffusion of small molecules across chitosan membranes

2.9.1 Permeation studies

The permeation studies were performed using an in-house built side-by-side diffusion cell (see details in Chapter 6). Membranes were previous equilibrated in the respective buffer solution and mounted between the half-cells of the receptor and donor compartments (1 cm^2 area of diffusion). The receptor compartment fluid was continuously pumped through a flow-through quartz cuvette with optical pathway (*l*) of 1 cm. The absorbance at a maximum wavelength (different for each solute) was monitored in a UV-1610 Shimadzu spectrophotometer. The volume of the monitoring system (tubing and quartz cuvette) was calibrated before each experiment and it was found to vary between 2.84 and 2.90 ml. The monitoring system was filled with fresh buffer and air bubbles were purged before each measurement. The inlet and outlet tubing was connected to the receptor cell previously filled

with 2.2 ml of fresh buffer. Then, the diffusion cell was immersed in a thermostatic bath at 37.0 ± 0.1 ºC. Finally, the donor cell was filled with 2.2 ml of the buffer solution containing the respective solute and the absorbance recorded. The solutions in both cells were stirred by magnetic bars at 800 rpm to eliminate the boundary layer effect. In preliminary experiments, we confirmed that the calculated permeability was kept constant above 400 rpm.

The permeability of the chitosan membranes was evaluated for small molecules of similar size, but holding different chemical moieties, either ionised (anionic) or neutral at physiological pH (see Figure 6.1). Moreover, solutes with different ionic charges were tested by choosing monoprotic and diprotic acids that are fully ionised at that pH (see Table 6.1). The solutions of the anionic solutes, such as benzoic acid (BA), salicylic acid (SA), phthalic acid (Ph), were prepared at 5 mM, 2 mM and 5 mM, respectively. Since these molecules at the working concentration are able to change the pH of the buffer solution, this was further corrected to pH 7.4 with NaOH solution. The solution of 2-phenylethanol was prepared at a concentration of 10 mM. The different concentrations used took into consideration the different molar absorptivities, in order to allow the detection of the solutes at the early stages of permeation experiments (see Table 6.1). The flux rate of those model molecules was determined in both phosphate buffer saline (PBS) solution and buffered trishydroxymethylaminomethane (TRIS)-Ca^{2+}/Mg^{2+} solutions, the same used in the water uptake experiments. After each assay, the swollen membrane thickness was taken as a mean of five values at different points measured with a low-pressure micrometer.

2.9.2 Determination of the partition coefficients

The partition coefficient (K) was considered the ratio of the solute concentration in the liquid fraction absorbed by each sample (C_m) to that in the bulk solution (C_s) [44]:

$$K = \frac{C_m}{C_s} \qquad (2.14)$$

It was determined in both PBS and buffered TRIS-Ca^{2+}/Mg^{2+} solutions. First the membrane samples were equilibrated for 48 h in a solution of each model molecule at a concentration (C_s) 5 times higher than that used in the permeation experiments. The pH of the buffer solutions was corrected to pH 7.4 with NaOH solution after the solubilisation of each acid solute. When compared with the amount of membrane sample, the volume of the concentrated solution was higher enough to consider that C_s did not vary during the solute uptake stage. The membrane was removed from the concentrated solution and the excess of liquid was removed blotting the membrane with filter paper. The water uptake of each sample was determined as described for the equilibrium water uptake experiments. Loaded

membranes were immersed in fresh buffer and this procedure was repeated until no further release was observed by UV spectrophotometry. The amount of the solute uptake was calculated as the total cumulative release and C_m was determined accordingly.

2.10 Biological characterisation of chitosan membranes

2.10.1 Cytotoxicity

The materials were cut in 1 x 1 cm^2 pieces and sterilized by ethylene oxide (EtO), as described elsewhere[45]. The sterilization procedure did not show any adverse effect on the samples (data not shown). The materials were immersed for 24 hours at 37ºC (with constant shaking) in Dulbecco's Modified Eagle's Medium (DMEM) without phenol red (Gibco BRL, USA), supplemented with 10% Foetal Bovine Serum (FBS) (BioChrome, Germany) and 1% antibiotic/antimycotic solution (Sigma, St. Louis, USA), at a ratio of 1.5 cm^2/ml. This is an advised procedure for biomaterials extraction to obtain the major leachables and determine their short-term effect in a dynamic environment[46]. The extracts were then filtered through a 0.45 μm pore size filter and then used for MTT (see details below) and total protein quantification tests.

2.10.2 MTT test

The 3-(4,5-dimethylthiazol-2-yl)-2,5-diphenyltetrazolium bromide (MTT) has a yellow tonality and is soluble in water. This compound can be converted by the mitochondrial enzyme succinate dehydrogenase in a purple colour salt insoluble in water. The insoluble salt absorbs at a wavelength of 570 nm and it is proportional to the amount of viable cells, since only viable cells can metabolise MTT [47-49].

A commercial cell line of rat lung fibroblasts – L929 (ECACC, UK) – was used in these studies. The cells were cultured in 75 cm^2 flasks (Costar). After detaching them from the culture flask by using a 0.25% trypsin-Ethylenediaminetetraacetic acid (EDTA) solution (SIGMA, St. Louis, USA) they were re-suspended in DMEM culture medium. The cells were plated in 96-well micrometer plates at a density of 2 x 10^4 cells/well. The plates were incubated for 48 hours in a humidified atmosphere of 5% CO_2 at 37ºC. After this, the culture medium was removed and the extracts were placed in contact with the cell monolayer and culture medium was used as control. The plates were incubated for 72 hours, and after

removal of the culture medium, 50 μl of MTT (Sigma, St. Louis, USA) solution (1 mg/ml in culture medium) was added and incubated 4 hours at 37ºC. To dissolve the formazan crystals that are formed, 100 μl of isopropanol were added and the plates were incubated for 15 minutes at 37ºC and then placed at room temperature in an orbital shaker to help dissolving the crystals. The optical densities at 570 nm and 650 nm (background) were read on a multiwell plate reader (Molecular Dynamics, Amersham, USA) against a blank of MTT solution and isopropanol. All the materials were tested in 10 replicates for each extract for at least three separate experiments with reproducible results.

2.10.3 Total protein quantification

The method used to quantify the total protein make use of the Micro BCA Protein Assay Reagent Kit (Pierce, USA) that uses bicinchoninic acid (BCA) as the detection reagent for Cu^{+}, which is formed when Cu^{2+} is reduced by proteins in an alkaline environment. The purple colour product is formed by the chelation of two molecules of BCA with one Cu^{+} ion. This complex is water-soluble and absorbs at 562 nm, and its absorbance is linearly correlated with protein concentration[50].

The procedure is very similar to the one of MTT. After the 72 hours incubation, the extracts are removed from contact with cells and these are washed with PBS solution 0.01 M, and 100 μl of PBS 0.01 M are added to each well. To each well 100 μl of the BCA reagent were added, the plates were agitated for 30 seconds and incubated for 2 hours at 37ºC. The plates were then cooled to room temperature and the optical densities were measured at 562 nm against a blank of PBS 0.01 M and BCA reagent. Total protein (in μg/ml) was determined using a BSA standard curve.

2.11 Cell sheet culture and detachment

2.11.1 Cell culture

A human foetal lung cell line (MRC-5), an immortalized cell line with fibroblast-like morphology, was obtained from European Collection of Cell Cultures (ECACC, UK) and was used in the cell culture studies. The cells were cultured in Dulbecco's Modified Eagle's Medium (DMEM; Sigma-Aldrich, Inc, USA) supplemented with 10000 U/ml penicillin-G sodium, 10000 μg/ml streptomycin sulfate and 25 μg/ml amphotericin B in a 0.85% saline

(Gibco, Invitrogen Corporation, UK) and 10% of heat-inactivated fetal bovine serum (FBS; Biochrom AG, Germany) in a humidified atmosphere with 5% of CO_2 at 37ºC. Membranes were cut with 14 mm diameter and placed onto 24 well culture plates. Prior culturing, all samples were sterilized by adding 1 ml of 70% ethanol aqueous solution for 90 minutes and subsequently washed with sterile phosphate buffered saline solution (PBS, Sigma Chemical Co., USA) to remove the remaining ethanol. Cells were seeded on the materials at a concentration of 7 x 10^4 cells/ml, adding 1 ml per well and incubated for 10 days, time at which the cells seeded on plasma treated materials (P-iPrOH75) were 100% confluent.

2.11.2 Cell sheet detachment and assessment of the cell viability

After 10 days of culture, plates were removed from the incubator and observed by light microscopy. The cells cultured on the different samples were continuously observed to assess the eventual detachment from the surface at room temperature (c.a. 16ºC). Cell viability was assessed after Calcein AM staining. A 2:1000 Calcein AM solution (Sigma, Germany) was prepared with DMEM culture medium and 1000 µl were added to each sample culture. Plates were incubated for 15 minutes at 37ºC in a humidified atmosphere of 5% CO_2 and cell fluorescence examined in an Axioplan Imager Z1 from Zeiss (Germany).

2.12 References

1. Terbojevich, M.; Cosani, A., Molecular weight determination of chitin and chitosan. In *Chitin handbook*, Muzzarelli, R.; Peter, M., Eds. European chitin society: 1997; pp 87-101.
2. Huggins, M. L., The Viscosity of Dilute Solutions of Long-Chain Molecules. IV. Dependence on Concentration. *Journal of the American Chemical Society* **1942,** 64, (11), 2716-2718.
3. Kraemer, E. O., Molecular Weights of Celluloses and Cellulose Derivates. *Industrial and Engineering Chemistry* **1938,** 30, (10), 1200-1203.
4. Delpech, M. C.; Oliveira, C. M. F., Viscometric study of poly(methyl methacrylate-g-propylene oxide) and respective homopolymers. *Polymer Testing* **2005,** 24, (3), 381-386.
5. Terbojevich, M.; Cosani, A.; Muzzarelli, R. A. A., Molecular parameters of chitosans depolymerized with the aid of papain. *Carbohydrate Polymers* **1996,** 29, (1), 63-68.
6. Baxter, A.; Dillon, M.; Taylor, K. D. A.; Roberts, G. A. F., Improved Method for IR Determination of the Degree of *N*-Acetylation of Chitosan. *International Journal of Biological Macromolecules* **1992,** 14, (3), 166-169.

7. Van de Velde, K.; Kiekens, P., Structure analysis and degree of substitution of chitin, chitosan and dibutyrylchitin by FTIR spectroscopy and solid state C-13 NMR. *Carbohydrate Polymers* **2004,** 58, (4), 409-416.

8. Brugnerotto, J.; Lizardi, J.; Goycoolea, F. M.; Arguelles-Monal, W.; Desbrieres, J.; Rinaudo, M., An infrared investigation in relation with chitin and chitosan characterization. *Polymer* **2001,** 42, (8), 3569-3580.

9. Duarte, M. L.; Ferreira, M. C.; Marvao, M. R.; Rocha, J., An optimised method to determine the degree of acetylation of chitin and chitosan by FTIR spectroscopy. *International Journal Of Biological Macromolecules* **2002,** 31, (1-3), 1-8.

10. Jiang, X. A.; Chen, L. R.; Zhong, W., A new linear potentiometric titration method for the determination of deacetylation degree of chitosan. *Carbohydrate Polymers* **2003,** 54, (4), 457-463.

11. Roberts, G. A. F., Determination of the degree of *N*-acetylation of chitin and chitosan. In *Chitin handbook*, Muzzarelli, R.; Peter, M., Eds. European chitin society: 1997; pp 127-132.

12. Liu, D. S.; Wei, Y. N.; Yao, P. J.; Jiang, L. B., Determination of the degree of acetylation of chitosan by UV spectrophotometry using dual standards. *Carbohydrate Research* **2006,** 341, (6), 782-785.

13. Muzzarelli, R. A. A.; Rocchetti, R., Determination of the Degree of Acetylation of Chitosans by 1st Derivative Ultraviolet Spectrophotometry. *Carbohydrate Polymers* **1985,** 5, (6), 461-472.

14. Tan, S. C.; Khor, E.; Tan, T. K.; Wong, S. M., The degree of deacetylation of chitosan: advocating the first derivative UV-spectrophotometry method of determination. *Talanta* **1998,** 45, (4), 713-719.

15. Prochazkova, S.; Varum, K. M.; Ostgaard, K., Quantitative determination of chitosans by ninhydrin. *Carbohydrate Polymers* **1999,** 38, (2), 115-122.

16. Raymond, L.; Morin, F. G.; Marchessault, R. H., Degree of Deacetylation of Chitosan Using Conductometric Titration and Solid-State NMR. *Carbohydrate Research* **1993,** 246, 331-336.

17. Varum, K. M.; Anthonsen, M. W.; Grasdalen, H.; Smidsrod, O., High-Field NMR-Spectroscopy of Partially N-Deacetylated Chitins (Chitosans) .1. Determination of the Degree of N-Acetylation and the Distribution of N-Acetyl Groups in Partially N-Deacetylated Chitins (Chitosans) by High-Field NMR-Spectroscopy. *Carbohydrate Research* **1991,** 211, (1), 17-23.

18. Hirai, A.; Odani, H.; Nakajima, A., Determination of Degree of Deacetylation of Chitosan by 1H-NMR Spectroscopy. *Polymer Bulletin* **1991,** 26, (1), 87-94.

19. Lavertu, M.; Xia, Z.; Serreqi, A. N.; Berrada, M.; Rodrigues, A.; Wang, D.; Buschmann, M. D.; Gupta, A., A validated 1H-NMR method for the determination of the degree of deacetylation of chitosan. *Journal of Pharmaceutical and Biomedical Analysis* **2003,** 32, (6), 1149-1158.

20. Ottoy, M. H.; Varum, K. M.; Smidsrod, O., Compositional heterogeneity of heterogeneously deacetylated chitosans. *Carbohydrate Polymers* **1996,** 29, (1), 17-24.

21. Duarte, M. L.; Ferreira, M. C.; Marvao, M. R.; Rocha, J., Determination of the degree of acetylation of chitin materials by C-13 CP/MAS NMR spectroscopy. *International Journal of Biological Macromolecules* **2001,** 28, (5), 359-363.

22. Heux, L.; Brugnerotto, J.; Desbrieres, J.; Versali, M. F.; Rinaudo, M., Solid state NMR for determination of degree of acetylation of chitin and chitosan. *Biomacromolecules* **2000,** 1, (4), 746-751.

23. Sorlier, P.; Denuziere, A.; Viton, C.; Domard, A., Relation between the degree of acetylation and the electrostatic properties of chitin and chitosan. *Biomacromolecules* **2001,** 2, (3), 765-772.

24. Viciosa, M. T.; Dionisio, M.; Silva, R. M.; Reis, R. L.; Mano, J. F., Molecular motions in chitosan studied by dielectric relaxation spectroscopy. *Biomacromolecules* **2004,** 5, (5), 2073-2078.

25. Garcia, M. C.; Torre, M.; Laborda, F.; Marina, M. L., Rapid separation of soybean globulins by reversed-phase high-performance liquid chromatography. *Journal of Chromatography A* **1997,** 758, (1), 75-83.

26. Vaz, C. M.; Fossen, M.; van Tuil, R. F.; de Graaf, L. A.; Reis, R. L.; Cunha, A. M., Casein and soybean protein-based thermoplastics and composites as alternative biodegradable polymers for biomedical applications. *Journal of Biomedical Materials Research Part A* **2003,** 65A, (1), 60-70.

27. Vaz, C. M.; van Doeveren, P. F. N. M.; Reis, R. L.; Cunha, A. M., Soy matrix drug delivery systems obtained by melt-processing techniques. *Biomacromolecules* **2003,** 4, (6), 1520-1529.

28. Vaz, C. M.; van Doeveren, P. F. N. M.; Yilmaz, G.; de Graaf, L. A.; Reis, R. L.; Cunha, A. M., Processing and characterization of biodegradable soy plastics: Effects of crosslinking with glyoxal and thermal treatment. *Journal of Applied Polymer Science* **2005,** 97, (2), 604-610.

29. Silva, R. M.; Elvira, C.; Mano, J. F.; San Roman, J.; Reis, R. L., Influence of beta-radiation sterilisation in properties of new chitosan/soybean protein isolate membranes for guided bone regeneration. *Journal of Materials Science-Materials in Medicine* **2004,** 15, (4), 523-528.

30. Vaz, C. M.; van Doeveren, P. F. N. M.; Reis, R. L.; Cunha, A. M., Development and design of double-layer co-injection moulded soy protein based drug delivery devices. *Polymer* **2003,** 44, (19), 5983-5992.

31. Renkema, J. M. S.; Lakemond, C. M. M.; de Jongh, H. H. J.; Gruppen, H.; van Vliet, T., The effect of pH on heat denaturation and gel forming properties of soy proteins. *Journal of Biotechnology* **2000,** 79, (3), 223-230.

32. Lopez-Perez, P. M.; Marques, A. P.; da Silva, R. M. P.; Pashkuleva, I.; Reis, R. L., Effect of chitosan membranes' surface modification via plasma induced polymerization on the adhesion of Osteoblast-like cells. *Journal of Materials Chemistry* **2007,** DOI: 10.1039/b707326g.

33. Boyan, B. D.; Hummert, T. W.; Dean, D. D.; Schwartz, Z., Role of material surfaces in regulating bone and cartilage cell response. *Biomaterials* **1996,** 17, (2), 137-146.

34. Ratner, B. D., Surface properties of materials. In *Biomaterials Science*, Ratner, B. D.; Hoffman, A. S.; Schoen, F. J.; Lemons, J. E., Eds. Academic Press: 1996; pp 21-35.

35. Tamada, Y.; Ikada, Y., Fibroblast growth on polymer surfaces and biosynthesis of collagen. *Journal of Biomedical Materials Research* **1994,** 28, (7), 783-789.

36. Owens, D. K.; Wendt, R. C., Estimation Of Surface Free Energy Of Polymers. *Journal Of Applied Polymer Science* **1969,** 13, (8), 1741-1747.

37. Samuels, R. J., Solid-State Characterization Of The Structure Of Chitosan Films. *Journal of Polymer Science Part B-Polymer Physics* **1981,** 19, (7), 1081-1105.

38. Ogawa, K.; Yui, T.; Miya, M., Dependence On The Preparation Procedure Of The Polymorphism And Crystallinity Of Chitosan Membranes. *Bioscience Biotechnology And Biochemistry* **1992,** 56, (6), 858-862.

39. Ogawa, K.; Hirano, S.; Miyanishi, T.; Yui, T.; Watanabe, T., A New Polymorph Of Chitosan. *Macromolecules* **1984,** 17, (4), 973-975.

40. Zhang, Y. Q.; Xue, C. H.; Xue, Y.; Gao, R. C.; Zhang, X. L., Determination of the degree of deacetylation of chitin and chitosan by X-ray powder diffraction. *Carbohydrate Research* **2005,** 340, (11), 1914-1917.

41. Mano, J. F.; Neves, N. M.; Reis, R. L., Mechanical Characterization of Biomaterials. In *Biodegradables Systems in Tissue Engieering and Regenerative Medicine*, Reis, R. L.; San Roman, J., Eds. CRC Press: 2005; pp 127-144.

42. Lakes, R.; Saha, S., Cement Line Motion In Bone. *Science* **1979,** 204, (4392), 501-503.

43. Jantarat, J.; Palamara, J. E. A.; Lindner, C.; Messer, H. H., Time-dependent properties of human root dentin. *Dental Materials* **2002,** 18, (6), 486-493.

44. Matsuyama, H.; Kitamura, Y.; Naramura, Y., Diffusive permeability of ionic solutes in charged chitosan membrane. *Journal of Applied Polymer Science* **1999,** 72, (3), 397-404.

45. Reis, R. L.; Mendes, S. C.; Cunha, A. M.; Bevis, M. J., Processing and in vitro degradation of starch/EVOH thermoplastic blends. *Polymer International* **1997,** 43, (4), 347-352.

46. Marques, A. P.; Reis, R. L.; Hunt, J. A., The biocompatibility of novel starch-based polymers and composites: in vitro studies. *Biomaterials* **2002,** 23, (6), 1471-1478.

47. Mosmann, T., Rapid Colorimetric Assay For Cellular Growth And Survival - Application To Proliferation And Cyto-Toxicity Assays. *Journal Of Immunological Methods* **1983,** 65, (1-2), 55-63.

48. Slater, T. F.; Sawyer, B.; Strauli, U., Studies On Succinate-Tetrazolium Reductase Systems .3. Points Of Coupling Of 4 Different Tetrazolium Salts. *Biochimica Et Biophysica Acta* **1963,** 77, (3), 383-&.

49. Winblade, N. D.; Schmokel, H.; Baumann, M.; Hoffman, A. S.; Hubbell, J. A., Sterically blocking adhesion of cells to biological surfaces with a surface-active copolymer containing poly(ethylene glycol) and phenylboronic acid. *Journal Of Biomedical Materials Research* **2002,** 59, (4), 618-631.

50. Smith, P. K.; Krohn, R. I.; Hermanson, G. T.; Mallia, A. K.; Gartner, F. H.; Provenzano, M. D.; Fujimoto, E. K.; Goeke, N. M.; Olson, B. J.; Klenk, D. C., Measurement Of Protein Using Bicinchoninic Acid. *Analytical Biochemistry* **1985,** 150, (1), 76-85.

Chapter 3

Straightforward determination of the degree of *N*-acetylation of chitosan by means of 1st derivative UV spectrophotometry

3.1 Abstract

The 1st derivative UV spectrophotometry has been herein proved to be a reliable method for the determination of the degree of *N*-acetylation (DA) of chitosan samples, previously dissolved in a diluted acetic acid aqueous solution. We derived a mathematical expression that allows for the determination of DA directly from the mass concentration of chitosan solutions and the first derivative value of its UV spectra at 202 nm (the acetic acid solutions zero crossing point), over the entire range of the DA of chitosan. This avoids the use of empiric correction curves for highly deacetylated samples. A simple calibration procedure consisted on the previous determination of the 1st derivative of the molar absorptivities of the two monosaccharides that compose this series of natural copolymers. A procedure is also proposed for the accurate mass determination of the hygroscopic chitosan. The proposed approach is important to automate the routine determination of the DA at large industrial scale, especially if taking into consideration the currently available potent multiwell microplate readers, which allow measuring hundreds of samples in just few minutes.

This chapter is based on the following publication:
Ricardo M.P. da Silva; João F. Mano; Rui L. Reis. Straightforward determination of the degree of *N*-acetylation of chitosan by means of 1st derivative UV spectrophotometry (submitted).

3.2 Introduction

Chitin is a structural polysaccharide that can be found in the cell wall of fungi and in the exoskeleton of most invertebrates, of which crustaceans are currently the major source of chitin for the industry [1]. This polysaccharide is similar to cellulose, both in function, chemical structure and abundance; chitin is likely one of the most abundant natural macromolecules in the biosphere. Besides its central importance as building and structural material in a great number of biological organisms, chitin is winning a central role as a raw material in engineering and emergent technologies, in great part owing to its soluble derivative, chitosan. Given its natural abundance, it promises to be one of the future important sources of renewable materials. In fact, more or less successfully, chitin and chitosan have been proposed for a broad range of industrial applications, including wastewater treatment, food, agriculture, cosmetics, biotechnological processes and separation technologies [2], as well as, for medical applications, such as biomaterials [3, 4] and tissue engineering [5-7]. It can be also used as a precursor to produce other materials through chemical modification [8, 9].

Chitin is poly[β-(1→4)-2-acetamido-2-deoxy-D-glucopyranose]. The *N*-deacetylation processes give origin to a series of copolymers varying in the relative amounts of its comonomers, β-(1→4)-2-acetamido-2-deoxy-D-glucopyranose (GluNAc) and β-(1→4)-2-amino-2-deoxy-D-glucopyranose units(GluN) [10]. The molar fraction of the GluNAc units is defined as degree of *N*-acetylation (DA). Chitosan is the most *N*-deacetylated part of this series of copolymers. Although the criteria that defines what is chitin or chitosan based on the DA value is somewhat controversial, chitosan is often regarded as the soluble copolymers in dilute acidic solutions, oppositely to the insoluble chitin. Much more relevant than the details on the nomenclature affairs, it is that both physicochemical [11-15] and biological properties [16] of these copolymers are strongly dependent on the DA. For instance, the dependence on the DA has been shown for properties such as: the polymer conformation in solution [11, 12], the supramolecular aggregation [13] and the p*Ka* [14]; the crystallinity [15, 17] and the mechanical properties of these biopolymers films [17]; the cellular uptake and the *in vitro* cytotoxicity of its molecules and nanoparticles [16]. Therefore, the chitin/chitosan biopolymer can only be correctly defined once its DA is known. The determination of this parameter is only apparently a simple analytical problem and, actually, it has revealed to be a rather complicate issue. A myriad of methods have been proposed and tuned over the past two decades, but all of them possess inherent drawbacks and limitations. The portfolio of methods includes techniques such as Fourier transformed infrared (FTIR) spectroscopy [18-20], potentiometric titration [21], elemental analysis [21, 22], ultraviolet (UV) spectrophotometry [22-24], ninhydrin assay [25], conductometric titration [26] and a range of nuclear magnetic resonance

(NMR) spectroscopic methods, both in liquid [10, 27, 28] and solid state [29-31], just to refer to most common.

Solid state methods, which do not require the materials dissolution, present the advantage of being applicable over the entire range of DA values, both for chitin and chitosan. Solution methods are limited to soluble samples and, by definition, can only be applied to determine the DA of chitosan (for DA < 0.60, approx.).

The most widely used solid state method for the DA determination is FTIR, but some bands depend on intricate associations with the typical hydrogen-bonding networks different for each chitin polymorphic form [18]. A great number of different bands and baselines have been suggested in the literature, but important variations can often be found in the respective results [18]. This fact makes the selection of suitable bands and baselines quite problematic. Statistical studies comparing the vast number of proposed bands and baselines combinations have been employed to assist in that selection based on robust criteria [19]. Despite its drawbacks, FTIR has been often preferred because it is a quick, user-friendly and low-cost method, but mostly because it can also be applied to the insoluble chitin. Nevertheless, the construction of a specific calibration line for each particular isolation and *N*-deacetylation procedure may be necessary to obtain reliable values of DA [19]. The calibration requires the use of standards previously assessed for the DA, which, in the case of insoluble samples, is normally done using solid state ^{13}C-NMR as a reference method [18-20].

The solid state NMR methods are powerful tools for determining the DA of chitin and chitosan. The ^{15}N Solid-state Cross Polarization Magic Angle Spinning NMR (^{15}N CP/MAS NMR) has been used to evaluate the acetyl content in the case of a complex association of chitin with other polysaccharides. The combination with ^{13}C CP/MAS NMR also allowed the determination of the chitin content in the structural polysaccharides in fungus [31]. The NMR methods are often referred as the gold standard techniques and employed to calibrate other techniques or to assess their accuracy [18-21, 24-26]. The NMR does not require the use of external standards, it provides a simultaneous checking for the present of some impurities and structural information can be inferred. The experimental parameters should be carefully adjusted in order that the signal is proportional to the concentration of the all sample nuclei. Comprehensive studies on the adjustment of the NMR assay parameters have been reported both for liquid ^{1}H-NMR [27, 28] and solid state ^{13}C CP/MAS NMR [30]. Unfortunately, the related costs and complicate technical considerations hinder its widespread as routine technique at the industrial scale and in non-specialised laboratories.

Amongst the solution methods, the first derivative UV spectrophotometry presents several advantages. It was conceived by Muzzarelli and Rocchetti to provide accurate and precise results in a simple and fast way for highly deacetylated chitosan, which can be hardly analysed by techniques that record the signals of the *N*-acetyl group [23]. Furthermore, this

method is insensitive to the acetic acid concentration, under reasonable limits, a typically residue from the manufacturing process; the use of water as a reference blank reduces light absorption in the reference system, thus permitting a better signal to noise ratio [23]; it tolerates the presence of remaining traces of protein contaminants [24]; calibration does not rely on other determinations of the DA of standard samples; and it only requires very small amounts of sample, simple reagents and instrumentation. The main disadvantages of the method are the requirement of an accurate determination of the weight, particularly difficult for the highly hygroscopic chitosan samples, and the need of using an empiric correction curve for DA<0.11 [23], due to the contribution of the GluN to the 1st derivative signal.

The GluN and GluNAc are two far UV chromophoric groups, which contribute in a simple addictive way to the total absorbance of the material at a particular wavelength, since they do not interact within the polymer in a manner that would affect absorption of UV radiation [22]. Based on this evidence Liu *et al* derived a linear relationship between the absorbance divided by the total molar concentration of the monomers and the DA. The main advantage of such approach is the absence of the necessity for corrections at lower DA [22]. In our approach, we derived a similar equation that combines the advantages and robustness of the 1st derivative method, with the exact mathematical description of the DA in function of the 1st derivative of the absorbance at 202 nm and the mass concentration of the polysaccharide solutions. It was also defined a solid criterion for the absorbance range within which the method remains valid. We believe that the proposed procedure, combining the accuracy and precision of the 1st derivative UV spectrophotometry with a straightforward determination of the DA, constitutes a breakthrough in the reliable determination of the DA of chitosan samples at a large industrial scale, specially if taking into consideration the currently available potent multiwell microplate readers, which can allow the fast measurement of hundreds of samples in just few minutes.

3.3 Materials and methods

3.3.1 Purification and characterisation of chitosan

Chitosan raw-materials from crab shells were purchased from Sigma-Aldrich (USA). The chitosan samples were purified once in an amount sufficient to perform all the experimental work reported, by re-precipitation in sodium hydroxide. First, the chitosan was dissolved in an aqueous acetic acid solution (1%) at ~1% (w/v). The insoluble material was removed by filtration with Whatman® ashless filter paper (20-25 μm). The obtained clear solution was

precipitated adding a NaOH solution (final pH ~ 8). The formed white gel was sieved to remove the exuded liquid and thoroughly rinsed with distilled water, until no changes on the pH were detected. The chitosan gel was further washed with ethanol, freeze-dried, ground to powder and dried at 60ºC overnight. Two different chitosan raw-materials varying in the degree of acetylation were labelled according to their nominal DA values as DA05 and DA20 (see Table 1). The average molecular weight was of found to be 790 kDa for DA05 and 770 kDa for DA20 by viscometry in CH_3COOH 0.5 M/ $NaCH_3COO$ 0.2 M, according to the Mark-Houwing theory ($k = 3.5 \times 10^{-4}$; $a = 0.76$) [32].

3.3.2 Preparation of chitosan samples with several DA by selective *N*-acetylation

The chitosan sample DA20 (5 g) was dissolved in 1% (w/v) of aqueous acetic acid (50 ml). A variable volume of acetic anhydride was mixed with 50 ml of ethanol, added slowly to the chitosan solution and stirred overnight. The ratio of the acetic anhydride to the chitosan GluN units was adjusted to obtain samples with different DA. The solutions were precipitated with acetone, followed by diethyl ether and dried under vacuum. The acetylated samples were then neutralised in 1N NH_4OH aqueous solution, thoroughly washed with distilled water and freeze-dried. The resultant sponges were milled with liquid nitrogen and the obtained flakes were dried at 80ºC under reduced pressure. The *N*-acetylated chitosan Fourier-transform infrared (FTIR) spectra were recorded in an IRPrestige 21 FTIR spectrophotometer (36 scans, resolution 4 cm^{-1}) from the solvent cast films, previously neutralised in 1N NH_4OH in water/methanol (1:3) and thoroughly dried under vacuum.

3.3.3 Thermogravimetric analysis (TGA)

In one of our previous works [33], we found that chitosan membranes contain residual moisture irrespective to the drying procedure. The hypothesis that this residual moisture could be caused by a fast water uptake from the atmosphere would make the accurate determination of the chitosan weight a tricky procedure. The water content of the chitosan samples was estimated by TGA (TA Instruments, model TGA Q500), immediately after being weighted for the UV determination of the DA. The thermograms were obtained under an atmosphere of flowing nitrogen. The chitosan powder (4-10 mg) was first heated at a 10ºC/min ramp, which was followed by an isothermal step of 20 min at 110ºC to assure complete dryness of the samples. Moisture content (*MC*(%)) was considered to be the weight loss at that time point. The temperature programme also included a cooling down period, under the same nitrogen

stream. Then, the dried sample was exposed to the air atmosphere and weighted again at preset time periods, by closing temporarily the TGA apparatus furnace. This procedure allowed us to estimate the time necessary for the dried chitosan materials to recover the initial water content when exposed to the atmospheric moisture.

3.3.4 Ultraviolet (UV) 1st derivative spectrophotometry

The monosaccharides, GluN (D-glucosamine hydrochloride, >99%, Mr 215.6) and GluNAc (>99%, Mr 221.2), were purchased from Sigma-Aldrich. The GluNAc was stored in the freezer and kept in a vacuum desiccator for at least 2 hours before use. One stock solution of acetic acid (AcOH) 0.1 M was prepared and another AcOH 0.01 M stock solution was obtained diluting the previous one. Standard monosaccharide solutions were prepared dissolving each sugar powder in acetic acid 0.01 M at several molarities, in the range of 3 mM to 0.2 M for GluN and from 0.01 mM up to 1 mM for GluNAc.

For the determination of the DA, chitosan samples were dried over vacuum at 80ºC. The dried chitosan powder uptakes the water from the atmosphere at a rate that is high enough to provoke water content shifts within two consecutive weightings of the same sample, as previously verified by means of thermogravimetric analysis (TGA). For this reason, chitosan samples were previously conditioned at the atmospheric moisture for 10 min and subsequently weighted. After that, the chitosan samples were subjected to TGA to determine the water content, as described above. The accurately weighted (10.0 mg) chitosan samples were dissolved in 2.00 ml of AcOH 0.1 M and diluted 10-fold with distilled water to obtain a final AcOH concentration of 0.01 M (chitosan was not dissolved directly in AcOH 0.01M, since it would be more time consuming). When required, further dilutions were performed using the AcOH 0.01 M stock solution to keep the AcOH concentration at this value. All solutions, including the AcOH 0.01M, were prepared from the same AcOH 0.1M stock solution. All the spectra (range 200-240 nm, step 1 nm) were recorded with a Bio-Tek® Synergy^{TM} HT microplate reader in a 96 well quartz plate from Hellma® using 300 µl of each solution. The empty quartz plate was read before each set of experiments and subtracted from measured spectra to attenuate possible differences in the residual absorbance, arising from an eventual drift in the plate thickness, scratches or occasional dirtiness. Distilled water was used as a blank. All measurements were preformed at least in triplicate.

3.3.5 Determination of the DA by ^{1}H-NMR

Three different solutions of each chitosan sample were prepared by stirring 10 mg of chitosan in 1 ml of 0.4% (w/v) DCl in D_2O solution at room temperature. In order to minimise the *N*-deacetylation catalysed by the presence of deuterium chloride, only freshly prepared solutions were used. The ^{1}H-NMR spectra were acquired in a Varian Unity Plus (300 MHz) spectrometer at 70ºC, temperature at which the solvent signal (HOD) does not interfere with the chitosan peaks. The acquisition (64 transients) started after 10 min, considered to be enough to reach the thermal equilibrium. The pulse repetition delay, 6 s, and the acquisition time, 2 s, were set to assure complete relaxation of the nuclei before each pulse application. This procedure (repetition time of 8 s) guarantees that the relative intensities of the resonances correlate with the exact number of nuclei originating that signal [28].

3.4 Results and discussion

3.4.1 Preparation of chitosan samples with different DA over the entire solubility range

The chitosan samples, both purified raw-materials (DA05 and DA20) and *N*-acetylated samples, are depicted in Table 1 and cover the entire DA range of the polysaccharide solubility. The ratio of acetic anhydride to GluN units was chosen in order to get samples with differences of around 10% between each DA value. The use of aqueous alcoholic acetic acid solutions for the reaction of chitosan with carboxylic anhydrides has been shown to avoid the *O*-acylation side reaction [34, 35]. The selective *N*-acetylation was confirmed by FTIR spectra, where the absorption bands typical of the *O*-acetyl groups were absent, ~1750 cm^{-1} (C=O) and ~1240 cm^{-1} (C-O) [34], in addiction to those assigned to the *N*-acetyl groups at ~1655 cm^{-1} (C=O) and ~1560 cm^{-1} (N-H).

The molecular weight was reported to not vary considerably if the *N*-acetylation is performed under mild conditions [14], similar to the ones used in this study. For this reason and since the molecular weight should obviously not influence the DA measure, it was only determined for the original purified raw-materials.

Table 3.1 Degree of *N*-acetylation (DA) by the 1st derivative UV spectrophotometry and by liquid phase ^{1}H-NMR using equations 3.16, 3.17 and 3.18; coefficient of variation (CV = σ / DA x 100), where σ is the standard deviation of three measurements; and moisture content (MC)

Sample	UV		^{1}H-NMR (3.16)		^{1}H-NMR (3.17)		^{1}H-NMR (3.18)		MC(%)
	DA	CV(%)	DA	CV(%)	DA	CV(%)	DA	CV(%)	
DA05	0.067	2.0	0.049	6.9	0.052	2.7	0.101	40.6	7.3
DA20	0.216	1.3	0.187	4.8	0.200	5.4	0.251	6.4	7.1
DA30 [a]	0.326	0.8	0.279	2.0	0.314	4.0	0.388	11.9	8.2
DA40 [a]	0.415	3.2	0.372	1.0	0.435	3.6	0.516	6.9	4.5
DA50 [a]	0.514	0.0	0.506	3.6	0.526	1.5	0.543	5.2	6.2
DA60 [a]	0.613	0.6	0.556	1.4	0.592	2.2	0.617	3.8	10.0

[a] *N*-acetylated from DA20 sample

3.4.2 Determination of the 1st derivative of the monosaccharides molar absorptivities

The high absorbance of the acetic acid at the working concentration disturbs the determination of both GluNAc (Figure 3.2) and GluN (Figure 3.3) residues, when using the zero order UV spectra (see also Figure 3.1a). The 1st derivative spectra of the AcOH solutions, reported in Figure 3.1b, share a common point at around 202 nm for concentrations from 0.005M up to 0.03 M, designated as the zero crossing point by Muzzarelli and Rocchetti [23]. In this sense, at the zero crossing point, the determination of the monosaccharides concentration should be relatively insensitive to fluctuations in the acetic acid concentration. It also corresponds to a stronger signal of the monosaccharides, if compared to the quite low contribution of the acetic acid, as can be observed in the Figure 3.1b.

The monosaccharides individual calibration curves were easily drawn through a linear regression between the concentration and the 1st derivative UV signal arising either from GluNAc (Figure 3.2) or GluN (Figure 3.3). This can be deduced from the Beer-Lambert law for diluted solutions, which correlates the concentration (*C*) with the absorbance (*A*), for a given wavelength (λ):

$$A(\lambda) = \varepsilon(\lambda) l C \qquad (3.1)$$

where ε is the molar absorptivity and *l*, the optical path length. Since both *l* and *C* are independent on the wavelength:

$$\frac{dA}{d\lambda} = \frac{d\varepsilon}{d\lambda} lC \qquad \text{or} \qquad \frac{dA}{d\lambda} = \varepsilon'(\lambda) lC \tag{3.2}$$

It should be noticed that the acetic acid gives also a signal at λ = 202 nm, thus the expressions should be corrected by:

$$A - A_{\text{AcOH}} = \varepsilon\, lC \tag{3.3}$$

$$\frac{dA}{d\lambda} - \left(\frac{dA}{d\lambda}\right)_{\text{AcOH}} = \varepsilon'\, lC \tag{3.4}$$

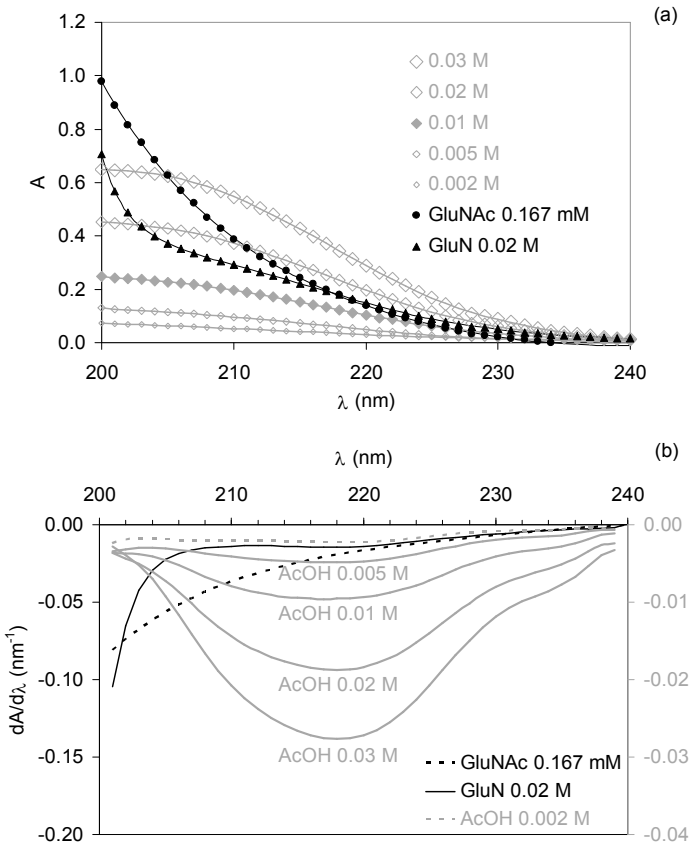

Figure 3.1 Zero order **(a)** and first derivative **(b)** UV spectra of the acetic acid (AcOH) solutions with different concentrations (grey) and of the monosaccharides standards (black) dissolved in AcOH 0.01M (closed dots). Each spectrum represents the average of three independent data sets.

In Figure 3.2c it is possible to observe that the GluNAc concentration (0.167 mM) above which Beer-Lambert law lost validity (equations 3.1 and 3.3 with ε no longer independent on the concentration), matches the same limit value observed for equation 3.4 (Figure 3.2b), as expected. The validity limit is regarded as the concentration above of which the linear correlation is lost ($r^2 < 0.99$). This linearity limit is not a problem concerning the estimation of

the GluN residues (20 mM), because this limit is never reached in the determination of the DA, even considering the maximum concentration of chitosan used and a theoretical DA of 0 (maximum GluN molar fraction).

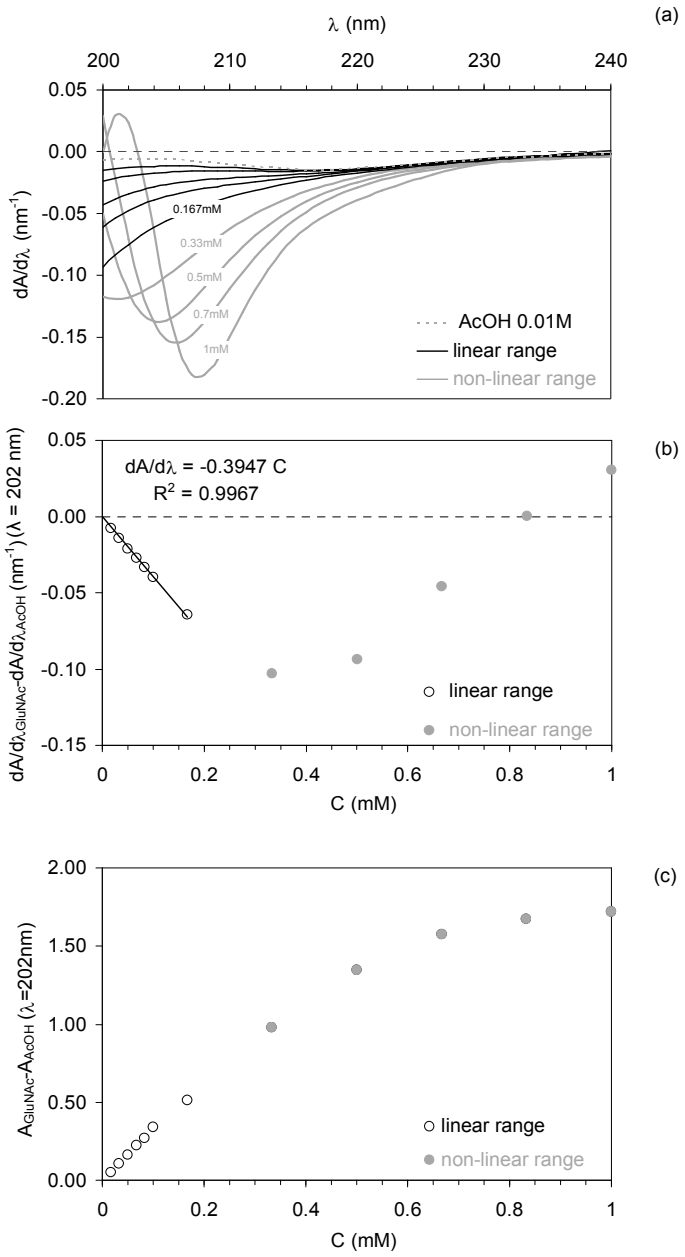

Figure 3.2 First derivative UV spectra **(a)** of GluNAc at several concentrations (0.0167 to 1 mM) dissolved in AcOH 0.01 M; First derivative **(b)** and zero order **(c)** UV spectral value at λ = 202 nm (after subtracting the contribution of the AcOH 0.01 M) in function of the GluNAc concentration. Each spectrum represents the average of three independent data sets.

On the other hand, the 1st derivative spectra of GluNAc surfer a continuous peak deviation as the concentration increases above the linearity limit (Figure 3.2a) and, as a consequence, the $dA/d\lambda$ at λ = 202 nm reaches a minimum at around 0.4 mM and start to increase again (Figures 3.2a and 3.2b). Therefore, one single measurement of $dA/d\lambda$ at λ = 202 nm could be assigned to two very different GluNAc concentrations. This would pose a difficulty to determine the DA of chitosan without ambiguity and would require the analysis of the all spectrum. In order to assure that the GluNAc concentration is within the linearity range one may alternatively use the following practical criterion:

$$\left(A - A_{AcOH}\right) < 0.5 \qquad (3.5)$$

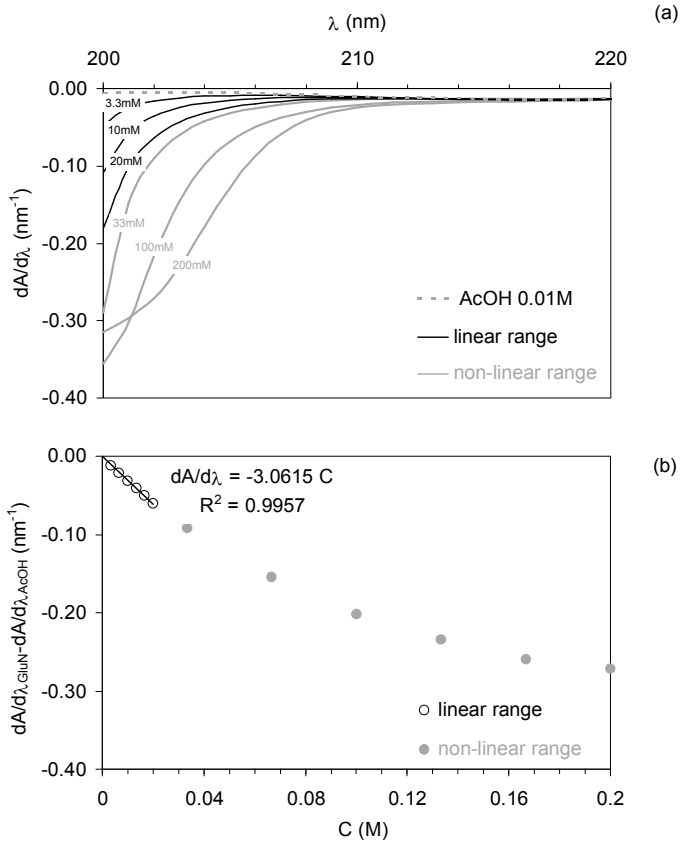

Figure 3.3 (a) First derivative UV spectra of GluN at several concentrations (3.33 to 200 mM) dissolved in AcOH 0.01 M; **(b)** First derivative UV spectral value at λ = 202 nm (after subtracting the contribution of the AcOH 0.01 M) in function of the GluN concentration. Each spectrum represents the average of three independent data sets.

Since the GluNAc absorbance at 202 nm is an increasing monotonic function of the concentration (Figure 3.2c), each absorbance value is unequivocally assigned to one

concentration value of the GluNAc. In this way, it is still possible to only use the spectral region in the neighbourhood of 202 nm (few data points) for the routine determination of the DA of chitosan samples.

Denoting the 1st derivative of the GluNAc and GluN molar absorptivities as ε_a and ε_g, respectively, the linear regression of the experimental data gives that:

$\varepsilon_a^{'} \, l = -394.7 \, \mathrm{M}^{-1}$ and $\varepsilon_g^{'} \, l = -3.061 \, \mathrm{M}^{-1}$

The optical path length (*l*) was estimated (approx. 0.93 cm) from the geometrical features of the microplate wells and the solution volume (300 µl) added to each well. The solution shape was considered to be roughly cylindrical, disregarding the meniscus concavity.

3.4.3 Determination of the DA by means of the 1st derivative UV spectrophotometry

The method is based on the assumption that the molar absorptivities of both GluN (ε_a) and GluNAc (ε_g) chromophoric groups does change when they are covalently bound through β-(1→4) glycosidic linkages. Being so, the monosaccharides contribute in an addictive way to the total absorbance, which in the presence of acetic acid can be expressed as:

$$A = \varepsilon_a \, lC_a + \varepsilon_g \, lC_g + \varepsilon_{AcOH} \, lC_{AcOH} \tag{3.6}$$

with concentrations (*C)* in mol/l. Since the optical path length (*l*) and the concentration (*C*) are independent on the wavelength, differentiating equation 3.6, it gives:

$$\frac{dA}{d\lambda} - \left(\frac{dA}{d\lambda}\right)_{AcOH} = \varepsilon_a^{'} lC_a + \varepsilon_g^{'} lC_g \tag{3.7}$$

The DA, defined as the molar fraction of the GluNAc units, can be expressed as the ratio between the GluNAc concentration and the total monosaccharides concentration (C_t):

$$\mathrm{DA} = \frac{C_a}{C_a + C_g} = \frac{C_a}{C_t} \tag{3.8}$$

Combining equations 3.7 and 3.8 and rearranging, it follows that:

$$\frac{1}{C_t}\left[\frac{dA}{d\lambda} - \left(\frac{dA}{d\lambda}\right)_{AcOH}\right] = \left(\varepsilon_a^{'} l - \varepsilon_g^{'} l\right)\mathrm{DA} + \varepsilon_g^{'} l \tag{3.9}$$

This equation is the basis of the method proposed herein. It is interesting to notice that the method developed by Muzzarelli and Rocchetti [23] is a particular case of the last equation. If fact, since $\left|\varepsilon_a^{'}\right| >> \left|\varepsilon_g^{'}\right|$ equation 3.9 can be simplified:

$$\frac{1}{C_t}\left[\frac{dA}{d\lambda} - \left(\frac{dA}{d\lambda}\right)_{AcOH}\right] \approx \left(\varepsilon_a^{'} l\right)\mathrm{DA} + \varepsilon_g^{'} l \tag{3.10}$$

If DA is not too small (those authors found that for DA > 0.11 the GluN does not interfere with the GluNAc determination), it can be further simplified, giving:

$$\left[\frac{dA}{d\lambda}-\left(\frac{dA}{d\lambda}\right)_{AcOH}\right]\approx\left(\varepsilon_a^{'}\ l\right)\mathrm{DA}\ C_t=\varepsilon_a^{'}\ l\ C_a \tag{3.11}$$

For DA < 0.11, Muzzarelli and Rocchetti [23] proposed a correction curve.

The molar concentration of both pyranosyl units (C_t) within a chitosan sample can not be achieved without knowing the DA. Thus, it is more convenient to express the copolymer concentration in terms of solute mass ($\overline{C_t}$) in g/l, which is defined experimentally. These two concentration values are related by the next equation:

$$\frac{\overline{C_t}}{C_t}=\left(M_a-M_g\right)\mathrm{DA}+M_g \tag{3.12}$$

where M_a and M_g are the molecular weights of the GluNAc and GluN units within the copolymer. Combining equations 3.9 and 3.12, it gives:

$$\frac{1}{\overline{C_t}}\left[\frac{dA}{d\lambda}-\left(\frac{dA}{d\lambda}\right)_{AcOH}\right]=\frac{\left(\varepsilon_a^{'}l-\varepsilon_g^{'}l\right)\mathrm{DA}+\varepsilon_g^{'}l}{\left(M_a-M_g\right)\mathrm{DA}+M_g} \tag{3.13}$$

and, rearranging,

$$\mathrm{DA}=\frac{\varepsilon_g^{''}l-\frac{M_g}{\overline{C_t}}\left(\frac{dA}{d\lambda}-\left(\frac{dA}{d\lambda}\right)_{AcOH}\right)}{\frac{M_a-M_g}{\overline{C_t}}\left(\frac{dA}{d\lambda}-\left(\frac{dA}{d\lambda}\right)_{AcOH}\right)-\left(\varepsilon_a^{'}l-\varepsilon_g^{'}l\right)} \tag{3.14}$$

The values of the 1st derivative of the molar absorptivities have been determined in a separate experiment (calibration). Also, the molecular weight of the monosaccharides within the copolymer are easily calculated (M_a = 203 g/mol and M_g = 161 g/mol). Therefore, equation 3.14 allows a straightforward determination of the DA, known the 1st derivative UV spectral signal at 202 nm of the chitosan solution at a suitable concentration. The results obtained for the different chitosan samples are depicted in Table 3.1. The determination of the mass concentration ($\overline{C_t}$) requires the accurate measurement of the chitosan weight. Since chitosan is very hygroscopic, concerns can be raised regarding the accuracy of this measurement. This issue was addressed by means of TGA and it is detailed in the following section.

3.4.4 Determination of the moisture content of chitosan

In order to assure the accurate chitosan mass measurement, the water uptake of thoroughly dried chitosan samples from the atmosphere was assessed under similar conditions used to weight the samples. It was found that the completely dried chitosan samples (after a TGA drying cycle) recover the initial moisture content in less than 10 min (see Figure 3.4b), when exposed to the room atmosphere. A longer exposition time point would be required to show that the typical equilibrium plateau has been already reached. Nevertheless, the total recovery of the initial moisture content value was considered as an evidence of that the 10 min exposition to room atmosphere gives a value that for our purpose was close enough to the equilibrium.

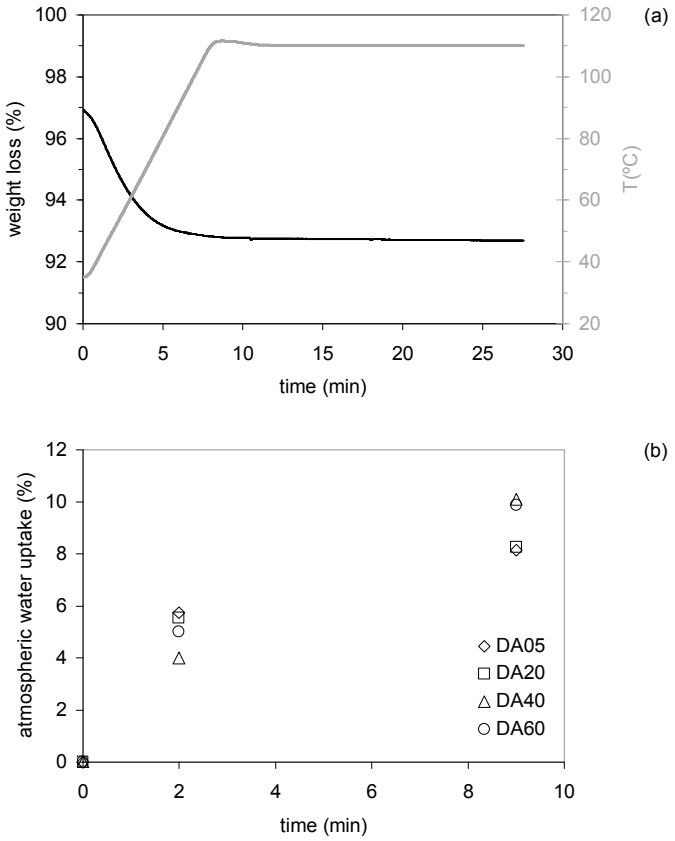

Figure 3.4 (a) Thermogram of DA05 conditioned at the room atmosphere for 10 min and accurately weighted for the UV spectra determination; **(b)** Water uptake (ratio between the weight increment and the initial dry weight) of the samples exposed to the room atmosphere during different times after a TGA drying cycle.

The fast atmospheric water uptake, calculated as the ratio between the weight increment and the initial dry weight, is enough to provoke water content shifts within two consecutive weightings of the same sample. Based on this result, an alternative procedure was adopted. Thoroughly dried samples were conditioned at the air atmosphere for around 10 min and accurately weighted (*W*). After that, the moisture content (MC(%)) of the samples was determined by TGA (see Figure 3.4a and Table 3.1) and the mass concentration was corrected according to equation 3.15.

$$\overline{C_t} = \frac{W \times \left(1 - MC(\%)/100\right)}{V} \qquad (3.15)$$

Although the difficulty of determining the accurate weight of a chitosan sample is often considered one of the drawbacks of the UV spectrophotometry based methods, we found that the DA value is relatively insensitive to a small drift in the moisture content. We simulate an absolute error of ±1% in the moisture content of our samples and encountered a relative error associated to the DA of ±1.3%. Besides, the proposed procedure should provide reliable chitosan weight determinations.

3.4.5 Comparison with the DA as determined by liquid phase ^{1}H-NMR

Proton chemical shifts (δ), relative to 3-(trimethylsilyl)propionic acid, were assigned as reported in the literature [27]. Data for the sample DA30: ^{1}H-NMR (D_2O, DCl) δ 2.05 (s, HAc of GluNAc), 3.20 (s, H2 of GluN), 3.6-4.0 (m, H2 of GluNAc and H3, H4, H5, H6, H6' of both monomers), 4.61 (s, H1a of GluNAc) and 4.90 (s, H1g of GluN) (see Figure 3.5).

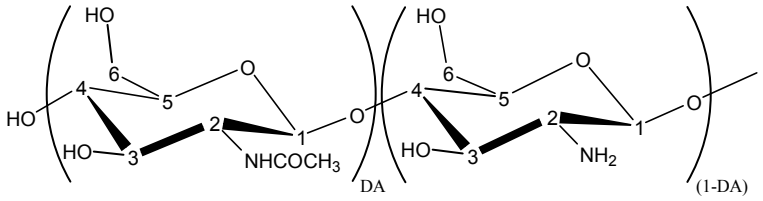

Figure 3.5 Chemical structure of chitosan.

The comparison between the DA values calculated using different combinations of peaks, can be used as an indicator of the ^{1}H-NMR method consistency. We have used several methods to calculate the DA, namely the method proposed by Hirai *et al* [27], which makes use of the peak areas from the protons H2, H3, H4, H5, H6, H6' to estimate the sum of both monomers and the signal arising from the acetyl group protons (HAc) to the amount of GluNAc:

$$DA = \frac{HAc/3}{(H2 + H3 + H4 + H5 + H6 + H6')/6} \quad (3.16)$$

The method proposed by Lavertu *et al* [28] uses the peak of proton H1g to estimate the amount of GluN and the signal from the acetyl group protons (HAc) to estimate the amount of GluNAc:

$$DA = 1 - \frac{H1g}{H1g + HAc/3} \quad (3.17)$$

We also calculated the DA using a combination of the two previous equations, as it follows:

$$DA = 1 - \frac{H1g}{(H2 + H3 + H4 + H5 + H6 + H6')/6} \quad (3.18)$$

The results obtained from these different calculation methods showed that, although the ^{1}H-NMR is regarded as having a good internal consistency, the determination of DA may be somewhat systematically affected by the choice of the peaks to be used in that calculation and in the way those peaks are combined to estimate the GluN and GluNAc quantities. None of the calculation methods make use of the peak assigned to the H1a proton of the GluNAc, because of its lower intensity for low DA values and, simultaneously, due to its proximity to the HOD signal. These equations represent the possible combinations of the other different sets of well resolved peaks (excluding H1a).

The coefficient of variation, which stands for the ratio between the standard deviation and the averaged DA value, was found to be considerably lower for the UV determination, confirming the higher precision of the method proposed in this work. The DA values achieved for the different chitosan samples using the 1st derivative UV spectrophotometry method were plotted against the values achieved for the same samples using each one of the calculation methods based on the ^{1}H-NMR spectra (Figure 3.6). Ideally, this representation should give a straight-line with slope 1 and y-intercept 0. In this respect, the equation 3.17 gives the best match with the UV method. However, any irrefutable conclusions can be drawn with respect to the accuracy, just based on this result, because we do not know what equation gives the most accurate results from the ^{1}H-NMR data. Especially when the reasons behind the discrepancy between the results are not known and logic criteria can not be established to disregard some of the equations.

On the other hand, albeit the average between the three methods is solely an algebraic combination of the three equations and do not assure that a value closer to the actual DA is obtained, the correlation between the averaged ^{1}H-NMR DA values and the UV method is noteworthy. The respective linear regression gives a correlation factor R^2=0.993 and a straight-line with slope 0.986 and y-intercept 0.0074. It should be noticed that the 1st derivative UV spectrophotometry and the liquid state ^{1}H-NMR are independent techniques, in

the sense that the calibration of the former does not rely on the DA values of chitosan standards obtained from other techniques, neither the ^{1}H-NMR required any calibration. Hence, the good correlation between both techniques constitutes a strong indication of the good accuracy of the 1st derivative UV spectrophotometry method over the whole DA range of the chitosan solubility and using equation 3.14, if a reliable measure of the chitosan weight is undertaken.

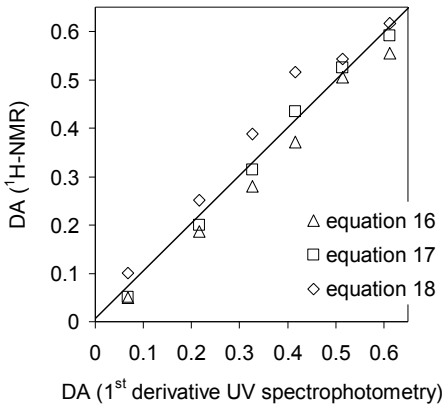

Figure 3.6 DA obtained by the proposed UV spectrophotometric method (equation 3.14) vs DA calculated from the ^{1}H-NMR data (equations 3.16 to 3.18). The straight-line represents the linear regression between the DA determined by the UV method and the average of each of the three different experimental values obtained for the same sample by ^{1}H-NMR ($y = 0.9868x + 0.0063$; $R^2 = 0.993$).

3.5 Conclusions

The 1st derivative UV spectrophotometry is a robust, accurate and precise technique for the determination of the DA of soluble chitosan samples. It presents several advantages such as: it is relatively tolerant to the presence of residual acetic acid and protein contaminants; it only requires a small amount of sample, simple reagents and equipments; and the high value of the molar absorptivity 1st derivative of the GluNAc should assure a good accuracy on the determination of the GluNAc residues even at very low concentrations (high DA). We derived a mathematical expression that described the DA as a function of the 1st derivative signal at 202 nm and the mass concentration of the polysaccharide solution, avoiding the use of empiric correction curves for the determination of the DA of highly deacetylated samples. The values of the DA for several chitosan samples on the entire range of the copolymer solubility confirmed the good precision of the method with typical coefficients of variation

around 1%. The comparison with an optimised ^{1}H-NMR determination reiterates the expected fine accuracy of the 1st derivative UV spectrophotometry.

3.6 Acknowledgments

This work was partially supported by the Portuguese Foundation for Science and Technology (FCT), through funds from the POCTI and/or FEDER programmes and through the scholarship SFRH/BD/6862/2001 granted to Ricardo M. P. da Silva. This work was carried out under the scope of the European NoE EXPERTISSUES (NMP3-CT-2004-500283) and also partially supported by the European Union funded STREP Project HIPPOCRATES (NMP3-CT-2003-505758). The authors thank Elisa Pinto for her kindly help and advice on setting up the ^{1}H-NMR instrumentation conditions.

3.7 References

1. Cauchie, H. M., Chitin production by arthropods in the hydrosphere. *Hydrobiologia* **2002,** 470, (1-3), 63-96.

2. Kumar, M. N. V. R., A review of chitin and chitosan applications. *Reactive & Functional Polymers* **2000,** 46, (1), 1-27.

3. Silva, R. M.; Silva, G. A.; Coutinho, O. P.; Mano, J. F.; Reis, R. L., Preparation and characterisation in simulated body conditions of glutaraldehyde crosslinked chitosan membranes. *Journal of Materials Science-Materials in Medicine* **2004,** 15, (10), 1105-1112.

4. Lopez-Perez, P. M.; Marques, A. P.; da Silva, R. M. P.; Pashkuleva, I.; Reis, R. L., Effect of chitosan membranes' surface modification via plasma induced polymerization on the adhesion of Osteoblast-like cells. *Journal of Materials Chemistry* **2007,** 17, (38), 4064-4071.

5. Baran, E. T.; Tuzlakoglu, K.; Salgado, A. J.; Reis, R. L., Multichannel mould processing of 3D structures from microporous coralline hydroxyapatite granules and chitosan support materials for guided tissue regeneration/engineering. *Journal of Materials Science-Materials in Medicine* **2004,** 15, (2), 161-165.

6. Tuzlakoglu, K.; Alves, C. M.; Mano, J. F.; Reis, R. L., Production and characterization of chitosan fibers and 3-D fiber mesh scaffolds for tissue engineering applications. *Macromolecular Bioscience* **2004,** 4, (8), 811-819.

7. Silva, G. A.; Ducheyne, P.; Reis, R. L., Materials in particulate form for tissue engineering. 1. Basic concepts. *Journal of Tissue Engineering and Regenerative Medicine* **2007,** 1, (1), 4-24.

8. Prabaharan, M.; Mano, J. F., Stimuli-responsive hydrogels based on polysaccharides incorporated with thermo-responsive polymers as novel biomaterials. *Macromolecular Bioscience* **2006,** 6, (12), 991-1008.

9. Jayakumar, R.; Prabaharan, M.; Reis, R. L.; Mano, J. F., Graft copolymerized chitosan - present status and applications. *Carbohydrate Polymers* **2005,** 62, (2), 142-158.

10. Varum, K. M.; Anthonsen, M. W.; Grasdalen, H.; Smidsrod, O., High-Field NMR-Spectroscopy of Partially N-Deacetylated Chitins (Chitosans) .1. Determination of the Degree of N-Acetylation and the Distribution of N-Acetyl Groups in Partially N-Deacetylated Chitins (Chitosans) by High-Field NMR-Spectroscopy. *Carbohydrate Research* **1991,** 211, (1), 17-23.

11. Lamarque, G.; Lucas, J. M.; Viton, C.; Domard, A., Physicochernical behavior of homogeneous series of acetylated chitosans in aqueous solution: Role of various structural parameters. *Biomacromolecules* **2005,** 6, (1), 131-142.

12. Sorlier, P.; Rochas, C.; Morfin, I.; Viton, C.; Domard, A., Light scattering studies of the solution properties of chitosans of varying degrees of acetylation. *Biomacromolecules* **2003,** 4, (4), 1034-1040.

13. Sorlier, P.; Viton, C.; Domard, A., Relation between solution properties and degree of acetylation of chitosan: Role of aging. *Biomacromolecules* **2002,** 3, (6), 1336-1342.

14. Sorlier, P.; Denuziere, A.; Viton, C.; Domard, A., Relation between the degree of acetylation and the electrostatic properties of chitin and chitosan. *Biomacromolecules* **2001,** 2, (3), 765-772.

15. Rinaudo, M., Chitin and chitosan: Properties and applications. *Progress in Polymer Science* **2006,** 31, (7), 603.

16. Huang, M.; Khor, E.; Lim, L. Y., Uptake and cytotoxicity of chitosan molecules and nanoparticles: Effects of molecular weight and degree of deacetylation. *Pharmaceutical Research* **2004,** 21, (2), 344-353.

17. Hwang, K. T.; Kim, J. T.; Jung, S. T.; Cho, G. S.; Park, H. J., Properties of chitosan-based biopolymer films with various degrees of deacetylation and molecular weights. *Journal of Applied Polymer Science* **2003,** 89, (13), 3476-3484.

18. Van de Velde, K.; Kiekens, P., Structure analysis and degree of substitution of chitin, chitosan and dibutyrylchitin by FT-IR spectroscopy and solid state C-13 NMR. *Carbohydrate Polymers* **2004,** 58, (4), 409-416.

19. Duarte, M. L.; Ferreira, M. C.; Marvao, M. R.; Rocha, J., An optimised method to determine the degree of acetylation of chitin and chitosan by FTIR spectroscopy. *International Journal Of Biological Macromolecules* **2002,** 31, (1-3), 1-8.

20. Brugnerotto, J.; Lizardi, J.; Goycoolea, F. M.; Arguelles-Monal, W.; Desbrieres, J.; Rinaudo, M., An infrared investigation in relation with chitin and chitosan characterization. *Polymer* **2001,** 42, (8), 3569-3580.

21. Jiang, X. A.; Chen, L. R.; Zhong, W., A new linear potentiometric titration method for the determination of deacetylation degree of chitosan. *Carbohydrate Polymers* **2003,** 54, (4), 457-463.

22. Liu, D. S.; Wei, Y. N.; Yao, P. J.; Jiang, L. B., Determination of the degree of acetylation of chitosan by UV spectrophotometry using dual standards. *Carbohydrate Research* **2006,** 341, (6), 782-785.

23. Muzzarelli, R. A. A.; Rocchetti, R., Determination Of The Degree Of Acetylation Of Chitosans By 1st Derivative Ultraviolet Spectrophotometry. *Carbohydrate Polymers* **1985,** 5, (6), 461-472.

24. Tan, S. C.; Khor, E.; Tan, T. K.; Wong, S. M., The degree of deacetylation of chitosan: advocating the first derivative UV-spectrophotometry method of determination. *Talanta* **1998,** 45, (4), 713-719.

25. Prochazkova, S.; Varum, K. M.; Ostgaard, K., Quantitative determination of chitosans by ninhydrin. *Carbohydrate Polymers* **1999,** 38, (2), 115-122.

26. Raymond, L.; Morin, F. G.; Marchessault, R. H., Degree of Deacetylation of Chitosan Using Conductometric Titration and Solid-State NMR. *Carbohydrate Research* **1993,** 246, 331-336.

27. Hirai, A.; Odani, H.; Nakajima, A., Determination of Degree of Deacetylation of Chitosan by 1H-NMR Spectroscopy. *Polymer Bulletin* **1991,** 26, (1), 87-94.

28. Lavertu, M.; Xia, Z.; Serreqi, A. N.; Berrada, M.; Rodrigues, A.; Wang, D.; Buschmann, M. D.; Gupta, A., A validated 1H-NMR method for the determination of the degree of deacetylation of chitosan. *Journal of Pharmaceutical and Biomedical Analysis* **2003,** 32, (6), 1149-1158.

29. Ottoy, M. H.; Varum, K. M.; Smidsrod, O., Compositional heterogeneity of heterogeneously deacetylated chitosans. *Carbohydrate Polymers* **1996,** 29, (1), 17-24.

30. Duarte, M. L.; Ferreira, M. C.; Marvao, M. R.; Rocha, J., Determination of the degree of acetylation of chitin materials by C-13 CP/MAS NMR spectroscopy. *International Journal Of Biological Macromolecules* **2001,** 28, (5), 359-363.

31. Heux, L.; Brugnerotto, J.; Desbrieres, J.; Versali, M. F.; Rinaudo, M., Solid state NMR for determination of degree of acetylation of chitin and chitosan. *Biomacromolecules* **2000,** 1, (4), 746-751.

32. Terbojevich, M.; Cosani, A.; Muzzarelli, R. A. A., Molecular parameters of chitosans depolymerized with the aid of papain. *Carbohydrate Polymers* **1996,** 29, (1), 63-68.

33. Viciosa, M. T.; Dionisio, M.; Silva, R. M.; Reis, R. L.; Mano, J. F., Molecular motions in chitosan studied by dielectric relaxation spectroscopy. *Biomacromolecules* **2004,** 5, (5), 2073-2078.

34. Hirano, S.; Ohe, Y.; Ono, H., Selective *N*-Acylation of Chitosan. *Carbohydrate Research* **1976,** 47, (2), 315-320.

35. Vachoud, L.; Zydowicz, N.; Domard, A., Formation and characterisation of a physical chitin gel. *Carbohydrate Research* **1997,** 302, (3-4), 169-177.

Chapter 4

Influence of β-radiation sterilization in properties of new chitosan/soybean protein isolate membranes for guided bone regeneration

4.1 Abstract

Novel chitosan (CTS) and Soybean Protein Isolate (SI) blended membranes were prepared. These membranes were produced by solvent casting. Besides combining the advantages of both materials, CTS/SI membranes exhibit a biphasic structure that will eventually originate *in situ* porous formation, through a two-step degradation mechanism. In this particular work the effect of β-radiation over the properties of these membranes was evaluated. β-radiation sterilisation was performed at three different doses (25, 50 and 100 kGy) and eventual surface chemical changes were evaluated by Fourier Transform Infrared with Attenuated Total Reflection (FTIR-ATR) and Contact Angle Measurements. Moreover, eventual bulk properties changes due to β-radiation were assessed by means of mechanical tensile tests and water uptake measurements. In general, no substantial changes were detected on the studied properties, with the exception of the surface energy that was found to be slightly increased for higher applied doses.

This chapter is based on the following publication:
R. M. Silva, C. Elvira, J. F. Mano, J. San Román, R. L. Reis. Influence of β-Radiation Sterilization in Properties of New Chitosan/Soybean Protein Isolate Membranes for Guided Bone Regeneration. **Journal of Materials Science: Materials in Medicine**, 15 (2004) 523-528.

4.2 Introduction

In many cases, bone healing and the formation of new bone are inhibited by the rapid appearance of connective tissue. The concept of guided bone regeneration (GBR) primarily consists in barrier membranes that prevent the in-growth of connective tissue. Furthermore, growth factors can be accumulated under the membrane [1, 2]. One interesting approach to develop suitable barrier membranes for GBR has been focused in proteins present in the extracellular matrix, namely on using collagen [3]. However, a lot of work has still to be done to develop an ideal GBR and the recent Bovine Spongiform Encephalopathy (BSE) crises lead to an increasing concern about the use of animal origin proteins in biomedical applications. Soybean protein isolate (SI) has been proposed as a non-animal origin protein substitute for several biomedical applications [4, 5]. SI is a mixture of globulin proteins on which Glycinin is present at about 40% (isoelectric point - pI 6,4) and β-conglycinin at about 28% (pI 4.8) [6]. SI is not totally soluble in water, but about 90% of the proteins present in soybean are soluble at some pH (water extractable) [7]. On the other hand, chitosan is a copolymer of *N*-acetylglucosamine (GluNAc) and glucosamine (GluN). It has been observed that GluN, a degradation product of chitosan, has a beneficial effect on treatment and symptoms of osteoarthritis as it helps to regenerate joint cartilage [8, 9]. Moreover it possesses excellent properties such as biocompatibility, biodegradability and non-toxicity [10] and its degradation products are non-toxic, nonimunogenic and noncarcinogenic [11]. Chitosan has been widely studied and proposed for many biomedical applications [12-17], namely for skin tissue regeneration, wound dressings, as barrier-membranes to prevent the ingrowth of undesirable connective tissue, sutures and carriers for sustained drug release [10].

Thus, blending both materials can combine the advantages of a protein material with the unique properties of chitosan. Furthermore, the organic fractions of biological mineralized structures (like bone and tooth) are mainly composed by protein/polysacharide systems. Furthermore, these systems should possess different degradation behaviours as the distinct phases are degraded by different enzymes (chitosan by lysozyme [18, 19] and SI by non-specific proteases). So, by controlling the insoluble fraction and distribution of the protein material, which depends on factors such as pH, mixture composition, polymer concentration, etc, it should be possible to tailor the degradation rate, leading to systems with a two-step degradation behaviour.

This work focus on the assessment of the influence of β-radiation sterilization in the properties of the novel blended membranes composed by chitosan and SI blends. The main effects that ionizing radiation exposure can eventually induce in exposed samples are, among others, crosslinking, chain scissions and oxidative processes [20]. Whenever occurring,

these changes should have a remarkable effect on properties such as mechanical properties, water uptake ability and surface energy. In this work, besides the referred properties, the eventual chemical changes were analyzed by Fourier Transform Infrared with Attenuated Total Reflection (FTIR-ATR) spectroscopy.

4.3 Materials and methods

4.3.1 Membranes preparation and β-radiation sterilisation

Chitosan (deacetylation degree of about 85%) was purchased from Sigma. SI was provided by *Loders Crocklaan BV* (Netherlands). Membranes (average thickness from 45 up to 65 μm) were prepared by solvent casting. Chitosan was dissolved in 1 wt.% of acetic acid solution (AcOH) at a concentration of 1 wt.%. SI was suspended in distilled water at room temperature under gentle stirring in order to avoid protein denaturation and consequently, foam formation. SI suspensions were added dropwise to chitosan solutions under constant stirring at different ratios (designated CTS100%, CTS75%, CTS50%, CTS25%, related to chitosan percentage), and pH was corrected to 4.0 with AcOH (equal to chitosan solution). Mixtures were poured into the moulds directly in the drying place and moulds were no longer moved or removed until complete drying, in order assure that the insoluble part of SI was uniformly distributed. Drying was performed at room temperature (ca. 20ºC) and relative humidity (ca. 55%). The air-exposed (AE) surface during the drying process presented some roughness at macroscopical level, whereas the mould-exposed (ME) surface presented a very smooth appearance. In this way, the surface characterization was carried on taking in consideration this feature. β-radiation sterilization was preformed by *Ionmed Esterilizatión*, SA (Spain) at different radiation doses (25, 50 and 100 kGy) using the electron accelerator Rhodotron TT2 (10 MeV). Both membrane surfaces were characterized morphologically by Scanning Electron Microscopy (SEM, Philips XL30) and Environmental Scanning Electron Microscopy (ESEM, Philips XL30).

4.3.2 Fourier Transform infrared with attenuated total reflection

Surface chemical modifications were assessed by Fourier Transform Infrared with Attenuated Total Reflection (FTIR-ATR) spectroscopy (Perkin-Elmer 457 Spectrometer). The Oxidative effects of radiation should be detected at surface level by changes in the FTIR-

ATR spectrum regions of 3000-3500 and 1650-1800 cm^{-1} [21]. This spectrum regions were analysed in more detail for chemical shifts, peak shape and intensity changes. Both, AE and ME surfaces were analysed.

4.3.3 Contact angle measurements

Contact Angle (θ) Measurements were undertaken by means of sessile drop method with contact angle measurement system G10 from Krűss at room temperature (ca. 20ºC). At least five measurements were performed for each solvent. Surface tension (σ), as well as its polar (σ_p) and dispersive (σ_d) components were determined by Owens and Wendt method [22], using the equipment software G402. Glycerol and methylene iodide were respectively used as polar and non-polar test liquids. Both AE and ME surfaces were tested.

4.3.4 Water uptake measurements

The water uptake measurements were carried out by means of immersing previously weighted (W_0) samples, in a phosphate buffer solution (pH 7.4, ionic strength 0.154 M, buffer conc. 50 mM) at 37ºC. Containers were sealed and placed in a thermostatic bath at 37 ± 1ºC. For each condition 4 samples were used. After each time period (from 10 seconds up to 48 h) samples were removed from containers, adsorbed water was removed by sandwiching between two paper towels and weighted immediately (W). The water uptake (WU) was calculated using the following equation:

$$WU = \frac{W - W_0}{W_0} = \frac{W}{W_0} \qquad (4.1)$$

4.3.5 Quasi-static mechanical properties

Membranes were cut into strips. Their dimensions were found to be typically about 8 x 1 x 0.045 mm. Thickness was taken as a mean of ten values at different points measured with a low-pressure micrometer. Their resistance to stretching was evaluated on a Perkin-Elmer DMA7e at a constant stress rate of 5 MPa/min using the tensile mode. In such experiments, the strain was monitored as a function of stress. Please note that such procedure is different from conventional mechanical tests where the stress is monitored as a function of strain, which varies at constant rate. However, one can also build stress-strain curves and obtain a

measure of the stiffness (by looking at the slope of the curve at early stages) and the strength (measured by the stress at break) of the sample, when experiments at constant stress rate are performed. Mechanical tests were carried out at room temperature (ca. 20 ºC) and relative humidity (ca. 70%). Secant modulus was calculated at 1% of elongation. Stress and strain at break were also estimated.

4.3.6 Density determination

The polymer blends density measurements were undertaken making use of n-heptane/dibromoethane soluble solvents system. The rational for the solvents choice was based on their density (polymer density limited by solvents density) and the fact that samples did not absorb any measurable quantity of both. Membranes were cut in at least 3 strips (ca. 1 x 20 mm). A test tube was filled with n-heptane and placed in a ultrasound bath for 5 min to eliminate air bubbles (at this stage membrane strips should be settled down at the bottom). Then, dibromoethane was added drop by drop until all polymer strips start to go up and tend to float. At this stage the liquid density, determined by pycnometry, should be an approximation of the polymer density. The procedure was repeated 3 times giving results with a good precision (maximum standard deviation of 0.0058). In general, measures revealed to be accurate since at the changing point the addition of a few drops did not change significantly the liquid density.

4.4 Results and discussion

4.4.1 Fourier Transform infrared with attenuated total reflection

FTIR analysis was applied in order to detect chemical modifications on irradiated samples by means of oxidation or crosslinking processes. The most representative signals (see Figure 4.1) are those in the 3400-3200 cm^{-1} range, corresponding to the stretching vibration of the chitosan hydroxyl groups, amine groups ($–NH_2$, -NH- and –NH) of the amino-acids (SI) and amide groups. The signals appearing at 1626 cm^{-1} can be assigned to the NH_2 bending vibration (chitosan), amide vibration (SI), and signals appearing at 1530 cm^{-1} to the aromatic ring of some amino acids of SI. In terms of different radiation doses no significant changes are observed in the corresponding signal also in comparison to non-irradiated samples, indicating that significant chemical modifications are not observed by this spectroscopic

technique when treating CTS/SI membranes with β-radiation under the mentioned conditions.

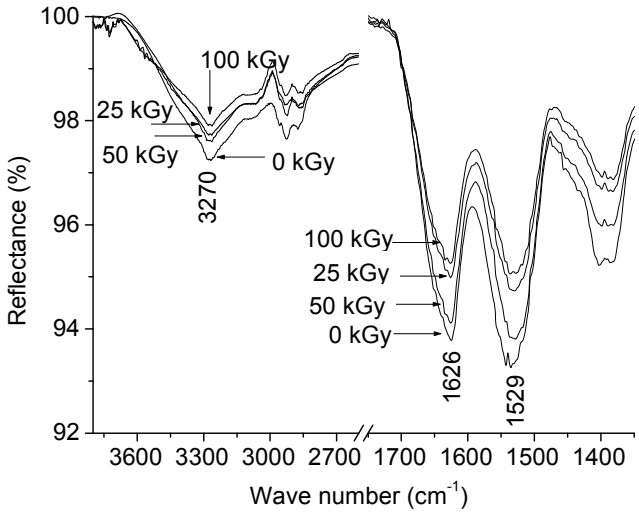

Figure 4.1 FTIR-ATR spectra of the ME surface of CTS75% membranes treated with different doses of β-radiation. Scale was adjusted to see in detail 3000-3500 and 1650-1800 cm^{-1} spectra regions.

4.4.2 Contact angle measurements

Contact Angle measurements were performed on all treated samples in order to determine the surface energy, the respective polar and dispersive contribution, and the possible changes due to the β-radiation treatment. The contribution of the dispersive (σ_d) and polar interactions (σ_p) to the surface energy was calculated by considering that the intermolecular attraction, which causes surface free energy (σ) results from a variety of intermolecular forces according to the additive rule. Thus, surface energy and contact angle of a liquid on a solid were calculated as described in the experimental part. Figure 4.2 shows the total surface energies and the respective polar and dispersive components values versus the β-radiation doses in the different CTS/SI formulations. In this figure it can be observed that as the SI percentage increases in the blends composition the surface energy also increases, as well as its polar and dispersive components. In Figure 4.2a it can be observed an increase in the dispersive energy component when increasing the β-radiation dose in formulations like CTS25%, CTS50%, CTS100%, whereas in the case of CTS75% σ_d is maintained constant. A similar behaviour is observed in the polar component energy values (Figure 4.2b) in CTS25%, CTS50% and CTS75%, whereas in CTS100% the σ_p decreases with the β-

radiation dose. Finally, the addition of both components to obtain the final surface energy (see Figure 4.2c) shows a general increase tendency, in about 2 mN/m units of energy, with respect to non-treated samples.

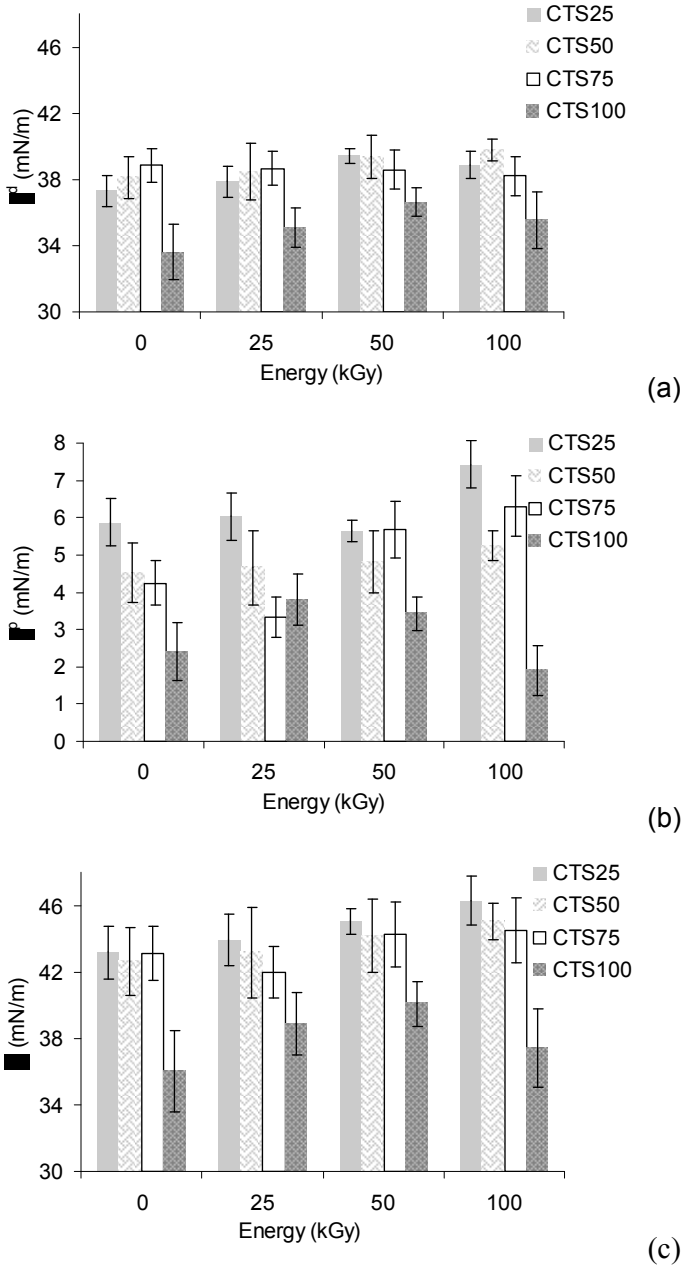

Figure 4.2 Dispersive **(a)** and polar **(b)** components of surface energy **(c)** measured at the ME surface in function of applied β-radiation dose. Data represents mean ± error at 95% of confidence level.

4.4.3 Morphological characterization by SEM and ESEM

The air-exposed (AE) surface exhibited a granulate aspect, in contrast with the smooth mould-exposed (ME) surface for all CTS/SI compositions, by simple eye observation. Reversely, AE surface present a smooth appearance at higher magnifications and it was possible to observe in the ME surface the presence of some globular structures incorporated in a continuous matrix, providing roughness at a lower scale (see Figure 4.3 and 4.4). This seems to indicate, in the authors' view, that during the drying time insoluble suspended SI particles settle down at the bottom. Therefore, bottom membrane surface can possibly present some SI insoluble particles, which are not totally covered by a chitosan layer. On contrary, in the upper surface a chitosan layer cover totally SI insoluble particles and accompany the gaps left by SI particles, originating the final rough appearance. Moreover, CTS100% membranes present both surfaces rather smooth at all magnifications used (results not shown). When comparing the membrane structures of the different blends with the ones of the CTS100%, one can correlate such granules with the SI insoluble part. This assumption is in a certain way supported by the fact that such granules present a higher swelling with respect to the surrounding matrix as it was possible to detect by ESEM (Figure 4.4), being SI more hydrophilic than chitosan. It was not detected any change in the membranes morphology after being sterilised by β-radiation at the tested doses.

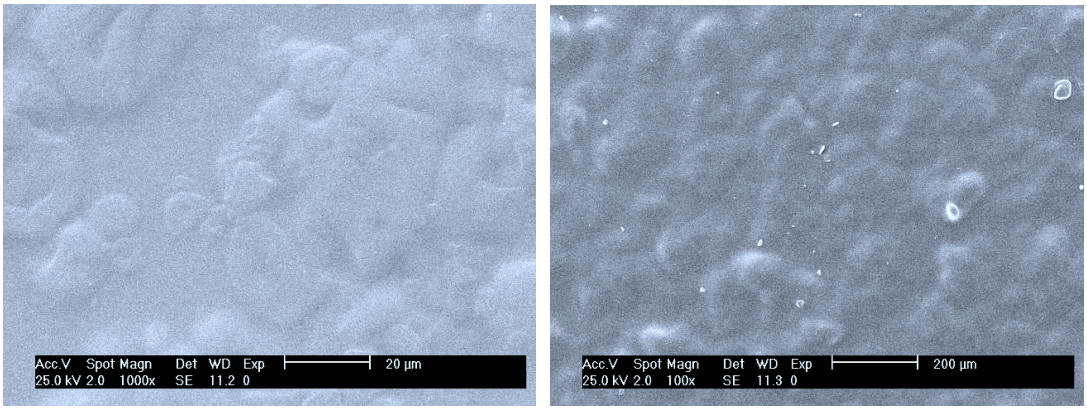

(a) (b)

Figure 4.3 SEM micrographs of CTS75% non-irradiated membranes: **(a)** ME surface (1000x) **(b)** AE surface (100x).

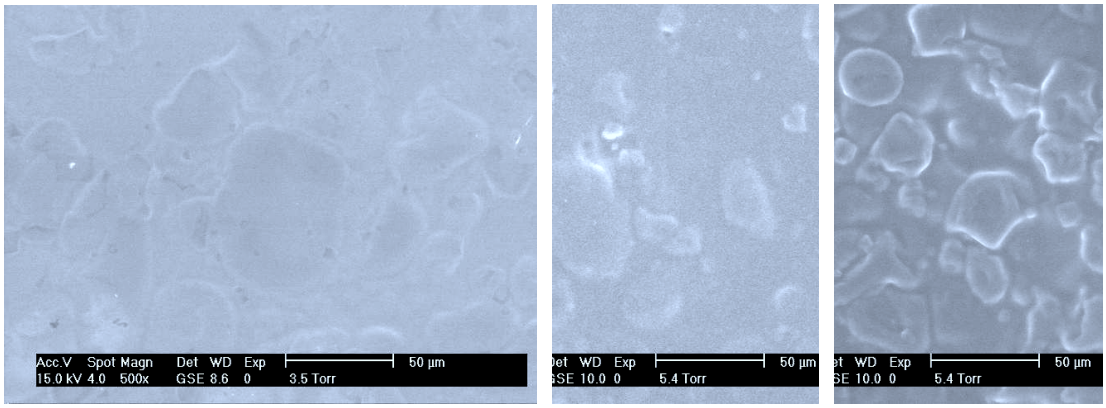

(a) (b) (c)

Figure 4.4 ESEM micrographs of CTS75% non-irradiated membranes in dry state (660 Pa) **(a)** and previously swollen in a buffer solutions at pH of 7.4 **(b)** and at 6.5 **(c)**.

4.4.4 Swelling kinetics

Figures 4.5a and 4.5b show two examples of the typical variation of the water uptake as a function of time. All formulations were found to reach the maximum of the hydration degree in less than 5 min. After that, it was observed a decrease in the water uptake towards the hydration equilibrium degree. This effect was more accentuated for the formulations with greater chitosan content, being likely due to the pH equilibration process inside the polymeric matrix. The hydration equilibrium degree values were taken after 2 days of immersion and it is shown to be independent of the β-radiation treatment. In respect to the CTS/SI blend composition no considerable differences could be observed (see Figure 4.5c).

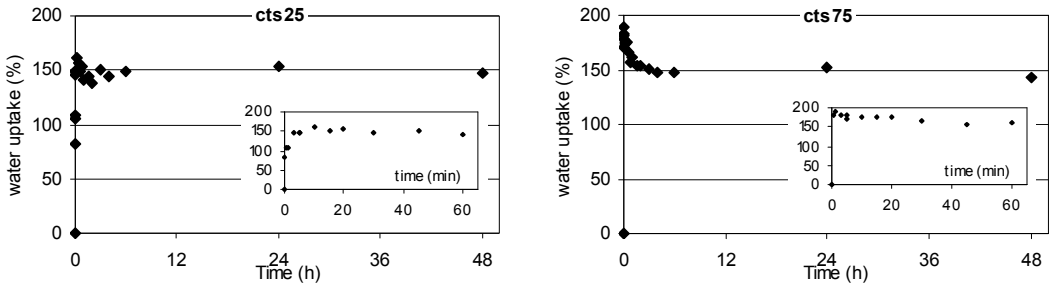

(a) (b)

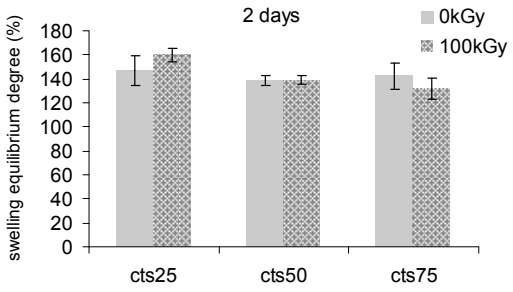

(c)

Figure 4.5 Swelling kinetics profile of non-irradiated CTS25% **(a)** and CTS75% **(b)** and the equilibrium hydration degree taken at 2 days of immersion in buffer solution (pH 7.4; IS 0.154 M; buffer conc. 50 mM) as a function of chitosan percentage in the blends for non-treated and exposed to β-radiation (100 kGy) membranes **(c)**. Data represents mean ± standard deviation of at least three samples.

4.4.5 Quasi-static mechanical properties

Tensile tests were carried out in order to evaluate the impact of β-radiation on the mechanical performance of the several formulations, since if crosslinking and/or polymer oxidative degradation/depolymerisation had occurred, it could cause important changes on those properties. It was impossible to test membranes with higher SI content, because of its high brittleness. In Figures 4.6a and 4.6c, it is represented the tensile strength and the secant modulus, respectively, as a function of the applied β-radiation dose. From those figures it can be observed that β-radiation did not affect the strength and the stiffness of the tested formulations, with the exception of CTS50% where the strength and the stiffness were found to increase when applying a β-radiation dose of 100 kGy. On the other hand, chitosan membranes (CTS100%) presented higher values of tensile strength at break (64.7 MPa) and modulus (2.5 GPa), than the blends. Furthermore, the amount of SI among the studied compositions did not change substantially these properties, which was found to be around 45 MPa and 2.0 GPa, respectively. The same behaviour was also observed for the strain at break (Figure 4.6c), being about 12% for chitosan membranes (CTS100%) and 3-4% for the blends. Moreover, the brittleness did not vary consistently with the β-radiation treatment, even when applying a 100 kGy β-radiation dose.

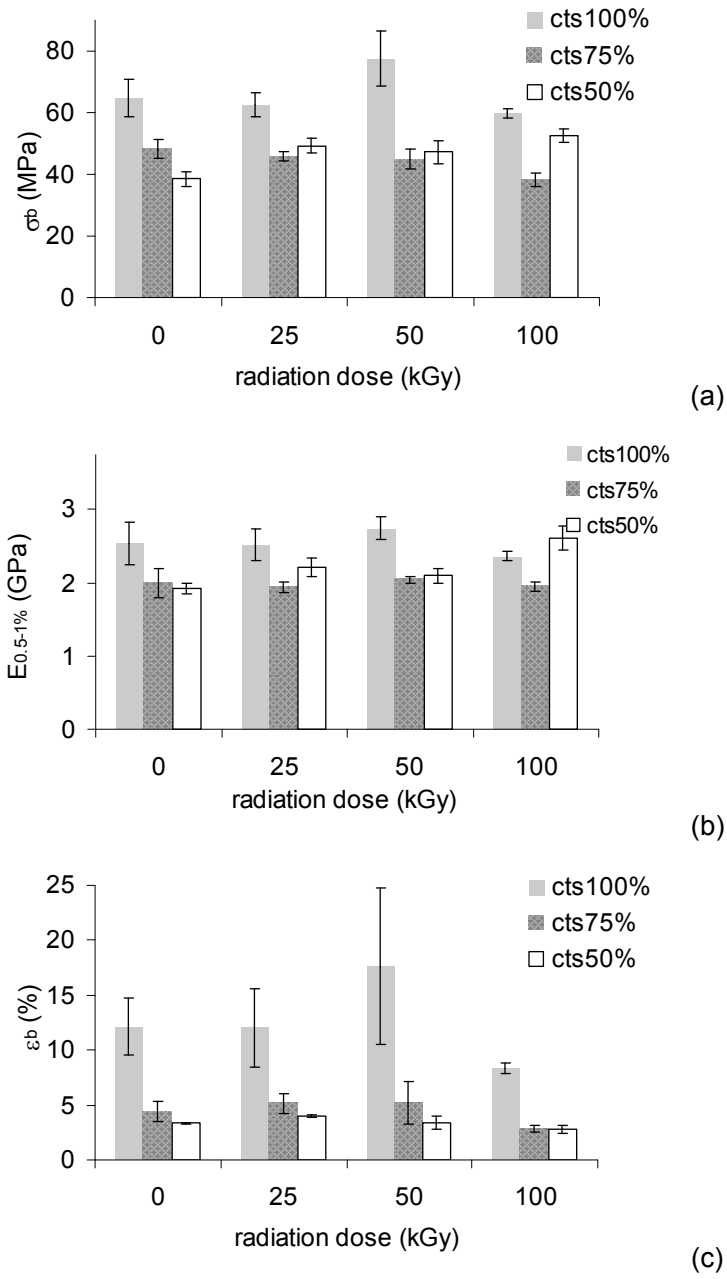

Figure 4.6 Membranes tensile properties of several CTS/SI blend compositions as a function of applied β-radiation dose: **(a)** secant modulus at 2% of elongation; **(b)** stress at break; **(c)** strain at break. Data represents mean ± standard deviation of at least three experiments.

4.4.6 Polymer density

Polymer density was determined in order to calculate the average molecular weight between possible crosslinks on irradiated samples. However, since the water uptake and the modulus of all formulation were not substantially affected by the β-radiation treatment, it is presented

as a further indication that no remarkable crosslinking reactions are taking place (see Table 4.1).

Table 4.1 Polymer density as a function of chitosan percentage in the blends for non-treated and exposed to β-radiation (100 kGy) membranes. Data represents mean ± error at 95% of confidence level

	Radiation dose (kGy)	
Sample	**0**	**100**
CTS100%	1.420 ± 0.025	1.424 ± 0.016
CTS 75%	1.386 ± 0.017	1.380 ± 0.010
CTS 50%	1.334 ± 0.008	1.355 ± 0.018
CTS 25%	1.314 ± 0.009	1.332 ± 0.005

4.5 Conclusions

Membranes presenting a very interesting morphology and correspondent properties could be obtained from combining chitosan and SI on blended membranes. The partial insolubility of SI at the processing pH, as well as its asymmetric distribution through the transversal section, being the SI insoluble particles concentrated at the ME surface, are desirable features to attain a controlled degradation rate *in vivo*. Furthermore, it can be foreseen a two-step degradation mechanism, eventually leading to *in situ* porous formation, which might be clinically useful. Moreover, since in general no remarkable differences were observed for the studied bulk and surface properties of the membranes, it might be possible to tailor their degradation and their biological response without changing their key properties, by means of controlling blends' composition.

β-radiation seems to be a suitable sterilization methodology to be used on chitosan/SI membranes aiming to be used in GBR. In fact, no considerable changes could be detected on the mechanical properties and equilibrium hydration degree. Furthermore, FTIR-ATR analyses indicated that no substantial chemical modifications occur when sterilising samples by β-radiation, for radiation doses up to 100 kGy. The most sensitive property to β-radiation exposure was the surface energy. In fact, a slight increase tendency was observed for the surface energy due to β-radiation.

4.6 Acknowledgements

R. M. Silva was supported by the PhD Scholarship SFRH/BD/6862/2001 from Portuguese Foundation for Science and Technology (FCT) under the POCTI Program. This work was partially supported by FCT through funds from the POCTI and/or FEDER programmes. *Ionmed Esterelizatión, SA* is also acknowledged by performing β-radiation sterilisation.

4.7 References

1. Ueyama, Y.; Ishikawa, K.; Mano, T.; Koyama, T.; Nagatsuka, H.; Suzuki, K.; Ryoke, K., Usefulness as guided bone regeneration membrane of the alginate membrane. *Biomaterials* **2002,** 23, (9), 2027-2033.
2. Imbronito, A. V.; Todescan, J. H.; Carvalho, C. V.; Arana-Chavez, V. E., Healing of alveolar bone in resorbable and non-resorbable membrane-protected defects. A histologic pilot study in dogs. *Biomaterials* **2002,** 23, (20), 4079-4086.
3. Jianqi, H.; Hong, H.; Lieping, S.; Genghua, G., Comparison of calcium alginate film with collagen membrane for guided bone regeneration in mandibular defects in rabbits. *Journal of Oral and Maxillofacial Surgery* **2002,** 60, (12), 1449-1454.
4. Vaz, C. M.; de Graaf, L. A.; Reis, R. L.; Cunha, A. M., In vitro degradation behaviour of biodegradable soy plastics: effects of crosslinking with glyoxal and thermal treatment. *Polymer Degradation and Stability* **2003,** 81, (1), 65-74.
5. Vaz, C. M.; van Doeveren, P. F. N. M.; Reis, R. L.; Cunha, A. M., Development and design of double-layer co-injection moulded soy protein based drug delivery devices. *Polymer* **2003,** 44, (19), 5983-5992.
6. Garcia, M. C.; Torre, M.; Laborda, F.; Marina, M. L., Rapid separation of soybean globulins by reversed-phase high-performance liquid chromatography. *Journal of Chromatography A* **1997,** 758, (1), 75-83.
7. Renkema, J. M. S.; Lakemond, C. M. M.; de Jongh, H. H. J.; Gruppen, H.; van Vliet, T., The effect of pH on heat denaturation and gel forming properties of soy proteins. *Journal of Biotechnology* **2000,** 79, (3), 223-230.
8. Fenton, J. I.; Chlebek-Brown, K. A.; Peters, T. L.; Caron, J. P.; Orth, M. W., The effects of glucosamine derivatives on equine articular cartilage degradation in explant culture. *Osteoarthritis and Cartilage* **2000,** 8, (6), 444-451.
9. Fenton, J. I.; Chlebek-Brown, K. A.; Peters, T. L.; Caron, J. P.; Orth, M. W., Glucosamine HCl reduces equine articular cartilage degradation in explant culture. *Osteoarthritis and Cartilage* **2000,** 8, (4), 258-265.

10. Ravi Kumar, M. N. V., A review of chitin and chitosan applications. *Reactive and Functional Polymers* **2000,** 46, (1), 1-27.

11. Muzzarelli, R. A. A., Biochemical Significance of Exogenous Chitins and Chitosans in Animals and Patients. *Carbohydrate Polymers* **1993,** 20, (1), 7-16.

12. Ito, M.; Hidaka, Y.; Nakajima, M.; Yagasaki, H.; Kafrawy, A. H., Effect of hydroxyapatite content on physical properties and connective tissue reactions to a chitosan-hydroxyapatite composite membrane. *Journal of Biomedical Materials Research* **1999,** 45, (3), 204-208.

13. Thacharodi, D.; Rao, K. P., Development and in vitro evaluation of chitosan-based transdermal drug delivery systems for the controlled delivery of propranolol hydrochloride. *Biomaterials* **1995,** 16, (2), 145-148.

14. Mi, F.-L.; Tan, Y.-C.; Liang, H.-F.; Sung, H.-W., In vivo biocompatibility and degradability of a novel injectable-chitosan-based implant. *Biomaterials* **2002,** 23, (1), 181-191.

15. Ma, J.; Wang, H.; He, B.; Chen, J., A preliminary in vitro study on the fabrication and tissue engineering applications of a novel chitosan bilayer material as a scaffold of human neofetal dermal fibroblasts. *Biomaterials* **2001,** 22, (4), 331-336.

16. Takechi, M.; Ishikawa, K.; Miyamoto, Y.; Nagayama, M.; Suzuki, K., Tissue responses to anti-washout apatite cement using chitosan when implanted in the rat tibia. *Journal of Materials Science-Materials in Medicine* **2001,** 12, (7), 597-602.

17. Prasitsilp, M.; Jenwithisuk, R.; Kongsuwan, K.; Damrongchai, N.; Watts, P., Cellular responses to chitosan in vitro: The importance of deacetylation. *Journal of Materials Science-Materials in Medicine* **2000,** 11, (12), 773-778.

18. Kurita, K.; Kaji, Y.; Mori, T.; Nishiyama, Y., Enzymatic degradation of [beta]-chitin: susceptibility and the influence of deacetylation. *Carbohydrate Polymers* **2000,** 42, (1), 19-21.

19. Tomihata, K.; Ikada, Y., In vitro and in vivo degradation of films of chitin and its deacetylated derivatives. *Biomaterials* **1997,** 18, (7), 567-575.

20. Silverman, J., Basic concepts of radiation processing. *Radiation Physics and Chemistry (1977)* **1977,** 9, (1-3), 1-15.

21. Baccaro, S.; Buontempo, U., Radiation induced oxidative degradation of ethylene-propylene rubber by IR spectroscopy. *International Journal of Radiation Applications and Instrumentation. Part C. Radiation Physics and Chemistry* **1992,** 40, (3), 175-180.

22. Owens, D. K.; Wendt, R. C., Estimation of Surface Free Energy of Polymers. *Journal of Applied Polymer Science* **1969,** 13, (8), 1741-&.

Chapter 5

Preparation and characterisation in simulated body conditions of glutaraldehyde crosslinked chitosan membranes

5.1 Abstract

Chitosan membranes, aimed at biomedical applications, were prepared by a solvent casting methodology. Crosslinking was previously performed in acetic acid solution with glutaraldehyde, in order to obtain different degrees of crosslinking. Some membranes were neutralised in a NaOH solution. Mechanical tensile tests comprised quasi-static experiments at constant stress rate and temperature sweep dynamic mechanical analysis tests. This included measurements with the samples immersed in isotonic saline solution (ISS) at 37ºC, in order to simulate physiological conditions, which were performed using a specific liquid container. It was observed that for higher crosslinking levels the membranes become stiffer but their strength decreases; these results are in agreement with swelling tests, also performed at body temperature. All the membranes exhibited similar and significant damping properties in wet conditions, which revealed to be stable in a broad temperature range. Weight loss measurements allowed showing that the developed membranes degrade slowly up to 60 days. Cytotoxicity screening, using cell culture tests, showed that such materials could be eventually adequate for being used in biomedical applications.

This chapter is based on the following publication:
R. M. Silva, G. A. Silva, O. P. Coutinho, J. F. Mano, R. L. Reis. Preparation and characterisation in simulated body conditions of glutaraldehyde crosslinked chitosan membranes. **Journal of Materials Science: Materials in Medicine**, 15 (2004), 1105-1112.

5.2 Introduction

Chitin is the second most abundant biopolymer in nature and the supporting material of crustaceans, insects, fungi, etc. Chitosan can be obtained by *N*-deacetylation of chitin, although this *N*-deacetylation is almost never complete. Thus, chitosan is a co-polymer of 2-amino-2-deoxy-D-glucopyranose (GluN) and 2-acetamido-2-deoxy-D-glucopyranose (GluNAc).

The ratio of GluN units to both glucopyranose structural units is known as the degree of deacetylation (DD) and has a striking effect on chitosan physical and chemical properties. The DD is typically of more than 75% [1]. The presence of free amino groups that can be protonated at acidic conditions make it soluble in dilute aqueous solutions of formic, acetic, lactic, citric and hydrochloric acid [2]. Chitosan acid-base equilibrium pKa depends on the net charge and its solubility occurs in the range of the degree of protonation of ca. 0.5. Chitosan (DD 88%) acetate neutral salt possesses a pKa of approx. 6.2 at that degree of protonation [3]. Chitosan can be hydrolysed by lysozyme present in human body fluids [4-7]. The degradation rate of chitosan by lysozyme depends on the DD, reaching a maximum at about 50%. In turn, no apparent lysozyme degradation was observed in chitosan with DD higher than 97% [8, 9].

This natural polymer is of special interest in the biomedical field, since it displays excellent properties such as biocompatibility, biodegradability, non-toxicity[1] and bioactivity [10], and its degradation products are non-toxic, non-immunogenic and non-carcinogenic [11]. Chitosan has been widely studied and proposed for biomedical applications, namely for skin tissue regeneration, wound dressings, as barrier-membranes to prevent the in-growth of undesirable connective tissue, sutures and for sustained drug release [1].

Crosslinking chitosan is an appropriate methodology for controlling its swelling rate, drug release rate and changing of mechanical properties. Some crosslinking reagents have been suggested in literature, like glutaraldehyde [12-16], sulphuric acid [17], genipin [18, 19] and oxidized glucose [20]. Glutaraldehyde is the most widely studied crosslinker of chitosan and it was often used as a comparison in the study of novel crosslinkers. The reaction with chitosan amine groups produces covalent crosslinking through a Schiff base reaction. Three different propositions are considered: (a) There is the formation of one Schiff base and the other aldehyde group of glutaraldehyde remains free (in this case no crosslinking is formed); (b) the crosslinking occurs with one glutaraldehyde molecule and two chitosan unities, involving the formation of two Schiff bases; (c) a great crosslinking chain is formed due to the polymerisation of glutaraldehyde. Chitosan dissolved in acetic acid pH 3-4 react with glutaraldehyde in short times, less that 1 hour. Therefore, the protonation of chitosan amine groups does not affect the reaction, while the concentration of glutaraldehyde strongly affects

the physical properties of the general compounds formed [21]. In this work, chitosan membranes with no, low or high crosslinking degree, as induced by glutaraldehyde were prepared and their degradation and swelling properties was evaluated.

The mechanical properties are usually an important criterion in selection of a material for biomedical applications. Water content of hydrogel materials can affect drastically its mechanical properties, especially when specimens are in contact with physiological fluids. In this sense, materials should be tested in water bath or in high humidity environment. Some authors [14, 18] have reported mechanical properties of chitosan membranes crosslinked with glutaraldehyde in dry state. However, some applications require the knowledge of mechanical properties measured in physiological conditions. In this work, an isotonic saline solution was used to simulate body fluid conditions and tests were preformed with samples immersed at 37ºC.

On the other hand, a material to be used as an implant or as a scaffold for tissue engineering applications must exhibit an appropriate biological behaviour in terms of interaction with living tissues [22]. The first step of the evaluation of these materials in terms of biological behaviour is their cytotoxicity testing *in vitro*, using immortalised cell lines [23]. Cytotoxicity deals mainly with substances that leach out of the proposed biomaterials [24], which in contact with cells allow for the evaluation of its possible toxicity over cells. Parameters like cell morphology, death, proliferation and adhesion are evaluated for a preliminary screening of the biocompatibility. Biochemical tests such as MTT test and total protein quantification are often used in these indirect contact studies. The MTT test has been widely used to measure cellular viability and proliferation [25-27], and the total protein test is a fairly accurate measure of cell proliferation [28].

5.3 Materials and methods

5.3.1 Membranes preparation

Chitosan origin from crab shells was purchased from Sigma-Aldrich. According to the manufacturer its degree of deacetylation (DD) is superior than 85%. Acetic acid, glutaraldehyde and other reagents were of reagent grade.

The chitosan solution was prepared by dissolving chitosan (1 wt.%) in acetic acid (1 wt.%) solution. Glutaraldehyde solutions with different concentrations were prepared diluting glutaraldehyde solution (50 wt.%) as it was provided by the manufacturer. The same volume of each glutaraldehyde solution was added to a certain amount of the previous chitosan

solution in order to obtain a glutaraldehyde to chitosan amine groups molar ratio (assuming the minimum degree of acetylation 85%) of 1% (CTS01), 10% (CTS10) and 20% (CTS20). Glutaraldehyde solution was added dropwise during 5 min under gentle stirring and the resultant solutions were let quiescent for about 1 h to remove any air bubble formed. Non-crosslinked chitosan membranes (CTS) were prepared in the same way, but no glutaraldehyde solution was added. Membranes were prepared by solvent casting. Solutions were poured into Petri dishes and dried at 37ºC. After drying, membranes were neutralised in NaOH 0.1 M solution for 10 min, washed thoroughly with distilled water and dried again at 37ºC. Some samples were not neutralised to be tested in dry state. Obviously, non-neutralised chitosan membranes can not be tested in solution, since they rapidly swell and dissolve due to the protonated amine groups

5.3.2 X-ray diffraction

The morphology of the studied film was analysed by X-ray diffraction using synchrotron radiation at the A2 Soft Condensed Matter Beamline of HASYLAB, DESY (Hamburg, Germany). 2D wide-angle X-ray scattering (WAXS) patterns were obtained employing an image plate, separated 22 cm from the sample.

5.3.3 Degradation and swelling kinetics

The water uptake measurements were carried out by means of immersing neutralised samples, previously weighted, in 30 ml of ISS (NaCl 0.154 M and pH = 7.4 $\pm$ 0.02). Containers were sealed and placed in a thermostatic bath at 37 $\pm$ 1ºC. After 15 min and 1, 2, 4, 8, 24 and 54 h samples were removed from containers, adsorbed water was removed by sandwiching between two paper towels and weighted immediately. The water uptake (*WU*) of all formulations was calculated using the following equation:

$$WU = \frac{W - W_0}{W_0} = \frac{W}{W_0} - 1 \qquad (5.1)$$

where W_0 is the initial weight of the sample and W is the weight of the sample at certain immersion time.

In vitro degradation of chitosan membranes was assessed again in 30 ml of ISS. Samples were previously weighted and then fully immersed in solution. Containers were sealed and placed in a thermostatic bath at 37 $\pm$ 1ºC. After each test period (7, 14, 30 and 60 days)

samples were dried until constant mass (W_1). The weight loss (WL) was calculated using the following equation:

$$WL = \frac{W_0 - W_1}{W_0} = 1 - \frac{W_1}{W_0} \quad (5.2)$$

where W_0 is the initial weight of the sample.

5.3.4 Quasi-static mechanical properties

Chitosan membranes neutralised in 0.1 M NaOH solution were cut into strips. Their dimensions were found to be typically about 15 x 2 x 0.02 mm after conditioning in ISS for 15 min. Thickness was taken as a mean of ten values at different points measured with a low-pressure micrometer. Their resistance to stretching was evaluated with a Perkin-Elmer DMA7e at a constant stress rate of 5 MPa/min using the tensile mode. In such experiments, the strain was monitored as a function of stress. Note that such procedure is different from conventional mechanical tests where the stress is monitored as a function of strain, which varies at constant rate. However, one can also build stress-strain curves and obtain a measure of the stiffness (by looking at the slope of the curve at early stages) and the strength (measured by the stress at break) of the sample, when experiments at constant stress rate are performed. The assays with samples immersed in solution were preformed using a liquid bath built in stainless steel. This bath can be fitted into the furnace of the DMA equipment. A schematic representation is shown in Figure 5.1.

Mechanical tests in immersed conditions were carried out in ISS at body temperature (37ºC). Samples were kept immersed for 15 min in order to reach the hydration and thermal equilibrium, after holding it in the test probe. Mechanical tests in a dry environment and in solution at room temperature (ca. 20ºC) were undertaken for comparison purposes. Non-neutralised chitosan membranes were only tested in a dry environment. Temperature was checked with an external temperature sensor after and before each test. The temperature read by the sensor fluctuated less then 0.1ºC during the experiments. Secant modulus was calculated at 2% of elongation. Stress and strain at break were also estimated.

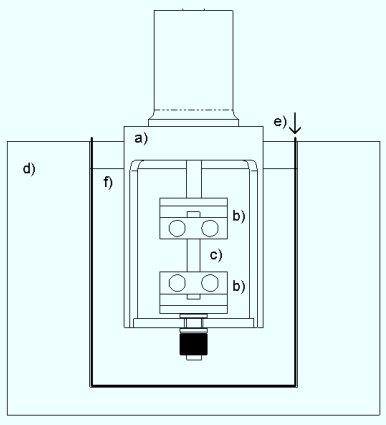

Figure 5.1 Schematic picture of DMAe7 Perkin-Elmer water bath system, used to test biomaterials in ISS. Legend: a) DMA tensile accessory; b) top and bottom clamps; c) sample (membrane); d) DMA furnace; e) metallic liquid reservoir; f) isotonic saline solution.

5.3.5 Dynamic mechanical analysis (DMA)

Dynamical mechanical measurements were carried out on chitosan membranes with a Perkin-Elmer DMA7e analyser at 1 Hz and heating rate of 2ºC/min. The tests were preformed with samples immersed in ISS, using the same system described above. In these measurements, sample and solution was carefully cooled down to near 0ºC, in order to avoid solution freezing and consequent sample damage. Experiments were stopped at about 80ºC. The dimensions were the same of those for quasi-static mechanical tests and thickness was taken by the method described in the previous section. It was considered that the cross-section area of the samples do not vary during the experiment.

During each DMA experiment, both the storage modulus, E', and the loss factor, tan δ, were measured as a function of temperature. The first corresponds to the real component of the complex modulus ($E^*=E'+iE''$), being a measure of the sample's stiffness, whereas the later gives the ratio between the amount of mechanical energy lost and stored during a cycle ($\tan\delta=E''/E'$), measuring the damping capability of the sample.

A sample of polybutadiene was tested both into solution and in the conventional dry state. This rubber material was found to not absorb any water by a simple gravimetric assay and so mechanical dynamic performance in wet conditions should not differ from conventional assay. In fact, it was found that both E' and tan δ are similar when measuring in both dry and wet conditions, indicating that the effect of the solution does not influence significantly the measurements.

5.3.6 Cytotoxicity

The materials were cut in 1 x 1 cm^2 pieces and sterilized by ethylene oxide (EtO), as described before [29]. The sterilization procedure did not show any adverse effect on the samples (data not shown).

The materials were immersed for 24 hours at 37ºC (with constant shaking) in DMEM culture media without phenol red (Gibco BRL, USA), supplemented with 10% Fetal Bovine Serum (FBS) (BioChrome, Germany) and 1% antibiotic/antimycotic solution (Sigma, St. Louis, USA), at a ratio of 1.5 cm^2/ml. This is an advised procedure for biomaterials extraction to obtain the major leachables and determine their short-term effect in a dynamic environment [23]. The extracts were then filtered through a 0.45 μm pore size filter and then used for MTT and total protein quantification tests.

5.3.7 MTT test

The MTT (3-(4,5-dimethylthiazol-2-yl)-2,5-diphenyltetrazolium bromide) has a yellow tonality and is soluble in water. This compound can be converted by the mitochondrial enzyme succinate dehydrogenase in a purple colour salt insoluble in water. The insoluble salt absorbs at a wavelength of 570 nm and it is proportional to the amount of viable cells, since only viable cells can metabolise MTT [26, 27, 30].

A commercial cell line of rat lung fibroblasts – L929 – was used in these studies. The cells were cultured in 75 cm^2 flasks (Costar). After detaching them from the culture flask by using a 0.25% trypsin-EDTA solution (SIGMA, St. Louis) they were re-suspended in DMEM culture medium. The cells were plated in 96-well micrometer plates at a density of 2 x 10^4 cells/well. The plates were incubated for 48 hours in a humidified atmosphere of 5% CO_2 at 37ºC. After this, the culture medium was removed and the extracts were placed in contact with the cell monolayer and culture medium was used as control. The plates were incubated for 72 hours, and after removal of the culture medium, 50 µl of MTT (Sigma, St. Louis, USA) solution (1 mg/ml in culture medium) was added and incubated 4 hours at 37ºC. To dissolve the formazan crystals that are formed, 100 µl of isopropanol were added and the plates were incubated for 15 minutes at 37ºC and then placed at room temperature in an orbital shaker to help dissolving the crystals. The optical densities at 570 nm and 650 nm (background) were read on a multiwell plate reader (Molecular Dynamics, Amersham, USA) against a blank of MTT solution and isopropanol. All the materials were tested in 10 replicates for each extract for at least three separate experiments with reproducible results.

5.3.8 Total protein quantification

The method used to quantify the total protein make use of the Micro BCA Protein Assay Reagent Kit (Pierce, USA) that uses bicinchoninic acid (BCA) as the detection reagent for Cu^{1+}, which is formed when Cu^{2+} is reduced by proteins in an alkaline environment. The purple colour product is formed by the chelation of two molecules of BCA with one Cu^{1+} ion. This complex is water-soluble and absorbs at 562 nm, and its absorbance is linearly correlated with protein concentration [28].

The procedure is very similar to the one of MTT. After the 72 hours incubation, the extracts are removed from contact with cells and these are washed with a phosphate buffer solution (PBS) 0.01 M, and 100 µl of PBS 0.01 M are added to each well. To each well 100 µl of the BCA reagent were added, the plates were agitated for 30 seconds and incubated for 2 hours at 37ºC. The plates were then cooled to room temperature and the optical densities were measured at 562 nm against a blank of PBS 0.01 M and BCA reagent. Total protein (in µg/ml) was determined using a BSA standard curve.

5.4 Results and discussion

5.4.1 Crystallinity

The 2D WAXS pattern of non-crosslinked chitosan (not shown) exhibited a Debye ring at $2\theta \approx 20^{o}$ and an isotropic crystalline orientation. This reflection is in agreement with the typical chitosan diffractogram [21, 31]. The equatorial cuts of such patterns for the studied chitosan membranes are shown in Figure 5.2. One clearly sees that for 1% crosslinking the crystallinity degree is highly depressed. The results for higher-crosslinked materials show that these membranes are amorphous.

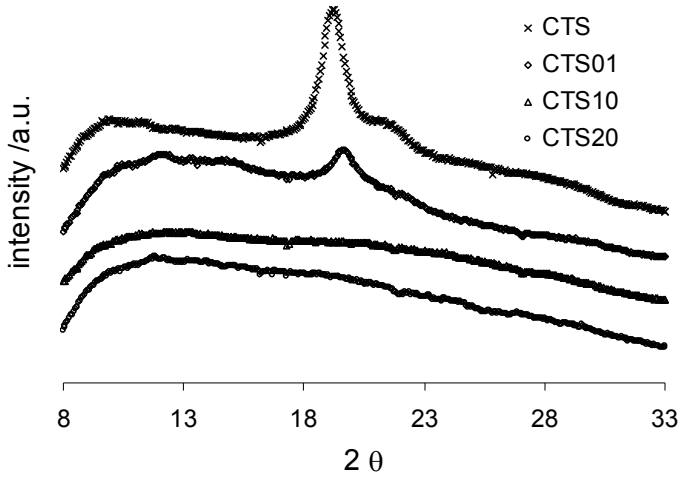

Figure 5.2 X-ray diffraction patterns of neutralised chitosan membranes non-crosslinked (CTS) and with crosslinker chitosan amine groups molar ratio of 1% (CTS01), 10% (CTS10) and 20% (CTS20).

5.4.2 Degradation and swelling kinetics

All samples reached the equilibrium hydration degree in about 15 min. This can be observed in Figure 5.3 which shows the swelling isotherms and respective pH drift. Chitosan membranes with lower crosslinking degree (CTS01) presented higher equilibrium hydration degree than non-crosslinked membranes (CTS) despite the crosslinking reactions. On the other hand, higher crosslinking degrees (CTS10 and CTS20) showed to be effective on lowering the equilibrium hydration degree. In fact, crystallinity decreases as crosslinking degree by glutaraldehyde increases, since crosslinks between two chitosan units or pendant glutaraldehyde with one aldehyde free may constitute an obstacle to chitosan molecules packing. The lower crystallinity enhance the water molecules accessibility. Thus, the hydration equilibrium degree should depend on the balance between crystallinity and crosslinking degree leading to a maximum somewhat between non-crosslinked membranes (CTS) and CTS10.

All formulations revealed to be very stable in the simulated body wet environment with a weight loss never superior than 12% after 60 days of immersion. Membranes degrade up to 30 days of immersion. After that, samples weight seems to stabilize and weight loss reach what can be roughly described as a plateau. These results may suggest that the low molecular mass fraction of the chitosan membranes is continuously released in the first 30 days. The higher molecular mass components are much more stable within the experimental time window studied.

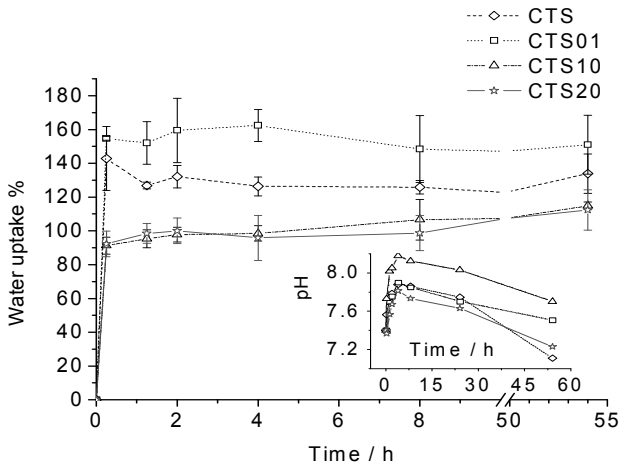

Figure 5.3 Swelling isotherms at 37ºC in ISS of chitosan membranes (CTS) and with crosslinker to chitosan amine groups molar ratio of 1% (CTS01), 10% (CTS10) and 20% (CTS20). Variation of pH during tests (inset graphics). Data represents mean ± standard deviation of at least three samples.

The results in Figure 5.4 show that the weight loss can be despised when performing mechanical tests on such membranes in wet state, since the time scale of such experiments is relatively short (only a few minutes) when compared to the time required to reach a significant weight loss.

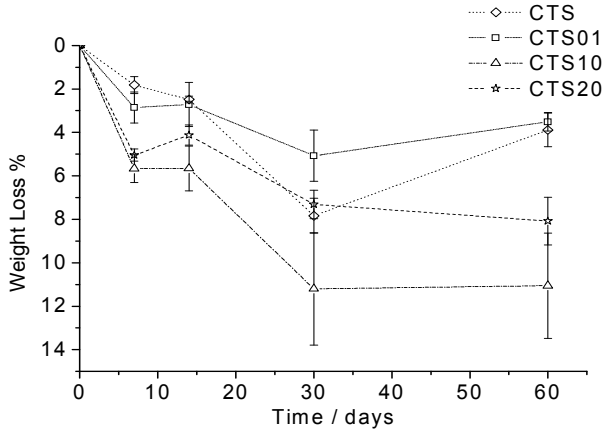

Figure 5.4 Degradation isotherms at 37ºC in ISS of chitosan membranes (CTS) and with crosslinker chitosan amine groups molar ratio of 1% (CTS01), 10% (CTS10) and 20% (CTS20). Data represents mean ± standard deviation of at least three samples.

5.4.3 Quasi-static mechanical properties

The results obtained for assays performed in dry state are presented in Table 5.1. No significant differences were found between neutralised and non-neutralised chitosan membranes for evaluated tensile mechanical properties in the dry state. Similar values of non-neutralised chitosan films have been reported by A. Bégin *et al* [2]. In order to evaluate the mechanical performance of the several prepared formulations in wet state, tensile tests were carried out in ISS. It was impossible to test membranes with higher degree of crosslinking (CTS20), because of its low resistance in wet state.

Table 5.1 Mechanical tensile properties of non-crosslinked chitosan (CTS) membranes (average ± standard deviation of at least three samples) performed in the dry state

	$E_{2\%}$ (GPa)	$\sigma_{at\ break}$ (MPa)	$\varepsilon_{at\ break}$ (%)
Non-neutralised	1.5 ± 0.6	52 ± 12	5.9 ± 0.5
Neutralised	1.8 ± 0.3	59 ± 11	4.9 ± 1.3

The mechanical resistance to stretching decreased sharply, when samples were swollen in the ISS. Secant modulus decreased about one hundredfold from 1.8 GPa to 13 MPa at room temperature, while stress at break decreased about tenfold from 59 MPa to 6.1 MPa at the same temperature. This is a consequence of the high equilibrium swelling degree. On the other hand, strain at failure increased from 4.9% to 59% due to the water plasticising effect. Typical stress-strain curves of samples tested as well as the corresponding relevant mechanical properties for all conditions studied are shown in Figure 5.5 and Figure 5.6, respectively.

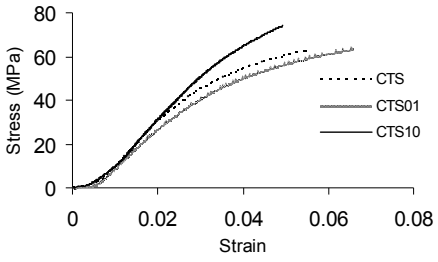

(a)

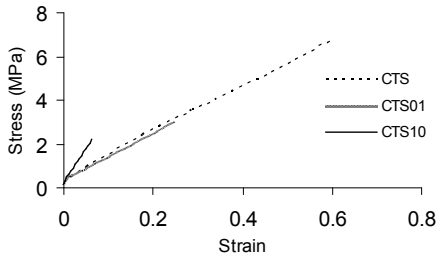

(b)

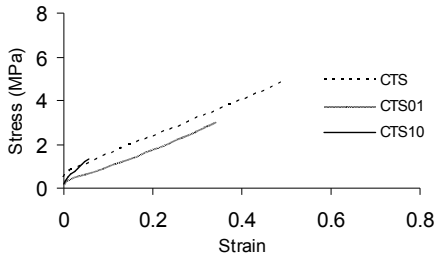

(c)

Figure 5.5 Typical stress-strain curves of membranes of non-crosslinked chitosan (CTS) and with crosslinker chitosan amine groups molar ratio of 1% (CTS01) and 10% (CTS10): **(a)** neutralised membranes tested in dry state at room temperature; **(b)** neutralised membranes tested in ISS at room temperature; **(c)** neutralised membranes tested in ISS at 37ºC.

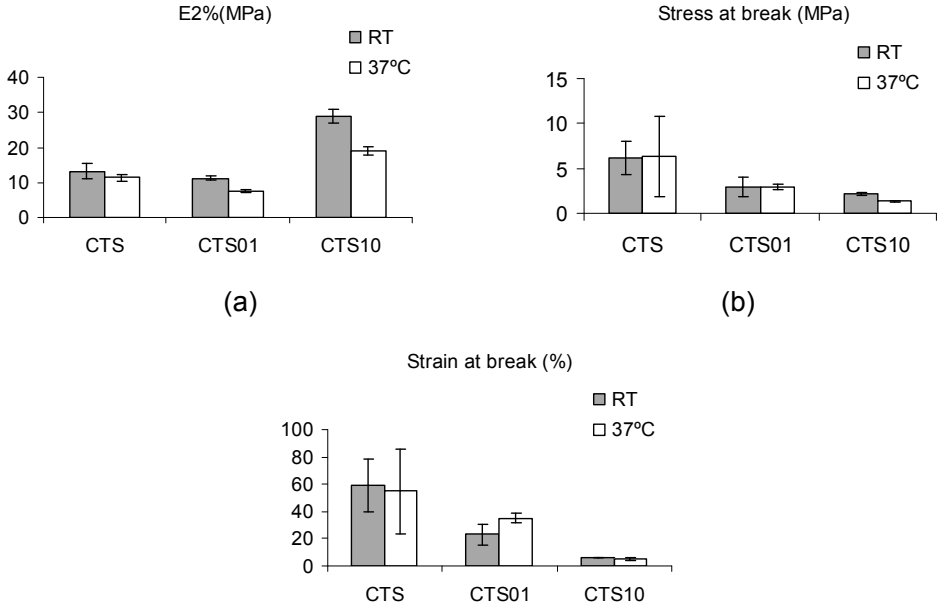

(a) (b)

(c)

Figure 5.6 Tensile properties of neutralised chitosan membranes non-crosslinked (CTS) and with crosslinker chitosan amine groups molar ratio of 1% (CTS01) and 10% (CTS10), measured in ISS: **(a)** secant modulus at 2% of elongation; **(b)** stress at break; **(c)** strain at break. Data represents mean ± standard deviation of at least three samples.

Secant tensile modulus at 2% decreased when a small amount of glutaraldehyde was used to crosslink chitosan (CTS01), for both temperatures tested. On the other hand, modulus increased for higher concentrations (CTS10). The minimum in stiffness found for CTS01 can be related with the maximum achieved for the equilibrium hydration degree for the same sample (Figure 5.3). However, a similar result was obtained for CTS01 tested in a dry

environment (results not showed). In this way, the balance between the effects of opposite variation of crystallinity and crosslinking degree may also have an effect on this behaviour, besides the hydration degree. It is well known that the elastic modulus increase when reducing the average molecular weight between crosslinks. However, in such a complex system where a semi-crystalline polymer is crosslinked with glutaraldehyde, which possesses a distinct chemical character from the original polymer, crystallinity, hydration degree and different hydrophilicity can also play a certain role. In this way, it is very difficult to correlate all those factors with the final viscoelastic properties of such materials.

At physiologic temperature the modulus decreased for each sample tested, relatively to what was observed at room temperature. Moreover, stress and strain at failure decreased when the crosslinking degree increased, since samples become fairly brittle for glutaraldehyde chitosan amine groups molar ratio of 10% (CTS10).

5.4.4 Dynamic mechanical analysis (DMA)

The storage modulus of non-crosslinked chitosan membranes (CTS) was almost constant during temperature scan, only showing a slight decrease around 40ºC (Figure 7a). On the other hand, both crosslinked samples (CTS01 and CTS10) storage modulus presented a continuous decrease with increasing temperature (Figures 7a and 7b) This is in agreement with the previously described decrease of the secant tensile modulus observed from room to physiological temperature. The slope of such curves seems to increase with crosslinking. All modulus values are quite similar to the values achieved for quasi-static tests and the same trends are basically observed.

The damping properties of the studied membranes are also depicted in Figure 5.7, as measured by the loss factor, tan δ. One founds values between 0.15 and 0.20, indicating a clear viscoelastic behaviour for the prepared chitosan membranes. This result is in accordance to the viscoelastic character also observed in meshes of chitosan fibres also analysed in wet conditions both by DMA and creep experiments [32]. It should be noticed in this context that most of the living tissues have viscoelastic properties. Thus, besides the conventional quasi-static mechanical properties, new materials to be used in biomedical applications should have compatible time-dependent mechanical (viscoelastic) features with the organs or tissues that they will contact with. Tests such as DMA experiments in simulated physiological conditions, as presented in this work, may constitute a valuable tool for this evaluation.

The results in Figure 5.7 indicates that crosslinking do not influence significantly the damping properties of the chitosan membranes. Moreover, for all formulations analysed, tan δ is

almost temperature independent, indicating that neither physical transition nor relaxation process take place within this temperature range.

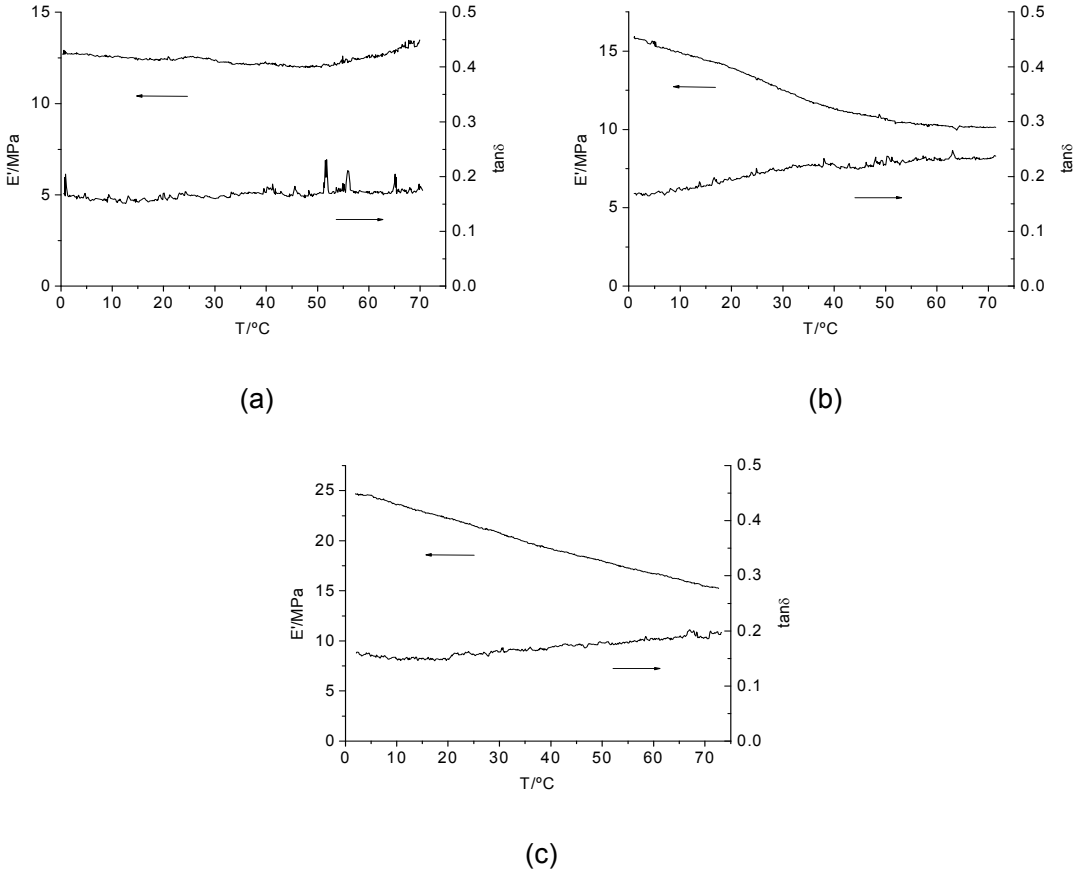

Figure 5.7 Storage modulus, *E*', and loss factor ,tan δ, at 1 Hz of neutralised chitosan membranes non-crosslinked (CTS) **(a)**, with crosslinker chitosan amine groups molar ratio of 1% (CTS01) **(b)** and 10% (CTS10) **(c)**, measured in ISS.

5.4.5 Cytotoxicity

Cells cultured in contact with the extracts of the materials after 72 hours displayed normal morphology when observed in an inverted light microscope. The results for the MTT test performed after 72 hours of contact of the extraction medium with cells are shown on Table 5.2, and allowed to assay, though qualitatively, the cellular viability. The percentage of cell viability plotted is related to the control, considering the control (cells with DMEM with 1% antibiotic/antimycotic and 10% FBS) to have 100% viability.

Table 5.2 MTT test and total protein quantification of neutralised chitosan membranes non-crosslinked (CTS) and with crosslinker to chitosan amine groups molar ratio of 1% (CTS01), 10% (CTS10) and 20% (CTS20). Data represents mean ± standard deviation of at least three samples

Sample	MTT value (%) *	Total Protein (µg)
control[Ŧ]	--	105.5 ± 22.9
CTS	74.9 ± 9.7	126.6 ± 23.9
CTS01	74.0 ± 9.3	87.8 ± 13.5
CTS10	75.4 ± 7.5	129.7 ± 15.8
CTS20	67.7 ± 9.9	132.0 ± 17.0

* viability related to the control, which is scored 100%
Ŧ Control: Cells with culture medium

All the samples present a viability percentage around 80%, which means that these materials do not exert a cytotoxic effect over the cells. It seems that growing concentrations of glutaraldehyde tend to have a negative effect over cell viability, although for the tested concentrations cell viability is maintained at a very good percentage (see Table 5.2). It is known from previous cytotoxic studies performed that increasing the glutaraldehyde concentration increases the cytotoxicity of the membranes (data not shown). Moreover, a similar trend was reported for collagen crosslinked with glutaraldehyde [33]. The results obtained can be considered as a good indicator of the biocompatibility of the tested materials, since it is known that for biodegradable polymers their degradation tends to induce a severe cytotoxic effect due to a pH drop (as for instance for polylactides and polyglycolides) [23].

As for the total protein quantification, Table 5.2 shows that only the cells in contact with the extract of the sample containing 1% glutaraldehyde as crosslinking agent (CTS01) displayed a slight smaller total protein content than the control. The other three samples (CTS, CTS10 and CTS20) displayed an even higher amount of total protein than the control. A possible explanation for this result is that the crosslinking strength of the membranes crosslinked with 1% of glutaraldehyde (CTS01) is lower than in the other conditions were glutaraldehyde is used as a crosslinker and, in this way, more leachables are obtained during the extraction in DMEM culture medium. So, the membranes non-crosslinked (CTS) would not leach components resulting from reaction with glutaraldehyde, while membranes crosslinked with 10 and 20% of glutaraldehyde (CTS10 and CTS20) would not leach those products in such an extent as in the formulation CTS01. In being so, the leachables of the formulation CTS01

will somehow inhibit the cellular activity, quantified by the protein production, but not diminishing their viability, as seen by MTT test.

The relation between the two tests (MTT and total protein quantification) is not, of course, straightforward, but some conclusions can be drawn from the comparison. The MTT test shows that all the conditions display similar viability patterns, around 80% when compared with the control, with the exception of the formulation CTS20 (a result in accordance with previous results obtained), that displays a level of 70% of viability. However, the total protein quantification shows that some of the conditions presented higher protein content than the control itself. This result can be explained by the fact that some of the leachables might in fact stimulate the activity of cells. In this way, the results between the two tests are perfectly complementary and coherent. Although further biocompatibility tests are needed, it is possible to say that the tested membranes have shown to be suitable for biomedical applications.

5.5 Conclusions

Different chitosan based membranes could be developed. A method was implemented to test tensile mechanical properties of chitosan-based membranes in ISS and 37ºC, in order to simulate body conditions. The mechanical resistance to stretching decreased sharply when swollen in an aqueous environment, mainly due to the high hydration equilibrium degree of chitosan materials. However, neutralised chitosan membranes and membranes crosslinked with small amounts of glutaraldehyde become more flexible, making them suitable for some biomedical applications, that could be wound dressing or as a barrier-membranes keeping space for bone regeneration and preventing the in-growth of undesirable connective tissue. Moreover, dynamic mechanical analysis in temperature scan mode confirmed the mechanical stiffness dependence on the temperature of crosslinked chitosan membranes. This dependence increased with the crosslinking degree. All formulations were found to be relatively stable in ISS up to 60 days. In fact, the weight loss was never superior than 12% and the membranes have kept its mechanical integrity.

All membrane formulations exhibit a viscoelastic behaviour which could have advantages in the mechanical compatibility with the tissues to be repaired.

The cell culture cytotoxicity studies performed indicate that there is a good interaction of the tested materials with the cells. The biochemical tests confirm that the viability of cells in contact with the extracts is maintained. In some cases an increased biochemical activity of cells is observed, which can be correlated indirectly with cell proliferation. In fact, the biological performance of the membranes seems to indicate that they can be used on the

proposed biomedical applications, although further cytocompatibility studies must be carried out before moving into any type of animal experimentation.

5.6 Acknowledgements

R. M. Silva was supported by the PhD Scholarship SFRH/BD/6862/2001 from the Portuguese Foundation for Science and Technology (FCT) under the POCTI programme. This work was partially supported by FCT through funds from the POCTI and/or FEDER programmes.

5.7 References

1. Kumar, M. N. V. R., A review of chitin and chitosan applications. *Reactive & Functional Polymers* **2000,** 46, (1), 1-27.
2. Begin, A.; Van Calsteren, M. R., Antimicrobial films produced from chitosan. *International Journal of Biological Macromolecules* **1999,** 26, (1), 63-67.
3. Rinaudo, M.; Pavlov, G.; Desbrieres, J., Influence of acetic acid concentration on the solubilization of chitosan. *Polymer* **1999,** 40, (25), 7029-7032.
4. Varum, K. M.; Holme, H. K.; Izume, M.; Stokke, B. T.; Smidsrod, O., Determination of enzymatic hydrolysis specificity of partially N-acetylated chitosans. *Biochimica Et Biophysica Acta-General Subjects* **1996,** 1291, (1), 5-15.
5. Varum, K. M.; Myhr, M. M.; Hjerde, R. J. N.; Smidsrod, O., In vitro degradation rates of partially N-acetylated chitosans in human serum. *Carbohydrate Research* **1997,** 299, (1-2), 99-101.
6. Aiba, S., Preparation of N-Acetylchitooligosaccharides from Lysozymic Hydrolysates of Partially N-Acetylated Chitosans. *Carbohydrate Research* **1994,** 261, (2), 297-306.
7. Nordtveit, R. J.; Varum, K. M.; Smidsrod, O., Degradation of partially N-acetylated chitosans with hen egg white and human lysozyme. *Carbohydrate Polymers* **1996,** 29, (2), 163-167.
8. Kurita, K.; Kaji, Y.; Mori, T.; Nishiyama, Y., Enzymatic degradation of beta-chitin: susceptibility and the influence of deacetylation. *Carbohydrate Polymers* **2000,** 42, (1), 19-21.
9. Tomihata, K.; Ikada, Y., In vitro and in vivo degradation of films of chitin and its deacetylated derivatives. *Biomaterials* **1997,** 18, (7), 567-575.

10. Kurita, K., Controlled functionalization of the polysaccharide chitin. *Progress in Polymer Science* **2001,** 26, (9), 1921-1971.

11. Muzzarelli, R. A. A., Biochemical Significance of Exogenous Chitins and Chitosans in Animals and Patients. *Carbohydrate Polymers* **1993,** 20, (1), 7-16.

12. Sridhar, S.; Susheela, G.; Reddy, G. J.; Khan, A. A., Crosslinked chitosan membranes: characterization and study of dimethylhydrazine dehydration by pervaporation. *Polymer International* **2001,** 50, (10), 1156-1161.

13. Krajewska, B., Diffusional properties of chitosan hydrogel membranes. *Journal of Chemical Technology and Biotechnology* **2001,** 76, (6), 636-642.

14. Risbud, M. V.; Bhat, S. V., Properties of polyvinyl pyrrolidone/beta-chitosan hydrogel membranes and their biocompatibility evaluation by haemorheological method. *Journal of Materials Science-Materials in Medicine* **2001,** 12, (1), 75-79.

15. Musale, D. A.; Kumar, A., Effects of surface crosslinking on sieving characteristics chitosan/poly(acrylonitrile) composite nanofiltration membranes. *Separation and Purification Technology* **2000,** 21, (1-2), 27-38.

16. Wang, X. P.; Feng, Y. F.; Shen, Z. Q., Pervaporation properties of a three-layer structure composite membrane. *Journal of Applied Polymer Science* **2000,** 75, (6), 740-745.

17. Ge, J. J.; Cui, Y. F.; Yan, Y.; Jiang, W. Y., The effect of structure on pervaporation of chitosan membrane. *Journal of Membrane Science* **2000,** 165, (1), 75-81.

18. Mi, F. L.; Tan, Y. C.; Liang, H. C.; Huang, R. N.; Sung, H. W., In vitro evaluation of a chitosan membrane cross-linked with genipin. *Journal of Biomaterials Science-Polymer Edition* **2001,** 12, (8), 835-850.

19. Mi, F. L.; Sung, H. W.; Shyu, S. S., Synthesis and characterization of a novel chitosan-based network prepared using naturally occurring crosslinker. *Journal of Polymer Science Part a-Polymer Chemistry* **2000,** 38, (15), 2804-2814.

20. Li, F.; Liu, W. G.; De Yao, K., Preparation of oxidized glucose-crosslinked N-alkylated chitosan membrane and in vitro studies of pH-sensitive drug delivery behaviour. *Biomaterials* **2002,** 23, (2), 343-347.

21. Monteiro, O. A. C.; Airoldi, C., Some studies of crosslinking chitosan-glutaraldehyde interaction in a homogeneous system. *International Journal of Biological Macromolecules* **1999,** 26, (2-3), 119-128.

22. Mendes, S. C.; Reis, R. L.; Bovell, Y. P.; Cunha, A. M.; van Blitterswijk, C. A.; de Bruijn, J. D., Biocompatibility testing of novel starch-based materials with potential application in orthopaedic surgery: a preliminary study. *Biomaterials* **2001,** 22, (14), 2057-2064.

23. Marques, A. P.; Reis, R. L.; Hunt, J. A., The biocompatibility of novel starch-based polymers and composites: in vitro studies. *Biomaterials* **2002,** 23, (6), 1471-1478.

24. Gomes, M. E.; Reis, R. L.; Cunha, A. M.; Blitterswijk, C. A.; de Bruijn, J. D., Cytocompatibility and response of osteoblastic-like cells to starch-based polymers: effect of several additives and processing conditions. *Biomaterials* **2001,** 22, (13), 1911-1917.

25. Salgado, A. J.; Gomes, M. E.; Chou, A.; Coutinho, O. P.; Reis, R. L.; Hutmacher, D. W., Preliminary study on the adhesion and proliferation of human osteoblasts on starch-based scaffolds. *Materials Science & Engineering C-Biomimetic and Supramolecular Systems* **2002,** 20, (1-2), 27-33.

26. Mosmann, T., Rapid Colorimetric Assay for Cellular Growth and Survival - Application to Proliferation and Cyto-Toxicity Assays. *Journal of Immunological Methods* **1983,** 65, (1-2), 55-63.

27. Slater, T. F.; Sawyer, B.; Strauli, U., Studies on Succinate-Tetrazolium Reductase Systems .3. Points of Coupling of 4 Different Tetrazolium Salts. *Biochimica Et Biophysica Acta* **1963,** 77, (3), 383.

28. Smith, P. K.; Krohn, R. I.; Hermanson, G. T.; Mallia, A. K.; Gartner, F. H.; Provenzano, M. D.; Fujimoto, E. K.; Goeke, N. M.; Olson, B. J.; Klenk, D. C., Measurement of Protein Using Bicinchoninic Acid. *Analytical Biochemistry* **1985,** 150, (1), 76-85.

29. Reis, R. L.; Mendes, S. C.; Cunha, A. M.; Bevis, M. J., Processing and in vitro degradation of starch/EVOH thermoplastic blends. *Polymer International* **1997,** 43, (4), 347-352.

30. Winblade, N. D.; Schmokel, H.; Baumann, M.; Hoffman, A. S.; Hubbell, J. A., Sterically blocking adhesion of cells to biological surfaces with a surface-active copolymer containing poly(ethylene glycol) and phenylboronic acid. *Journal of Biomedical Materials Research* **2002,** 59, (4), 618-631.

31. Hwang, K. T.; Kim, J. T.; Jung, S. T.; Cho, G. S.; Park, H. J., Properties of chitosan-based biopolymer films with various degrees of deacetylation and molecular weights. *Journal of Applied Polymer Science* **2003,** 89, (13), 3476-3484.

32. Tuzlakoglu, K.; Alves, C. M.; Mano, J. F.; Reis, R. L., Production and characterization of chitosan fibers and 3-D fiber mesh scaffolds for tissue engineering applications. *Macromolecular Bioscience* **2004,** 4, (8), 811-819.

33. Scotchford, C. A.; Cascone, M. G.; Downes, S.; Giusti, P., Osteoblast responses to collagen-PVA bioartificial polymers in vitro: the effects of cross-linking method and collagen content. *Biomaterials* **1998,** 19, (1-3), 1-11.

Chapter 6

Transport of small anionic and neutral solutes through chitosan membranes: dependence on crosslinking and chelation of divalent cations

6.1 Abstract

Chitosan membranes were prepared by solvent casting and crosslinked with glutaraldehyde at several ratios under homogenous conditions. The crosslinking degree, varying from 0 to 20%, is defined as the ratio between the total aldehyde groups and the amine groups of chitosan. Permeability experiments were conducted using a side-by-side diffusion cell to determine the flux of small molecules of similar size, but holding different chemical moieties, either ionised (benzoic acid, salicylic acid and phthalic acid) or neutral (2-phenylethanol) at physiological pH. The permeability of the different model molecules revealed to be dependent on the affinity of those structurally similar molecules to chitosan, i.e., related to the partition coefficient determined in an independent experiment. The permeability of the salicylate anion was enhanced by the presence of metal cations commonly present in biological fluids, such as calcium and magnesium, but remained unchanged for the neutral 2-phenylethanol. This effect could be explained by the chelation of metal cations on the amine groups of chitosan, which increased the partition coefficient. The crosslinking degree was also correlated with the permeability and partition coefficient. The change in the permeation properties of chitosan to anionic solutes in the presence of these metallic cations is an important result, and should be taken into consideration when trying to make *in vitro* predictions of the drug release from chitosan based controlled release systems.

This chapter is based on the following publication:
Ricardo M.P. da Silva, Sofia G. Caridade, Julio San Román, João F. Mano; Rui L. Reis. Transport of small anionic and neutral solutes through chitosan membranes: dependence on crosslinking and chelation of divalent cations (submitted).

6.2 Introduction

Chitin is a structural polysaccharide of the cell wall of fungi and of the exoskeleton of most invertebrates, of which crustaceans are the major source for the industry [1]. The chitin similarities to cellulose encompass function, chemical structure and abundance. It is estimated as being one of the most abundant natural macromolecules in the biosphere [1]. Besides its importance as building and structural material in biological organisms, chitin is becoming a key raw material in engineering and emergent technologies, largely due to its soluble derivative, chitosan. Chitosan has been proposed for a large number of applications in the biomedical field [2-11], in great part owning to its biocompatibility, biodegradability and non-toxicity [12]. In fact, this natural derived polymer has been proposed for controlled drug release devices [2, 3], rate controlling membranes in transdermal delivery systems [4, 5], biomaterials [6-8] and tissue engineering [9-11]. Although, it was found that native chitosan membranes do not support cell adhesion and proliferation [13, 14], we have recently be able to render chitosan membranes surface properties appropriate for cell adhesion and behaviour [8, 9]. Recent strategies, incorporated growth factors in chitosan-based scaffolds demonstrated the usefulness of the chitosan permeability for the local drug controlled release inside the scaffolds [15-17]. On the other hand, survival of *ex vivo* constructed tissues after transplantation is often limited by insufficient oxygen and nutrient supply. Strategies aiming at the improvement of neovascularization of engineered tissues are considered a key issue [18, 19]. Scaffolds can work as an additional route for the elimination of excreted toxic products and for the supply of nutrients, if those molecules can permeate through the polymeric support. Although, this would not constitute a truly alternative strategy for the improvement of neovascularization of engineered tissues, it would help on the survival of the tissue engineered transplants.

Both in tissue engineering and drug delivery strategies the knowledge and control of the permeability of chitosan-based materials is very important. On the other hand, the well-known ability of chitosan to complex with divalent cations [20-23] can interfere with the permeability of anionic molecules through chitosan materials in physiological medium. In fact, human blood plasma possess typical Ca^{2+} and Mg^{2+} concentration of 2.5 and 1.5 mM [24]. To our knowledge, until now the studies on the permeability of chitosan to several model drugs and solutes have ignored this hypothesis. In the present study, we tested the influence of the binding ability of divalent cations on the permeation of small anionic solutes and its dependence on the crosslinking degree.

Finally, the importance of studying the influence of ionic species able to complex with polyelectrolytes on the permeability is not limited to the chitosan-based permeable system

that is presented as a case-study. In fact, there is a broad list of other polyelectrolytes, both polysaccharides [25-27] and synthetic polymers [28-30], which are able to form complexes with multivalent ions. Polyelectrolyte hydrogels are important systems for controlled drug release applications, due to their (pH and electric) stimuli-responsive nature [31-33].

6.3 Materials and methods

6.3.1 Purification and characterisation of chitosan

Chitosan (CTS) raw-material obtained from crab shells was purchased from Sigma-Aldrich (USA) and purified by re-precipitation. First, the chitosan was dissolved in an aqueous acetic acid solution (1% w/v) at ~1% (w/v). The solution was filtered through a Whatman® ashless filter paper (20-25 μm) to remove the insoluble material and producing a clear solution. This solution was precipitated adding a NaOH solution (final pH ~ 8) forming a white gel, which was sieved to remove the exuded liquid and thoroughly rinsed with distilled water, until no changes on the pH were detected. The chitosan gel was further washed/dehydrated with ethanol, freeze-dried, ground to powder and dried at 60ºC overnight. All other reagents were used without further purification.

The chitosan average molecular weight was of found to be 790 kDa by viscometry in CH_3COOH 0.5 M/ $NaCH_3COO$ 0.2 M, according to the Mark-Houwing theory ($k = 3.5x10^{-4}$; $a = 0.76$) [34]. The degree of *N*-deacetylation (DD) was found to be 93.3% by means of 1st derivative UV spectrophotometry, using both glucosamine (GluN) and *N*-acetylglucosamine (GluNAc) standards for calibration [35].

6.3.2 Preparation of chitosan membranes by solvent casting

The chitosan solution was prepared by dissolving chitosan (1 wt.%) in 1 wt.% acetic acid solution. Glutaraldehyde (GA) solutions at concentrations ranging from 0.1 M to 5 x 10^{-4} M were prepared. The amount of chitosan amine groups (NH_2) (GluN units) can be determined using the following expression:

$$n_{(GluN)} = \frac{m_{(CTS)}}{\left[M_g + \frac{1-DD}{DD} M_a \right]} \qquad (6.1)$$

where M_a = 203 g/mol and M_g = 161 g/mol are the molecular weights of the GluNAc and GluN units within the copolymer, $m_{(CTS)}$ is dry weight of chitosan in grams and $n_{(GluN)}$ is the molar amount of amine groups in that weight of chitosan.

Then, defining the crosslinking degree (x) as the percentage of aldehyde (CHO) groups with respect to the initial free NH_2 groups (CHO/NH_2 ratio), we can write:

$$x(\%) = \frac{n_{(CHO)}}{n_{NH_2}} \times 100 = \frac{2n_{(GA)}}{n_{(GluN)}} \times 100 \qquad (6.2)$$

and it follows that:

$$x(\%) = \frac{2V_{(GA)}C_{(GA)} \times \left(M_g + \frac{1-DD}{DD} M_a \right)}{m_{(CTS)}} \times 100 \qquad (6.3)$$

where $V_{(GA)}$ and $C_{(GA)}$ are respectively the volume and concentration of the glutaraldehyde solutions. Actually, the crosslinking degree defined by equation 6.2 is the reagents feed ratio, since the real crosslinking efficiency depends upon the chemical conversion and on the occurrence of other parallel reactions, which can form either any or longer crosslinks.

The glutaraldehyde solution volume added to a certain amount of the previous chitosan solution was kept constant. The several crosslinking degrees were obtained by only changing the concentration of glutaraldehyde, according to equation 6.3. In this way, the reaction volume and polymer concentration was kept constant for all the samples, varying only the molar amount of glutaraldehyde added. The glutaraldehyde solutions was added dropwise during 5 min under gentle stirring and the resultant solutions were let quiescent for about 1 h to remove any air bubble formed. Non-crosslinked chitosan membranes (CTS00) were prepared in the same way, but no glutaraldehyde solution was added. Solutions were poured into Petri dishes and dried at room conditions. The resultant membranes were neutralised in NaOH 0.1 M solution for 10 min, washed thoroughly with distilled water and dried again. Samples were labelled according to their crosslinking degree as CTS[x(%)]. For instance, samples with x = 0.1%, 1% and 20% were labelled as CTS0.1, CTS01 and CTS20, respectively.

6.3.3 Fourier Transform infrared spectroscopy with attenuated total reflection (FTIR - ATR)

Membranes of both non-crosslinked chitosan (CTS00) and crosslinked at the highest ratio (CTS20) were analysed by infrared spectroscopy to assess the proposed mechanisms for the reaction of chitosan with glutaraldehyde, which may depend on the reaction conditions [20,

[36, 37]. Spectra were recorded in an IRPrestige 21 FTIR spectrophotometer from Shimadzu (Kyoto, Japan) with the attenuated total reflection accessory (128 scans, resolution 4 cm^{-1}).

6.3.4 X-ray diffraction (XRD)

The morphology of the membranes was analysed recording the wide-angle X-ray scattering (WAXS) pattern in a Philips PW1710 reflection diffractometer (Almelo, the Netherlands), with a step (2θ = 0.02º) scanning time of 2 s and Cu-Kα-radiation generated at 40 kV and 30 mA.

6.3.5 Water contact angle measurements

The influence of the glutaraldehyde crosslinking on the hydrophilicity of the materials was assessed evaluating the surface wettability by water contact angle measurements. Static contact angle measurements were carried out by the sessile drop method using a contact angle meter OCA 15+ with high-performance image processing system from DataPhysics Instruments (Filderstadt, Germany). A drop (1 μL) of water was added by a motor driven syringe at room temperature. Two different samples of each material were used and at least three measurements were carried out for each sample.

6.3.6 Equilibrium swelling studies

The water uptake measurements were undertaken in two different buffer systems, both at pH 7.4 and ionic strength 0.154 M. Phosphate buffer saline (PBS) solution was prepared dissolving PBS tablets from Sigma in a suitable amount of water (NaCl 0.137 M; KCl 0.0022 M; phosphate buffer 0.01M; pH 7.4 at 25ºC). A second solution (TRIS-Ca^{2+}/Mg^{2+}) was prepared with 1.5mM of $MgCl_2$ and 2.5 mM $CaCl_2$, to give the typical Ca^{2+} and Mg^{2+} concentration of this cations in the human blood plasma [24]. This solution was buffered with 0.01M TRIS and adding HCl until pH was 7.40 ± 0.05 at 25ºC. Ionic strength was corrected with NaCl to give 0.154 M.

The equilibrium water uptake was determined immersing previously weighted chitosan membranes in these buffer systems at 37 ± 1 ºC. We previously found that the water uptake kinetics is very fast, reaching the equilibrium in less than 15 min [6]. After around 4 h, equilibrated samples were blotted with filter paper to remove the adsorbed water and

weighted immediately. The equilibrium water uptake (WU_{eq}) was calculated using the following equation:

$$WU_{eq} = \frac{W - W_0}{W_0} \quad (6.4)$$

where W_0 is the initial weight of the sample and W is the weight of the swelled sample.

6.3.7 Permeation studies

The permeation studies were performed using an in-house built side-by-side diffusion cell (see Figure 6.1). Membranes were previous equilibrated in the respective buffer solution and mounted between the half-cells of the receptor and donor compartments (1 cm^2 area of diffusion). The receptor compartment fluid was continuously pumped through a flow-through quartz cuvette with optical pathway (l) of 1 cm. The absorbance at a maximum wavelength (different for each solute) was monitored in a UV-1610 Shimadzu spectrophotometer. The volume of the monitoring system (tubing and quartz cuvette) was calibrated before each experiment and it was found to vary between 2.84 and 2.90 ml. The monitoring system was filled with fresh buffer and air bubbles were purged before each measurement. The inlet and outlet tubing was connected to the receptor cell previously filled with 2.2 ml of fresh buffer. Then, the diffusion cell was immersed in a thermostatic bath at 37.0 ± 0.1ºC. Finally, the donor cell was filled with 2.2 ml of the buffer solution containing the respective solute and the absorbance recorded. The solutions in both cells were stirred by magnetic bars at 800 rpm to eliminate the boundary layer effect. In preliminary experiments, we confirmed that the calculated permeability was kept constant above 400 rpm.

The permeability of the chitosan membranes was evaluated for small molecules of similar size, but holding different chemical moieties, either ionised (anionic) or neutral at physiological pH (see Figure 6.2). Moreover, solutes with different ionic charges were tested by choosing monoprotic and diprotic acids that are fully ionised at that pH (see Table 6.1). The solutions of the anionic solutes, such as benzoic acid (BA), salicylic acid (SA), phthalic acid (Ph), were prepared at 5 mM, 2 mM and 5 mM, respectively. Since these molecules at the working concentration are able to change the pH of the buffer solution, this was further corrected to pH 7.4 with NaOH solution. The solution of 2-phenylethanol (PE) was prepared at a concentration of 10 mM. The different concentrations used took into consideration the different molar absorptivities, in order to allow the detection of the solutes at the early stages of permeation experiments (see Table 6.1). The flux rate of those model molecules was determined in both PBS and buffered TRIS-Ca^{2+}/Mg^{2+} solutions, the same used in the water

uptake experiments. After each assay, the swollen membrane thickness was taken as a mean of five values at different points measured with a low-pressure micrometer.

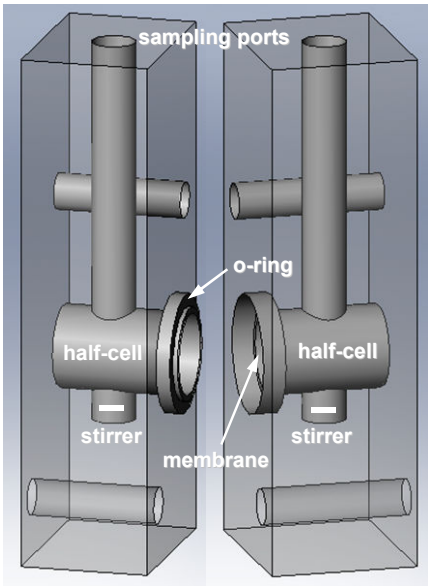

Figure 6.1 Schematic representation of the in-house built side-by-side diffusion cell.

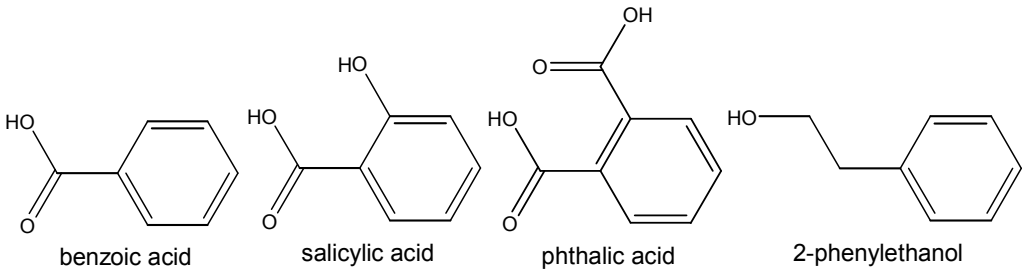

Figure 6.2 Chemical structures of the model solutes used in the permeation studies.

Table 6.1 Acidity constants (pK_a), wavelength of maximum UV absorbance ($\lambda_{máx}$), molar absorptivity (ε) at $\lambda_{máx}$ for the different model solutes and optical pathway (l) of the flow-through cuvette

Solute	**pK_{a1}**	**pK_{a2}**	**$\lambda_{máx}$ (nm)**	**1/(εl) (mM)**
benzoic acid (BA)	4.20[38]	-	270	1.747
salicylic acid (SA)	3.23[38]	-	297	0.2816
phthalic acid (Ph)	2.73[39]	4.78[39]	273	1.192
2-phenylethanol (PE)	-	-	258	5.244

6.3.8 Determination of the partition coefficients

The partition coefficient (*K*) was considered the ratio of the solute concentration in the liquid fraction absorbed by each sample (C_m) to that in the bulk solution (C_s) [40]:

$$K = \frac{C_m}{C_s} \tag{6.5}$$

It was determined in both PBS and buffered TRIS-Ca^{2+}/Mg^{2+} solutions. First the membrane samples were equilibrated for 48 h in a solution of each model molecule at a concentration (C_s) 5 times higher than that used in the permeation experiments. The pH of the buffer solutions was corrected to pH 7.4 with NaOH solution after the solubilisation of each acid solute. When compared with the amount of membrane sample, the volume of the concentrated solution was higher enough to consider that C_s did not vary during the solute uptake stage. The membrane was removed from the concentrated solution and the excess of liquid was removed blotting the membrane with filter paper. The water uptake of each sample was determined as described for the equilibrium water uptake experiments. Loaded membranes were immersed in fresh buffer and this procedure was repeated until no further release was observed by UV spectrophotometry. The amount of the solute uptake was calculated as the total cumulative release and C_m determined accordingly.

6.4 Results and discussion

6.4.1 Analysis of the crosslinking reaction

Several mechanisms have been proposed for the reaction of chitosan with glutaraldehyde, the simplest involving the formation of one Schiff base between one of the aldehyde groups and an amine group of chitosan, remaining the other aldehyde group free [20, 37]. This aldehyde group may react with other chitosan chains to form a crosslink, but can also remain free, immobilised within the formed polymer network [37]. A third mechanism may encompass the polymerisation of gluraldehyde which would form longer crosslinking bridges [20, 37]. Roberts *et al* [36] found that under several reaction conditions only a very small proportion (< 0.15%) of the aldehyde groups undergone an aldol condensation reaction leading to α,β-unsaturated aldehyde groups. In turn, Monteiro *et al* [20] found evidence of double ethylenic bonds above a certain glutaraldehyde/chitosan proportion. In our study, the ratio CHO/NH_2 should be low enough to keep the glutaraldehyde polymerisation at a very small proportion. The infrared spectrum of the membranes with the highest crosslinking degree (CTS20) is quite similar to

the spectrum of the non-crosslinked membrane (CTS00) (Figure 6.3). In the chitosan spectrum, the band at 1651 cm^{-1} (amide I) is assigned to the remaining acetyl groups of chitosan and the NH_2 characteristic absorption band is observed at 1591 cm^{-1} (amide II). In the spectrum of CTS20 the amide I band increases proportionally to the amide II band. The contribution of the imine (C=N) bond at around 1660 cm^{-1} [20, 37] from the formed Schiff bases upon crosslinking superimpose the amide I band of chitosan, leading to that change in the spectrum.

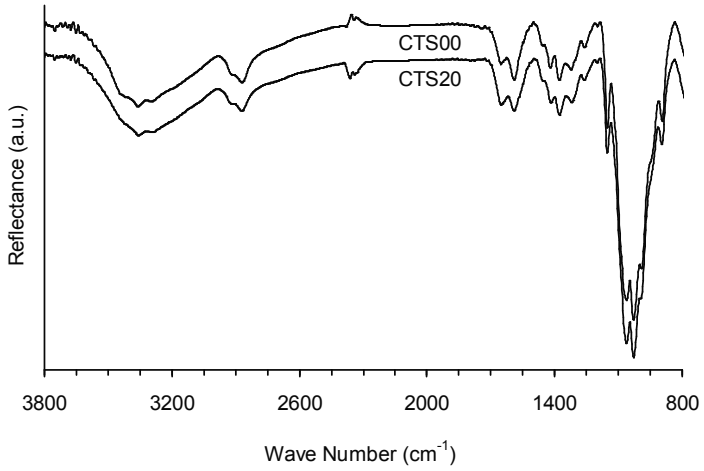

Figure 6.3 FTIR-ATR spectra of non-crosslinked chitosan membranes (CTS00) and at the highest crosslinking degree (CTS20).

On the other hand, it is not observed the signal of the carbonyl groups at around 1720-1730 cm^{-1}. Since in this region of the spectrum of chitosan did not present any absorption band, this constitutes a good indication that under this homogeneous reaction conditions, most of the glutaraldehyde molecules established crosslinks between chitosan chains, being involved in the formation of two Schiff bases. It should be notice that under heterogeneous reaction conditions it has been reported the appearance of this CHO band [37]. Finally, the water contact angle almost did not change with the reaction with glutaraldehyde molecules (Table 6.2), indicating that the overall hydrophilicity of the membranes was not affected.

Table 6.2 Water contact angle of non-crosslinked chitosan membranes (CTS00) and at the highest crosslinking degree (CTS20) (average ± standard deviation)

Sample	Contact angle (º)
CTS00	93.2 ± 2.1
CTS20	91.0 ± 0.9

6.4.2 Morphological characterisation of chitosan membranes

Chitosan is a semi-crystalline polymer from which several polymorphs have been mentioned in the literature [41-43]. Chitosan molecular weight [42], DD [44] and different membrane processing methods gave origin to substantial variations in the presence and amounts of the different polymorphs [42, 43].

Samuels [41] reported that chitosan has two distinct crystal forms, both orthorhombic. The crystal type I has the strongest reflection at 2θ = 11.4º, whereas the type II crystal strongest reflection falls at 2θ = 20.1º. As can be observed in Figure 6.4, the non-crosslinked chitosan membranes (CTS00) showed the strongest reflection at 2θ ≈ 20º and a weaker reflection at 2θ ≈ 10º, according to the typical chitosan diffractogram. Moreover, it was also possible to observe a reflection at around 2θ ≈ 15º. Ogawa *et al* [42, 43] described that annealed chitosan membranes cast from acetic acid and neutralised with NaOH may also present an anhydrous crystal form exhibiting a strong reflection at 2θ ≈ 15º. The crosslinking of chitosan under homogenous conditions produce a gradual effect on the WAXS patterns, manifested by a decrease in the reflection at 2θ ≈ 15º already noticed at low degrees of crosslinking (CTS0.5) and the weakening and disappearance of reflections at 2θ ≈ 10º and 2θ ≈ 15º on approaching the maximum crosslinking degree (CTS20). Surprisingly, the reflection at 2θ ≈ 20º related to the type II crystal did not disappear, showing that the chitosan membranes retain the semi-crystalline morphology up to a crosslinking degree of 20%.

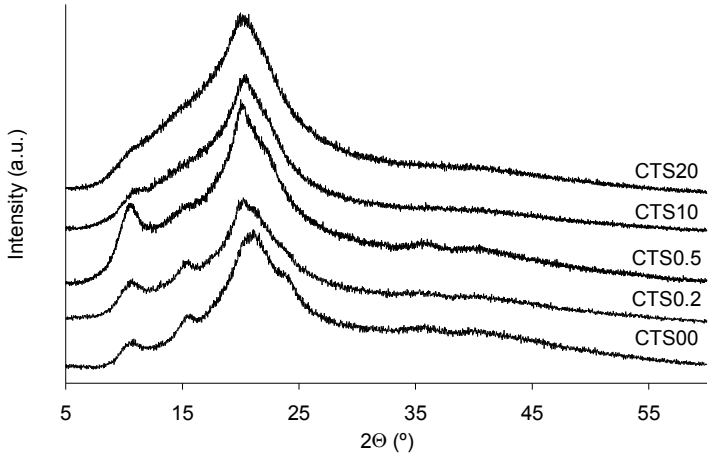

Figure 6.4 WAXS diffraction patterns for chitosan membranes with crosslinking degrees ranging from 0 up to 20%.

These results do not agree with our previous findings [6] that crystallinity was highly depressed for lower crosslinking degrees and that for higher degrees membranes were completely

amorphous. Nevertheless, those membranes had been prepared from chitosan with lower DD [6], which can explain the difference in the results.

6.4.3 Chitosan membranes equilibrium swelling degree and the influence of crosslinking

The chitosan membranes equilibrium water uptake increased steadily until a crosslinking degree of approx. 10% (CTS10), oppositely to what would be expected (see Figure 6.5). It is well documented that as higher is the crosslinking degree of a hydrogel, as lower is its swelling ratio. Crosslinking reduces the number average molecular weight between crosslinks and the mesh size, imposing restrictions to the entrance of water molecules and to the polymer chains relaxation [45, 46]. In fact, a further increase in the crosslinking degree of the chitosan membranes was effective in lowering the equilibrium water uptake.

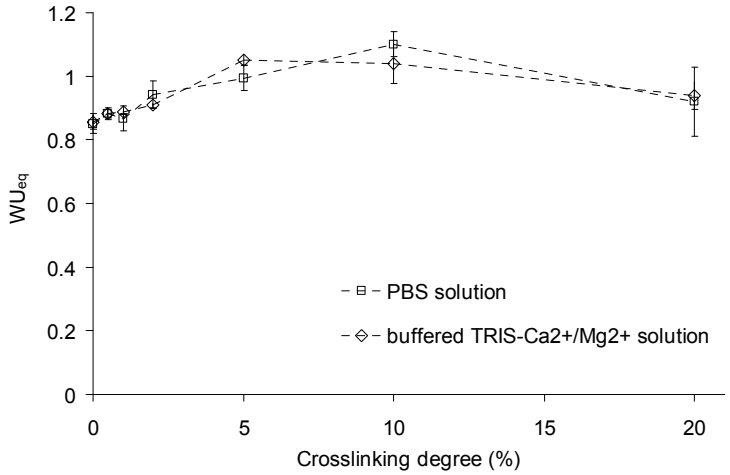

Figure 6.5 Water uptake (equation 6.4) of chitosan membranes in function of the crosslinking degree, either determined in PBS solution or in buffered TRIS-Ca^{2+}/Mg^{2+} solution. Data represents mean ± standard deviation for n=3.

This atypical behaviour of the chitosan membranes at the low range crosslinking degrees have been already described in one of our previous works in which membranes were prepared using chitosan with lower DD [6]. That result had been well correlated with a sharp reduction in the crystallinity degree already noticeable for faintly crosslinked membranes [6]. In the herein reported results the decrease in the crystallinity, which is only related to the disappearance of reflections at $2\theta \approx 10^{o}$ and $2\theta \approx 15^{o}$ (Figure 6.4), can also explain the increase in the equilibrium water uptake shown in Figure 6.5. Chitosan chains possess a large number of chemical moieties able to perform hydrogen bonds, and then it is reasonable

to consider that a certain number of hydrogen bonds may be disorderedly established between polymer chains in the amorphous regions. It is also reasonable to considering that the absorbed water in the swollen state did not disrupt all these physical crosslinks. In fact, at low activities water sorption in chitosan membranes occur on polymer-specific sites [47] until a limit of 2 water molecules per monomer unit. Above this limit, the sorption behaviour is consistent with the formation of clusters of water molecules [47]. Water molecules may bind both on hydroxyl and amino groups [48], which suggests that those polymer-specific sites are the pyranosyl side substituents and confirm that not all of these groups able to hydrogen bond are available to bind water molecules. Being so, the introduction of small amounts of crosslinker produces steric hindrance, which can reduce the ability of the polymer to establish intermolecular hydrogen bonds, enhancing the water molecules accessibility. The hydration water uptake should depend simultaneously on the balance between crystallinity, hydrogen bonding between chitosan chains in the amorphous phase and the crosslinking degree.

Finally, the equilibrium water uptake was insensitive to the presence of Ca^{2+} and Mg^{2+} in the buffer solution. The well-known ability of chitosan to form complexes with divalent cations [21, 22] did not influence the water uptake ability, at least at the physiological concentrations of calcium and magnesium.

6.4.4 Permeability of chitosan membranes

The diffusive mass transport is described by the Fick's first law:

$$J = -D\frac{dC}{dy} \tag{6.6}$$

where J is the flux, D is the diffusion coefficient, C is the solute concentration and y is the distance in the direction perpendicular to the membrane.

The simplest solution of the diffusion equation can be obtained at the steady-state, where flux is a constant and it can be maintained if the solute concentration is kept constant at the both donor (C_D) and receptor (C_R) half-cells. The Fick's first law may be then rewritten as:

$$J = -DK\frac{(C_D - C_R)}{0 - \delta} = \frac{P}{\delta}(C_D - C_R) \tag{6.7}$$

where K is the partition coefficient (equation 6.5), δ is the membrane thickness and P the permeability, such as:

$$P = DK \tag{6.8}$$

The solute flux can be determined measuring the concentration in the receptor compartment, using the following equation:

$$J = \frac{V_R}{A}\left(\frac{dC_R}{dt}\right) \tag{6.9}$$

where V_R is the volume of the receptor half-cell (including the volume of the UV spectrophotometry monitoring system) and A is the membrane useful mass transfer area.

The initial permeation stage is termed the lag time, when the drug is not detected in the receptor compartment. After the lag time, the concentration gradient inside the membrane is completely developed and the steady-state permeation stage is observed. At this pseudo-steady-state the concentration can be considered to vary linearly with time, this is, the flux is approximately constant [40, 49, 50]. The assumption is valid for the sink conditions, which are maintained while $C_D >> C_R$, this is:

$$C_D - C_R \approx C_D \tag{6.10}$$

Typical curves of the early permeation stage of the studied drugs through chitosan membranes are shown in Figure 6.6, normalised by the membrane thickness, which show a linear profile without a measurable lag time. This means that flux is constant within that time interval and that the sink conditions are maintained. The slope of the permeation curves was estimated by linear regression at that early release stage (correlation factor > 0.99).

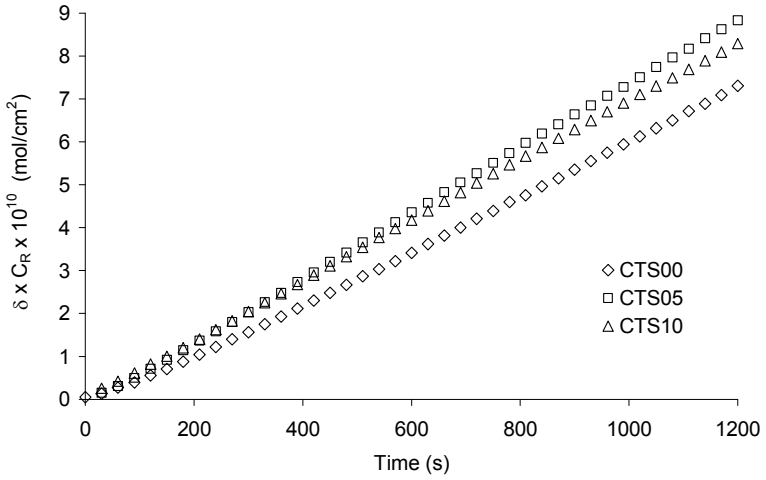

Figure 6.6 Typical curves of the variation of the concentration (C_R) of salicylic acid in the receptor compartment normalised by the membrane thickness (δ).

The permeability, P, was then calculated combining and rearranging equations 6.7, 6.9 and 6.10 to obtain:

$$P = \frac{V_R}{A}\left(\frac{dC_R}{dt}\right)\frac{\delta}{C_D} \tag{6.11}$$

where C_D is taken as the initial concentration at the donor compartment.

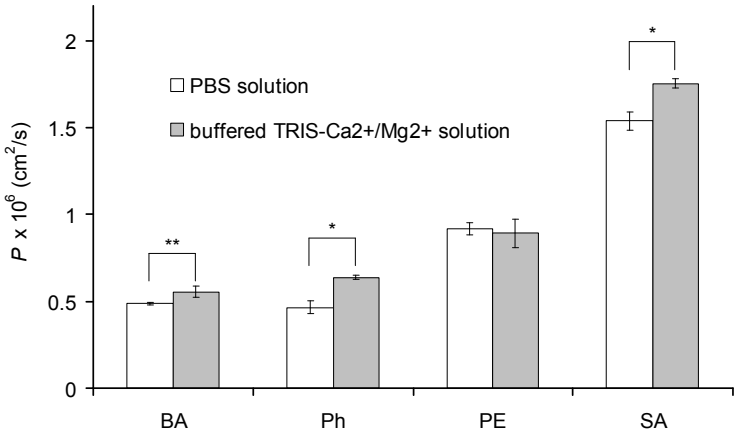

(a)

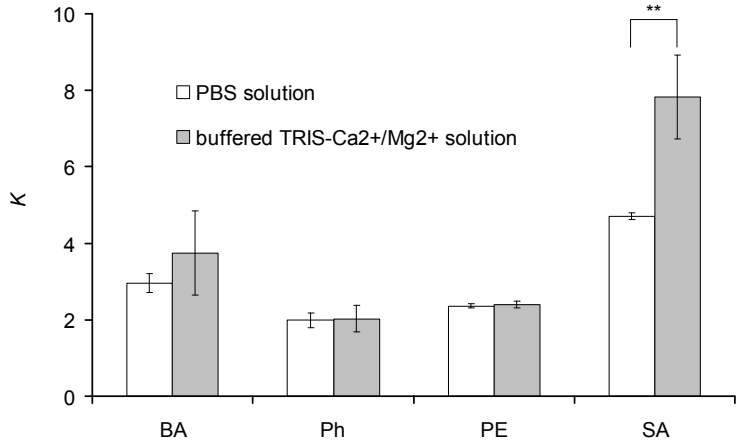

(b)

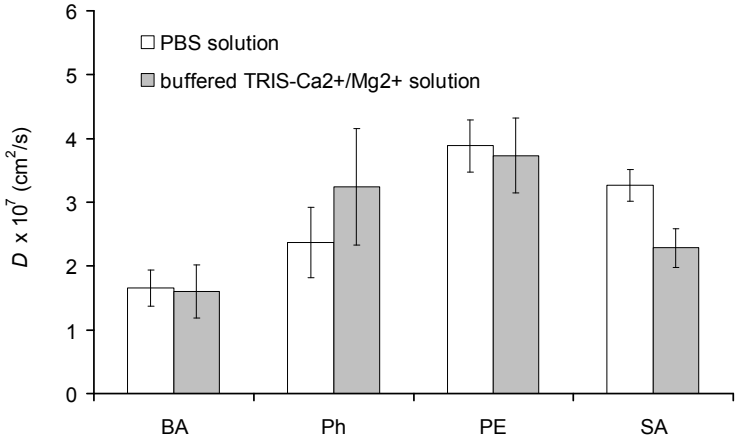

(c)

Figure 6.7 Permeability **(a)**, partition **(b)** and apparent diffusion **(c)** coefficients of benzoic acid (BA), salicylic acid (SA), phthalic acid (Ph) and 2-phenylethanol (PE), determined for the chitosan membranes in either PBS solution or in buffered TRIS-Ca^{2+}/Mg^{2+} solution. Data represents mean ± standard deviation for n = 3 (*p < 0.01; **p < 0.05).

The apparent diffusion coefficients (*D*) were determined using equation 6.8, considering the propagation of random errors associated with the experimental measurement of *K* and *P*. In Figure 6.7 it possible to observe the values of *D*, *K* and *P* for permeation of the different solutes through non-crosslinked chitosan membranes (CTS00).

The permeability of the different model solutes (see Figure 6.7a) increased according to the following sequence: SA > PE > Ph ~ BA. The great difference in the permeability of salicylic acid with respect to the other molecules is mainly due to its higher affinity to the chitosan matrix, as confirmed by its much higher partition coefficient (see Figure 6.7b). Chitosan membranes do not hold charged amine groups at the physiological pH [51], thus electrostatic interactions are not expected to occur directly with the charged anionic solutes. The affinity of the model solutes to the membrane should be related to other type of interactions. On the other hand, chitosan has the ability to form charged complexes with divalent cations [21, 22]. Interestingly, the buffer system that included Ca^{2+} and Mg^{2+} at the typical concentrations in the human blood plasma, induced an increase in the permeability of the anionic solutes (SA, Ph and BA), but did not have a statistically significant effect on the neutral one (PE) (Figure 6.7a). In the case of SA, the increase in the permeability in the presence of divalent ions can be again correlated with the increase in the partition coefficient.

The side-by-side diffusion cell was also used to evaluate the transport properties of the low molecular weight molecules through chitosan membranes with different crosslinking degrees. The SA was chosen to evaluate the effect of crosslinking in the permeation properties of chitosan membranes (see Figure 6.8).

The permeability of chitosan membranes to the SA followed the same tendency of the equilibrium water uptake, increasing until a crosslinking degree of approx. 5% (CTS05) and then decreasing steadily until 20% (Figure 6.8a). The permeability measured in the presence of Ca^{2+} and Mg^{2+} in the buffer solution followed the same tendency, but it presented higher values for each sample. The permeability measured in the presence or the absence of those cations differs of the same value throughout the crosslinking degree scale. The apparent diffusion coefficient showed a similar dependence on the crosslinking degree, but the difference between the two buffer solution groups decreased with the crosslinking degree, converging for higher crosslinking degrees (Figure 6.8c). On the other hand, the partition coefficient of the SA increased almost linearly with the crosslinking degree from 0 up to 20%. It is interesting to notice that the partition coefficients measured in the different buffers also seem to converge to the same value as the crosslinking degree increases (Figure 6.8b). This result gives a strong indication that the higher affinity of SA to the chitosan membranes in the presence of Ca^{2+} and Mg^{2+} at the physiological concentration is directly related to the complexation of these divalent cations with the chitosan. In fact, It has been reported that crosslinking chitosan with glutaraldehyde decreases the Cu^{2+} binding capacity [20].

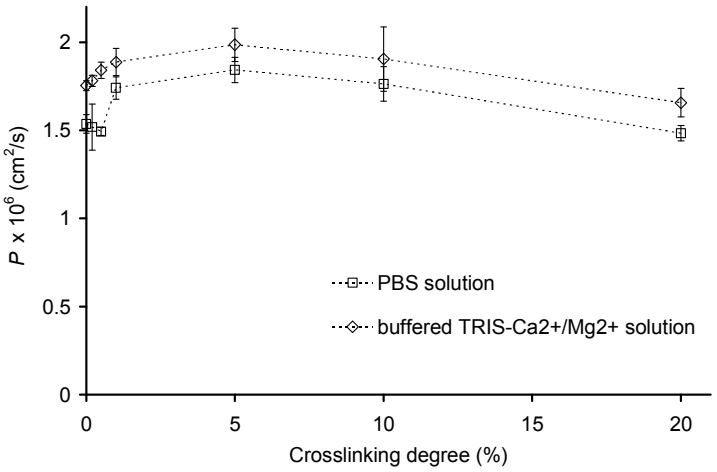

(a)

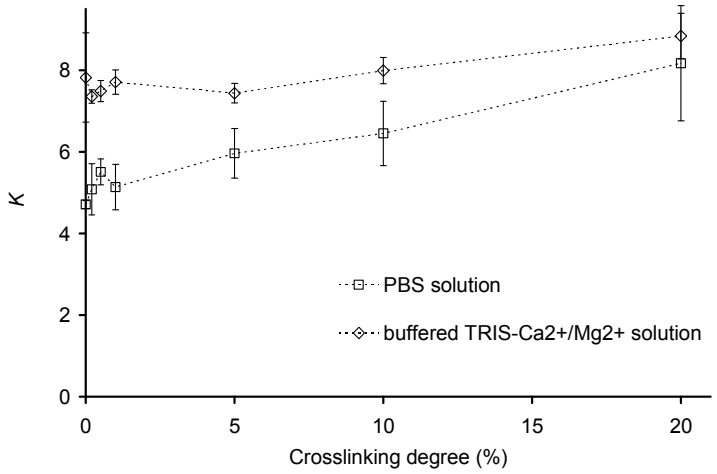

(b)

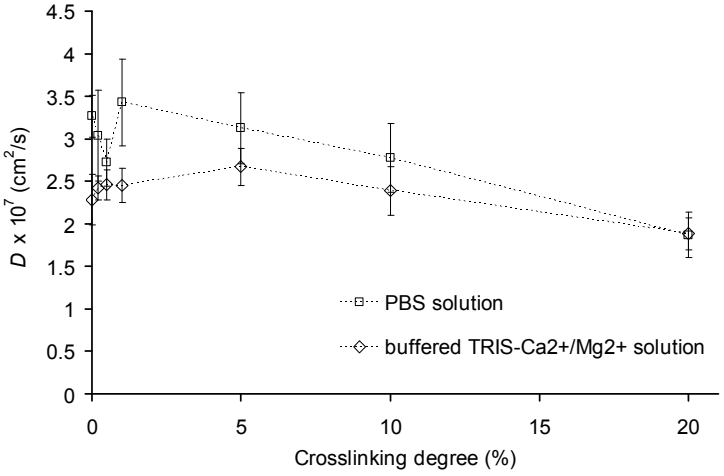

(c)

Figure 6.8 Permeability **(a)**, partition **(b)** and apparent diffusion **(c)** coefficients of salicylic acid determined in either PBS solution or in buffered TRIS-Ca^{2+}/Mg^{2+} solution as a function of the membranes crosslinking degree. Data represents mean ± standard deviation (n = 3).

This should not be surprising, because the several mechanisms proposed for the complex formation involve bounding of the metal ion to one or several amine groups [21, 23], which availability decrease as the crosslinking degree increases. The change in the permeation properties of chitosan to anionic solutes in the presence of these metallic cations is an important result and should be taken into consideration in the *in vitro* predictions of the drug release from chitosan based controlled drug release systems. Moreover, the influence of these divalent cations on the permeation properties of chitosan, if generalised to other polyelectrolytes able to form ionic complexes, can also raise concerns on how the ionic environment at the physiological conditions will affect the final performance of controlled drug release devices based on these polyelectrolytes.

6.5 Conclusions

Although the crosslinking of chitosan under homogenous conditions produce a gradual effect on the WAXS patterns, manifested by a weakening and disappearance of reflections at $2\theta \approx 10^{\circ}$ and $2\theta \approx 15^{\circ}$, the reflection at $2\theta \approx 20^{\circ}$ related to the type II crystal did not disappear, showing that the chitosan membranes retain the semi-crystalline morphology up to a crosslinking degree of 20%.

The equilibrium water uptake and the permeability of chitosan membranes followed a similar tendency, increasing until an intermediate crosslinking degree (10% and 5%, respectively) and then decreasing. The buffer system that included Ca^{2+} and Mg^{2+} at the typical concentrations in the human blood plasma, induced an increase in the permeability of the anionic solutes, but did not have any effect on the neutral one. The higher affinity of SA to the chitosan membranes in the presence of Ca^{2+} and Mg^{2+} at the physiological concentration seems to be directly related to the complexation of these divalent cations with chitosan. The permeation properties of chitosan to anionic solutes dependence on the presence of such metallic cations is an important result, which should be taken into consideration when trying to make *in vitro* predictions of the drug release from chitosan-based controlled release systems. We also hypothesise that a similar effect of these metallic cations can also be found in hydrogels prepared from other polyelectrolyte sources able to form ion-polymer complexes.

6.7 Acknowledgements

This work was partially supported by the Portuguese Foundation for Science and Technology (FCT), through funds from the POCTI and/or FEDER programmes and through the scholarship SFRH/BD/6862/2001 granted to Ricardo M. P. da Silva. This work was carried out under the scope of the European NoE EXPERTISSUES (NMP3-CT-2004-500283) and was also partially supported by the EU funded projects HIPPOCRATES (STREP – NMP3-CT-2003-505758) and PROTEUS (INTERREG III A – SP1.P151/03).

6.9 References

1. Cauchie, H. M., Chitin production by arthropods in the hydrosphere. *Hydrobiologia* **2002,** 470, (1-3), 63-96.

2. Wang, C.; Ye, W.; Zheng, Y.; Liu, X.; Tong, Z., Fabrication of drug-loaded biodegradable microcapsules for controlled release by combination of solvent evaporation and layer-by-layer self-assembly. *International Journal of Pharmaceutics* **2007,** 338, (1-2), 165-173.

3. Prabaharan, M.; Mano, J. F., Chitosan-based particles as controlled drug delivery systems. *Drug Delivery* **2005,** 12, (1), 41-57.

4. Siddaramaiah; Kumar, P.; Divya, K. H.; Mhemavathi, B. T.; Manjula, D. S., Chitosan/HPMC polymer blends for developing transdermal drug delivery systems. *Journal of Macromolecular Science-Pure And Applied Chemistry* **2006,** A43, (3), 601-607.

5. Thacharodi, D.; Panduranga Rao, K., Rate-controlling biopolymer membranes as transdermal delivery systems for nifedipine: Development and in vitro evaluations. *Biomaterials* **1996,** 17, (13), 1307.

6. Silva, R. M.; Silva, G. A.; Coutinho, O. P.; Mano, J. F.; Reis, R. L., Preparation and characterisation in simulated body conditions of glutaraldehyde crosslinked chitosan membranes. *Journal of Materials Science-Materials In Medicine* **2004,** 15, (10), 1105-1112.

7. Silva, R. M.; Elvira, C.; Mano, J. F.; San Roman, J.; Reis, R. L., Influence of beta-radiation sterilisation in properties of new chitosan/soybean protein isolate membranes for guided bone regeneration. *Journal of Materials Science-Materials In Medicine* **2004,** 15, (4), 523-528.

8. Lopez-Perez, P. M.; Marques, A. P.; da Silva, R. M. P.; Pashkuleva, I.; Reis, R. L., Effect of chitosan membrane surface modification via plasma induced polymerization on the adhesion of osteoblast-like cells. *Journal of Materials Chemistry* **2007,** 17, (38), 4064-4071.

9. Tuzlakoglu, K.; Alves, C. M.; Mano, J. F.; Reis, R. L., Production and characterization of chitosan fibers and 3-D fiber mesh scaffolds for tissue engineering applications. *Macromolecular Bioscience* **2004,** 4, (8), 811-819.

10. Silva, G. A.; Ducheyne, P.; Reis, R. L., Materials in particulate form for tissue engineering. 1. Basic concepts. *Journal of Tissue Engineering and Regenerative Medicine* **2007,** 1, (1), 4-24.

11. Baran, E. T.; Tuzlakoglu, K.; Salgado, A. J.; Reis, R. L., Multichannel mould processing of 3D structures from microporous coralline hydroxyapatite granules and chitosan support materials for guided tissue regeneration/engineering. *Journal of Materials Science-Materials in Medicine* **2004,** 15, (2), 161-165.

12. Kumar, M., A review of chitin and chitosan applications. *Reactive & Functional Polymers* **2000,** 46, (1), 1-27.

13. Zhu, X.; Chian, K. S.; Chan-Park, M. B. E.; Lee, S. T., Effect of argon-plasma treatment on proliferation of human-skin-derived fibroblast on chitosan membrane in vitro. *Journal of Biomedical Materials Research Part A* **2005,** 73A, (3), 264-274.

14. Mori, T.; Okumura, M.; Matsuura, M.; Ueno, K.; Tokura, S.; Okamoto, Y.; Minami, S.; Fujinaga, T., Effects of chitin and its derivatives on the proliferation and cytokine production of fibroblasts in vitro. *Biomaterials* **1997,** 18, (13), 947-951.

15. Lee, J. E.; Kim, S. E.; Kwon, I. C.; Ahn, H. J.; Cho, H.; Lee, S. H.; Kim, H. J.; Seong, S. C.; Lee, M. C., Effects of a chitosan scaffold containing TGF-beta 1 encapsulated chitosan microspheres on in vitro chondrocyte culture. *Artificial Organs* **2004,** 28, (9), 829-839.

16. Lee, J. Y.; Nam, S. H.; Im, S. Y.; Park, Y. J.; Lee, Y. M.; Seol, Y. J.; Chung, C. P.; Lee, S. J., Enhanced bone formation by controlled growth factor delivery from chitosan-based biomaterials. *Journal of Controlled Release* **2002,** 78, (1-3), 187-197.

17. Lee, J. E.; Kim, K. E.; Kwon, I. C.; Ahn, H. J.; Lee, S. H.; Cho, H. C.; Kim, H. J.; Seong, S. C.; Lee, M. C., Effects of the controlled-released TGF-beta 1 from chitosan microspheres on chondrocytes cultured in a collagen/chitosan/glycosaminoglycan scaffold. *Biomaterials* **2004,** 25, (18), 4163-4173.

18. Finkenzeller, G.; Torio-Padron, N.; Momeni, A.; Mehlhorn, A. T.; Stark, G. B., In vitro angiogenesis properties of endothelial progenitor cells: A promising tool for vascularization of ex vivo engineered tissues. *Tissue Engineering* **2007,** 13, (7), 1413-1420.

19. Laschke, M. W.; Harder, Y.; Amon, M.; Martin, I.; Farhadi, J.; Ring, A.; Torio-Padron, N.; Schramm, R.; Rucker, M.; Junker, D.; Haufel, J. M.; Carvalho, C.; Heberer, M.; Germann, G.; Vollmar, B.; Menger, M. D., Angiogenesis in tissue engineering: Breathing life into constructed tissue substitutes. *Tissue Engineering* **2006,** 12, (8), 2093-2104.

20. Monteiro, O. A. C.; Airoldi, C., Some studies of crosslinking chitosan-glutaraldehyde interaction in a homogeneous system. *International Journal of Biological Macromolecules* **1999,** 26, (2-3), 119-128.

21. Rhazi, M.; Desbrieres, J.; Tolaimate, A.; Rinaudo, M.; Vottero, P.; Alagui, A.; El Meray, M., Influence of the nature of the metal ions on the complexation with chitosan. Application to the treatment of liquid waste. *European Polymer Journal* **2002,** 38, (8), 1523-1530.

22. Bravo-Osuna, I.; Millotti, G.; Vauthier, C.; Ponchel, G., In vitro evaluation of calcium binding capacity of chitosan and thiolated chitosan poly(isobutyl cyanoacrylate) core-shell nanoparticles. *International Journal of Pharmaceutics* **2007,** 338, (1-2), 284.

23. Guibal, E., Interactions of metal ions with chitosan-based sorbents: a review. *Separation And Purification Technology* **2004,** 38, (1), 43-74.

24. Oyane, A.; Kim, H. M.; Furuya, T.; Kokubo, T.; Miyazaki, T.; Nakamura, T., Preparation and assessment of revised simulated body fluids. *Journal of Biomedical Materials Research Part A* **2003,** 65A, (2), 188-195.

25. Braccini, I.; Grasso, R. P.; Perez, S., Conformational and configurational features of acidic polysaccharides and their interactions with calcium ions: a molecular modeling investigation. *Carbohydrate Research* **1999,** 317, (1-4), 119-130.

26. Backfolk, K.; Lagerge, S.; Rosenholm, J. B.; Eklund, D., Aspects on the interaction between sodium carboxymethylcellulose and calcium carbonate and the relationship to specific site adsorption. *Journal of Colloid And Interface Science* **2002,** 248, (1), 5-12.

27. Debon, S. J. J.; Tester, R. F., In vitro binding of calcium, iron and zinc by non-starch polysaccharides. *Food Chemistry* **2001,** 73, (4), 401-410.

28. Han, S. C.; Choo, K. H.; Choi, S. J.; Benjamin, M. M., Modeling manganese removal in chelating polymer-assisted membrane separation systems for water treatment. *Journal of Membrane Science* **2007,** 290, (1-2), 55-61.

29. Konradi, R.; Ruhe, J., Interaction of poly(methacrylic acid) brushes with metal ions: An infrared investigation. *Macromolecules* **2004,** 37, (18), 6954-6961.

30. Navarro, R. R.; Wada, S.; Tatsumi, K., Heavy metal precipitation by polycation-polyanion complex of PEI and its phosphonomethylated derivative. *Journal of Hazardous Materials* **2005,** 123, (1-3), 203-209.

31. Murdan, S., Electro-responsive drug delivery from hydrogels. *Journal of Controlled Release* **2003,** 92, (1-2), 1-17.

32. Cafaggi, S.; Russo, E.; Stefani, R.; Leardi, R.; Caviglioli, G.; Parodi, B.; Bignardi, G.; De Totero, D.; Aiello, C.; Viale, M., Preparation and evaluation of nanoparticles made of chitosan or N-trimethyl chitosan and a cisplatin-alginate complex. *Journal of Controlled Release* **2007,** 121, (1-2), 110-123.

33. Liu, D. Z.; Sheu, M. T.; Chen, C. H.; Yang, Y. R.; Ho, H. O., Release characteristics of lidocaine from local implant of polyanionic and polycationic hydrogels. *Journal of Controlled Release* **2007,** 118, (3), 333-339.

34. Terbojevich, M.; Cosani, A.; Muzzarelli, R. A. A., Molecular parameters of chitosans depolymerized with the aid of papain. *Carbohydrate Polymers* **1996,** 29, (1), 63-68.

35. da Silva, R.; Mano, J.; Reis, R., An exact mathematical description for the straightforward determination of the degree of N-acetylation of chitosan by the 1st derivative UV spectrophotometry. *Submitted* **2007**.

36. Roberts, G. A. F.; Taylor, K. E., Chitosan gels, 3. The formation of gels by reaction of chitosan with glutaraldehyde. *Die Makromolekulare Chemie* **1989,** 190, (5), 951-960.

37. Tual, C.; Espuche, E.; Escoubes, M.; Domard, A., Transport properties of chitosan membranes: Influence of crosslinking. *Journal of Polymer Science Part B-Polymer Physics* **2000,** 38, (11), 1521-1529.

38. Robinson, D.; Smith, J. N.; Williams, R. T., Studies In Detoxication .52. The Apparent Dissociation Constants Of Some Glucuronides, Mercapturic Acids And Related Compounds. *Biochemical Journal* **1953,** 55, (1), 151-155.

39. Gluck, S. J.; Steele, K. P.; Benko, M. H., Determination of acidity constants of monoprotic and diprotic acids by capillary electrophoresis. *Journal Of Chromatography A* **1996,** 745, (1-2), 117-125.

40. Matsuyama, H.; Kitamura, Y.; Naramura, Y., Diffusive permeability of ionic solutes in charged chitosan membrane. *Journal of Applied Polymer Science* **1999,** 72, (3), 397-404.

41. Samuels, R. J., Solid-State Characterization Of The Structure Of Chitosan Films. *Journal of Polymer Science Part B-Polymer Physics* **1981,** 19, (7), 1081-1105.

42. Ogawa, K.; Yui, T.; Miya, M., Dependence On The Preparation Procedure Of The Polymorphism And Crystallinity Of Chitosan Membranes. *Bioscience Biotechnology And Biochemistry* **1992,** 56, (6), 858-862.

43. Ogawa, K.; Hirano, S.; Miyanishi, T.; Yui, T.; Watanabe, T., A New Polymorph Of Chitosan. *Macromolecules* **1984,** 17, (4), 973-975.

44. Zhang, Y. Q.; Xue, C. H.; Xue, Y.; Gao, R. C.; Zhang, X. L., Determination of the degree of deacetylation of chitin and chitosan by X-ray powder diffraction. *Carbohydrate Research* **2005,** 340, (11), 1914-1917.

45. Stringer, J. L.; Peppas, N. A., Diffusion of small molecular weight drugs in radiation-crosslinked poly(ethylene oxide) hydrogels. *Journal of Controlled Release* **1996,** 42, (2), 195-202.

46. Amende, M. T.; Hariharan, D.; Peppas, N. A., Factors Influencing Drug And Protein-Transport And Release From Ionic Hydrogels. *Reactive Polymers* **1995,** 25, (2-3), 127-137.

47. Despond, S.; Espuche, E.; Cartier, N.; Domard, A., Hydration mechanism of polysaccharides: A comparative study. *Journal of Polymer Science Part B-Polymer Physics* **2005,** 43, (1), 48-58.

48. Rueda, D. R.; Secall, T.; Bayer, R. K., Differences in the interaction of water with starch and chitosan films as revealed by infrared spectroscopy and differential scanning calorimetry. *Carbohydrate Polymers* **1999,** 40, (1), 49-56.

49. am Ende, M. T.; Hariharan, D.; Peppas, N. A., Factors Influencing Drug And Protein-Transport And Release From Ionic Hydrogels. *Reactive Polymers* **1995,** 25, (2-3), 127-137.

50. Kierstan, K. T. E.; Beezer, A. E.; Mitchell, J. C.; Hadgraft, J.; Raghavan, S. L.; Davis, A. F., UV-spectrophotometry study of membrane transport processes with a novel diffusion cell. *International Journal of Pharmaceutics* **2001,** 229, (1-2), 87-94.

51. Wang, Q. Z.; Chen, X. G.; Liu, N.; Wang, S. X.; Liu, C. S.; Meng, X. H.; Liu, C. G., Protonation constants of chitosan with different molecular weight and degree of deacetylation. *Carbohydrate Polymers* **2006,** 65, (2), 194-201.

Chapter 7

Poly(*N*-isopropylacrylamide) surface grafted chitosan membranes as a new substrate for cell sheet engineering and manipulation

7.1 Abstract

The immobilisation of poly(*N*-isopropylacrylamide) (PNIPAAm) on chitosan membranes was performed in order to render membranes with thermo-responsive surface properties. The aim was to create membranes suitable for cell culture and in which confluent cell sheets can be recovered by simply lowering the temperature. The chitosan membranes were immersed in a solution of the monomer that was polymerised via radical initiation. The composition of the polymerisation reaction solvent, which was a mixture of a chitosan non-solvent (isopropanol) and a solvent (water), provided a tight control over the chitosan membranes swelling capability. The different swelling ratio, obtained at different solvent composition of the reaction mixture, drives simultaneously the monomer solubility and diffusion into the polymeric matrix, the polymerisation reaction rate, as well as the eventual chain transfer to the side substituents of the pyranosyl groups of chitosan. A combined analysis of the modified membranes chemistry by proton nuclear magnetic resonance (^{1}H-NMR), Fourier Transform spectroscopy with attenuated total reflection (FTIR-ATR) and X-ray photoelectron spectroscopy (XPS) showed that it was possible to control the chitosan modification yield and depth in the solvent composition range between 75% and 100% of isopropanol. Plasma treatment was also applied to the original chitosan membranes in order to improve cell adhesion and proliferation. Chitosan membranes, which had been previously subjected to oxygen plasma treatment, were then modified by means of the previously described methodology. A human foetal lung fibroblast cell line was cultured until confluence on the plasma treated thermo-responsive chitosan membranes and cell sheets were harvested lowering the temperature.

This chapter is based on the following publication:
Ricardo M.P. da Silva, Paula M. López-Pérez, Carlos Elvira, João F. Mano, Julio San Román, Rui L. Reis. Poly(*N*-isopropylacrylamide) surface grafted chitosan membranes as a new substrate for cell sheet engineering and manipulation (submitted).

7.2 Introduction

Poly(*N*-isopropylacrylamide) (PNIPAAm) is a soluble polymer in cold water that present a sudden precipitation upon heating above the lower critical solution temperature (LCST), at around 32ºC in pure water [1-3]. This transition involves the breakage of intermolecular hydrogen bonds with the water molecules, which are replaced by intramolecular hydrogen bonds amongst the dehydrated amide groups. Subsequently, the PNIPAAm molecules assume a globule conformation, exposing the hydrophobic isopropyl groups to the water interface [4, 5]. Therefore, when immobilised onto a solid substrate, the LCST behaviour of PNIPAAm render the surface with thermo-responsive wettability [6]. The temperature control over the wettability of the PNIPAAm grafted substrates has been used to modulate protein adsorption [7-9] and confluent cells cultured on such substrates can be recovered as a contiguous cell sheet just by lowering the temperature [6, 10-12]. In conventional cell culture on tissue culture polystyrene (TCPS), cells are harvested disaggregating the extracellular matrix (ECM) through the enzymatic action of trypsin and by simultaneously chelating the Ca^{2+} and Mg^{2+} ions with ethylenediaminetetraacetic acid (EDTA). However, non-specific proteases may damage critical cell surface proteins, such as ion channels and receptors, which constitute a major drawback of this cell harvesting method [13-17]. Besides that, the recovery of the cells, together with the intact newly deposited ECM, represents an increased therapeutic potential with respect to the same single cells harvested by the conventional proteolytic methods, unable to keep cells confluence.

The so-called cell sheet engineering has been mainly performed using TCPS dishes grafted with PNIPAAm [6], which are rigid non-swollen supports. The confluent cell sheets cultured in these thermo-responsive substrates present relatively long detachment times. Several attempts have been made to accelerate the thermal harvesting process, such as grafting PNIPAAm onto porous supports [18] and co-grafting PNIPAAm with poly(ethylene glycol) (PEG) [19]. The potential of cell sheet engineering in the regenerative medicine field has been fostered by the development of manipulation techniques which allow transferring the fragile cell sheets from the thermo-responsive culture substrate to the desired place [20-22]. Single cell sheets has been transplanted directly to human patients for cornea regeneration tissues [23], but they can also be layered in order to recreate thicker tissue-like constructs with homotypic [24] or heterotypic [22] cells. However, the number of cell sheets that can be effectively layered without core ischemia or hypoxia is limited, because of restrictions on the delivery of nutrients and accumulation of metabolic wastes [11]. The thermo-responsive surfaces fabricated to harvest intact cell sheets can also be used to keep the multilayered cell sheets in culture for a certain period of time and to allow the thermal recovery of the thicker

constructs. It should be noticed that the thermo-responsive PNIPAAm grafted TCPS substrates commonly used to culture single cell sheets are impermeable, which would decrease the rate of elimination of metabolic wastes and of nutrients supplying, since the construct side facing the culture surface would be wasted as a potential mass transfer area.

In this work, we propose a methodology to grafted PNIPAAm on chitosan membranes aiming at being used as novel substrates for cell sheet engineering and manipulation. Chitosan is the soluble derivative of chitin obtained by *N*-deacetylation, which biocompatibility and non-toxicity make it an excellent candidate as a raw material in the biomedical field [25]. Chitosan has been proposed for a range of controlled drug release formulations [26, 27], as rate controlling membranes in transdermal delivery systems [28, 29], as a biomaterial [30-32] and for tissue engineering [33-37]. We previously developed chitosan membranes that possess adequate permeation properties for the rapid elimination or delivery of small molecules [38]. The use of these membranes grafted with PNIPAAm, if able to functioning as substrate for the thermal recovery of confluent cell sheets, would increase the mass transfer area for nutrients and metabolic wastes, hopefully supporting the culture of thicker layered cell sheet constructs. Moreover, the PNIPAAm grafted chitosan membranes reported herein will also be useful to transfer the cell sheets directly to the host site with minimal manipulation. Finally, fully hydrated chitosan membranes should be easily adaptable to several anatomical shapes, owning to its mechanical flexibility [30].

7.3 Materials and methods

7.3.1 Chitosan material and other reagents

Chitosan raw-material from crab shells were purchased from Sigma-Aldrich and purified prior to use. Chitosan was dissolved at ~1% (w/v) in an aqueous acetic acid solution (1% w/v). The solution was filtered to remove the insoluble material. The clear solution obtained was precipitated adding a NaOH solution to form a white gel, which was sieved to remove the exuded liquid. This gel was thoroughly washed with distilled water (until no changes on the pH were detected), further washed/dehydrated with ethanol, freeze-dried, ground to powder and dried at 60ºC overnight. *N*-isopropylacrylamide (NIPAAm) (Acros-Organics) was recrystallised from a n-hexane/diethyl ether (5:1) mixture and dried overnight to remove residual solvent. All other reagents were used without further purification.

The chitosan average molecular weight was of found to be 660 kDa by viscometry in CH_3COOH 0.5 M/ $NaCH_3COO$ 0.2 M, according to the Mark-Houwing theory ($k = 3.5x10^{-4}$; a

= 0.76) [39]. The degree of *N*-deacetylation (DD) was found to be 65.4% by means of 1st derivative UV spectrophotometry, using both glucosamine (GluN) and *N*-acetylglucosamine (GluNAc) standards for calibration [40].

7.3.2 Preparation of chitosan membranes by solvent casting

The chitosan solution was prepared by dissolving chitosan (1% wt.) in acetic acid solution (1% wt.). The solutions were carefully stirred in order to avoid the formation of any air bubble, poured on Petri Dishes (5 mg of chitosan/cm^2) and dried at room temperature in a dust free environment. The resultant membranes (thickness approx. 50 μm) were neutralised in NaOH 0.1 M solution for 10 min and washed thoroughly with distilled water. The obtained membranes (CTS) were hold in a frame and dried again, presenting a smooth surface without the typical wrinkles derived from the material shrinking during the drying process.

7.3.3 Swelling of chitosan membranes in mixtures of isopropanol and water

The swelling of chitosan membranes in mixtures of a non-solvent (isopropanol) and a solvent (water) was determined by immersing previously weighted chitosan membranes in mixtures of these solvents at compositions varying from pure water to pure isopropanol. After around 2 h, equilibrated samples were blotted with filter paper to remove the adsorbed solvent and weighted immediately. The equilibrium swelling ratio (S_{eq}) was calculated using the following equation:

$$S_{eq}(\%) = \frac{W - W_0}{W_0} \times 100 \qquad (7.1)$$

where W_0 is the initial weight of the sample and W is the weight of the swelled sample.

7.3.4 Surface modification by plasma treatment

In one of our previous works [32], plasma treatment of chitosan membranes was very effective on improving the viability and proliferation of osteoblast-like cells. In this sense, the surface of some chitosan membranes was modified by plasma treatment according to that procedure [32], before PNIPAAm grafting. Briefly, the plasma treatment was performed using a radio frequency (13.56 MHz) Plasma Prep5 equipment from Gala Intrument. Samples were exposed to O_2 plasma at 30 W of power during 15 min. The pressure in the reactor was

maintained under 20 Pa by regulating the gas flow. The samples were only further processed after 48 h in order to assure that free radicals formed during the plasma treatment have been quenched.

7.3.5 PNIPAAm grafting onto and into chitosan membranes

The monomer (NIPAAm) was dissolved in several compositions of these isopropanol/water mixtures varying in the volume ratio from (50:50) to pure isopropanol (100:0). The initiator, 2,2'-Azobis-isobutyronitrile (AIBN), was dissolved in each solvent mixture used in the respective monomer solution. Chitosan membranes were immersed in the monomer solutions. Both monomer and initiator solutions were deoxygenated under slow nitrogen flow for 10 min. The polymerisation was initiated adding the AIBN solution to the monomer solutions and the reaction was performed at 60ºC under N_2 atmosphere for 18h. The volumes of NIPAAM and AIBN solutions give a final monomer concentration of 0.25 g/mL and AIBN to NIPAAm molar ratio of 1%. The grafted membranes were washed thoroughly with water/acetone (25:75) to remove un-reacted monomer and unbound polymer. Samples were labelled as iPrOH100, iPrOH90, iPrOH75 and iPrOH50, according to the volume of isopropanol used in the non-solvent/solvent mixture composition. The same PNIPAAm grafting procedure was also applied to plasma treated chitosan membranes at an isopropanol/water composition of 75:25 (P-iPrOH75).

7.3.6 Assessment of chitosan membranes chemical modification

PNIPAAm grafted membranes were analysed by Fourier Transform Infrared spectroscopy with the attenuated total reflection (FTIR-ATR) to assess the existence of major chemical changes occurring at lower depth. Spectra were recorded in a Perkin-Elmer (Waltham, USA) Spectrum One spectrophotometer (32 scans, resolution 4 cm^{-1}). Proton nuclear magnetic resonance (^{1}H-NMR) was used to estimate the total amount of grafted PNIPAAm, which were thought to be detectable for samples in which grafting reaction was performed in solvents with higher water content. Around 10 mg of each membrane sample was dissolved in 1 ml of 0.4% (w/v) of deuterium chloride (DCl) in D_2O solution at room temperature. PNIPAAm spectrum was obtained dissolving in D_2O. The ^{1}H-NMR spectra were acquired in a VARIAN INOVA-300 (300MHz) spectrometer.

7.3.7 X-Ray photoelectron spectroscopy (XPS)

Possible chemical changes occurred on the surfaces after the modification were evaluated by XPS. The spectra were obtained using an ESCALAB 200A instrument from VG Scientific (UK) with PISCES software for data acquisition and analysis. A monochromatic Al-Kα radiation (hv=1486.60 eV) operating at 15 kV (300 W) was used. The measurements were performed in a constant Analyser Energy mode (CAE) and take off angle of 90º relative to the sample surfaces. Survey spectra were acquire using a pass energy of 50 eV, over a binding energy range of 0 to 1100 eV, and were used to calculate the elemental composition of the surfaces. Element atomic percentages were calculated from the integrated intensities of the survey spectra using the sensitivity factor of the instrument data system. High resolution spectra for different regions (C1s, O1s and N1s) were obtained using a pass energy of 20 eV and were peak-fitted using a least-squares peak analysis software, XPSPEAK version 4.1, using the Gaussian/Lorenzian sum function. Background counts were subtracted using a linear baseline and the sample charging was corrected assigning a binding energy of 285.0 eV to the saturated hydrocarbons C1s peak.

7.3.8 Water uptake kinetics and equilibrium hydration degree

The water uptake measurements were undertaken in phosphate buffer saline (PBS) solution, prepared dissolving PBS tablets from Sigma in a suitable amount of water (NaCl 0.137 M; KCl 0.0022 M; phosphate buffer 0.01 M; pH 7.4 at 25ºC). The water uptake was determined immersing previously weighted chitosan membranes in buffer solution at 37 ± 1ºC. After each time period samples were blotted with filter paper to remove the adsorbed water and weighted immediately. The calculation of the water uptake (*WU*) was also based on equation 7.1. The equilibrium hydration degree (WU_{eq}) in PBS solution was taken as the last point of the water sorption kinetic curves.

7.3.9 Cell culture

A human foetal lung cell line (MRC-5), an immortalized cell line with fibroblast-like morphology, was obtained from European Collection of Cell Cultures (ECACC, UK) and was used in the cell culture studies. The cells were cultured in Dulbecco's Modified Eagle's Medium (DMEM; Sigma-Aldrich, Inc, USA) supplemented with 10000 U/ml penicillin-G sodium, 10000 µg/ml streptomycin sulfate and 25 µg/ml amphotericin B in a 0.85% saline

(Gibco, Invitrogen Corporation, UK) and 10% of heat-inactivated fetal bovine serum (FBS; Biochrom AG, Germany) in a humidified atmosphere with 5% of CO_2 at 37ºC. Membranes were cut with 14 mm diameter and placed onto 24 well culture plates. Prior to culturing, all samples were sterilized by adding 1 ml of 70% ethanol aqueous solution for 90 minutes and subsequently washed with sterile phosphate buffered saline solution (PBS, Sigma Chemical Co., USA) to remove the remaining ethanol. Cells were seeded on the materials at a concentration of $7x10^4$ cells/ml, 1 ml per well and incubated for 10 days, time at which the cells seeded on plasma treated materials (P-iPrOH75) were 100% confluent.

7.3.10 Cell sheet detachment and assessment of the cell viability

After 10 days of culture, plates were removed from the incubator and observed by light microscopy. The cells cultured on the different samples were continuously observed to assess the eventual detachment from the surface at room temperature (c.a. 16ºC). Cell viability was assessed after Calcein AM staining. A 2:1000 Calcein AM solution was prepared with DMEM culture medium and 1000 µl were added to each sample culture. Plates were incubated for 15 minutes at 37ºC in a humidified atmosphere of 5% CO_2 and cell fluorescence examined in an Axioplan Imager Z1 from Zeiss.

7.4 Results and discussion

7.4.1 Isopropanol-water mixtures solvent uptake

The control of the swelling capability of the chitosan membranes can be tightly achieved by changing the composition of isopropanol and water mixtures. As it can be observed in Figure 7.1, the swelling equilibrium degree varies linearly with the volume composition of the solvent mixtures for concentrations of isopropanol higher than 10%. The swelling decreases steadily with increasing proportions of isopropanol. On the other hand, the membranes did not swell at all for the pure non-solvent. This result should allow engineering membrane surfaces with different grafting yields and depths, by changing simultaneously the monomer uptake by the membranes (solubility), diffusion into the polymer matrix and the monomer reaction rate on the surface or inside the swollen membranes. Of course, the solvent composition is restricted to the isopropanol volume ratio (higher that 50%) in which monomer and initiator are soluble at the polymerisation temperature (60ºC).

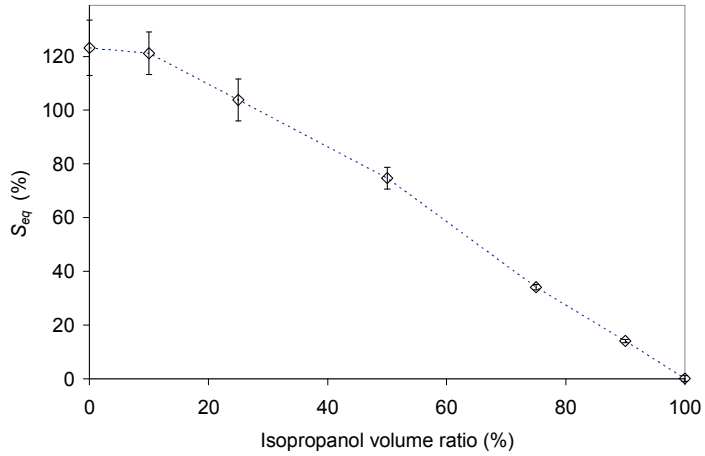

Figure 7.1 The equilibrium swelling ratio (S_{eq}) of chitosan membranes in mixtures of isopropanol and water at varying compositions represented in function of the isopropanol volume ratio.

7.4.2 Assessment of chitosan membranes chemical modification

The FTIR spectrum of PNIPAAm presents two intense bands at 1650 cm^{-1} and 1544 cm^{-1} (Figure 7.2a), which are related to the amide groups. The first is assigned to the stretching vibration of C=O group (amide I), whereas the second corresponds to the bending vibration of NH and the symmetric stretching of N-C=O (amide II). The three bands appearing at 2972, 2932, and 2874 cm^{-1} can be assigned to the stretching vibration of the C-H bonds from the isopropyl groups and polymer backbone. The band at 2972 cm^{-1} is particular intense.

In the chitosan membranes (CTS) spectrum (Figure 7.2b), amide II band is observed at 1590 cm^{-1}. The intensity of the band at 1645cm^{-1}, which is assigned to stretching vibration of carbonyl group (amide I), is in good agreement with the low deacetylation degree of the used chitosan. The bands assigned to the stretching vibration of C-O-C linkages in the polysaccharide structure appear at 1151, 1060, 1027 and 895 cm^{-1}. The weak bands at 2927 and 2874 cm^{-1} correspond to the stretching vibration of the C-H bonds.

The non-swollen membranes modified in pure isopropanol exhibit an infrared spectrum very similar to the non-modified membranes (CTS) (Figure 7.2b). Nevertheless, it does not mean that the surface has not been modified, because in the FTIR-ATR technique the penetration depth of the IR radiation beam is around 1 - 5 μm into the polymer membrane at each internal reflection [41]. Therefore, information cannot be inferred if the modification only affects the topmost layers of the sample, as it would be expected for the non-swollen membranes.

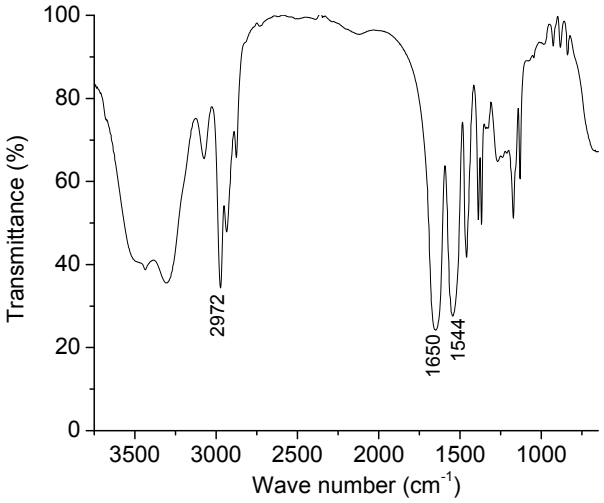

(a)

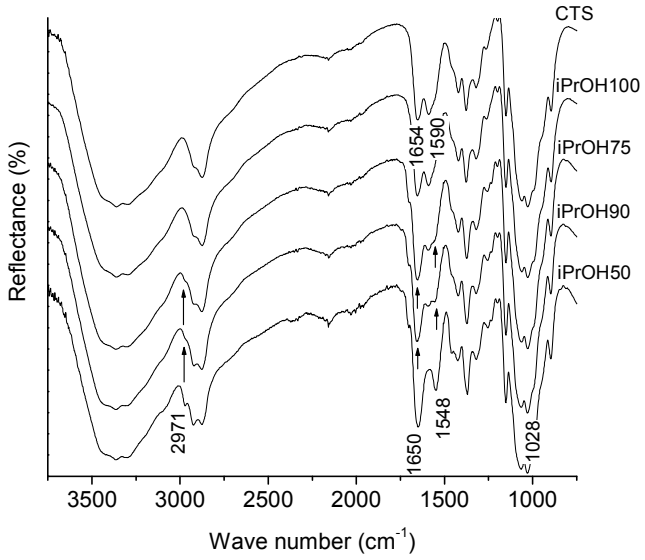

(b)

Figure 7.2 (a) FTIR-ATR spectrum of PNIPAAm; **(b)** comparative spectra of non-grafted chitosan membranes (CTS) and grafted in mixtures of isopropanol and water at varying compositions (iPrOH100, iPrOH90, iPrOH75 and iPrOH50).

In the membrane samples modified in an isopropanol content higher than 90% a shoulder or band appears at the amide II region between 1590 and 1548 cm^{-1} (see Figure 7.2b), which becomes more intense as the solvent swelling ratio increases (from 100% to 50% of isopropanol), indicating a gradual increase in the amount of PNIPAAm. In fact, in the spectrum of iPrOH50 the amide II band suffered a displacement to 1548 cm^{-1}, which is consistent with the wave number of that band in PNIPAAm. It is also observed an increase

on the intensities of the amide I band that can be explained due to the cumulative contribution of PNIPAAm amide groups (C=O) and of the chitosan acetyl groups (C=O). Furthermore, the relative intensity of the characteristic chitosan C-H stretching bands at 2874 and 2927 cm^{-1} changed gradually and a new band appears at 2972 cm^{-1} (iPrOH50), which corresponds to the particularly intense C-H stretching band in the PNIPAAm spectrum. The described spectral changes point out an increase in the amount of PNIPAAm in a superficial region of the membranes (1-5 μm) when going from iPrOH90 to iPrOH50, i.e., when increasing the polymerisation solvent swelling ratio.

The ^{1}H-NMR spectroscopy results (Figure 7.3) give quantitative information with respect to the bulk modification yield. PNIPAAm pure homopolymer (see Figure 7.4) was previously dissolved in D_2O and the proton chemical shifts (δ) were assigned: δ 1.00 ($-CH_3$, isopropyl group), 1.42 ($-CH_2-$, polymer chain), 1.78 (-CH-, polymer chain) and 3.76 (-CH-, isopropyl group). Only the first 2 peaks are well resolved from the chitosan spectrum. On the other hand, the chitosan peak assigned to the H2 proton (δ 2.95) of the GluN units is the only peak well resolved both from the PNIPAAm spectrum and from the HOD signal.

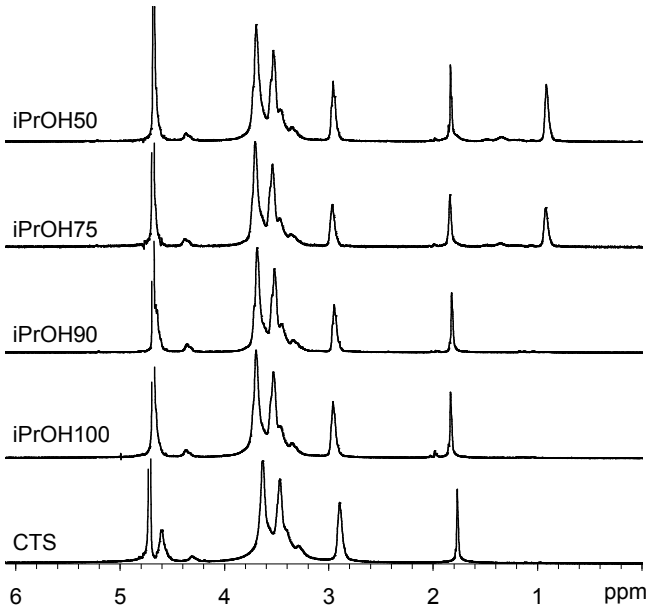

Figure 7.3 ^{1}H-NMR spectra of non-grafted chitosan membranes (CTS) and grafted in mixtures of isopropanol and water at varying compositions (iPrOH100, iPrOH90, iPrOH75 and iPrOH50).

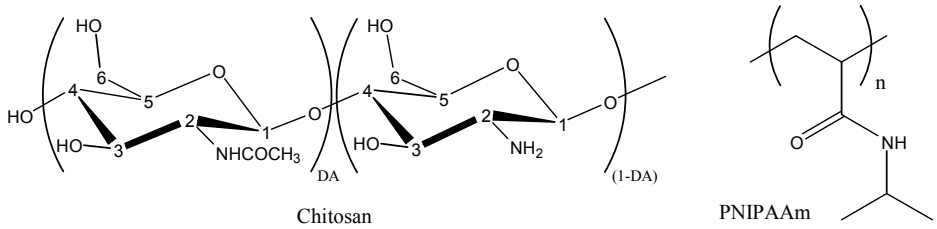

Figure 7.4 Chemical structures of chitosan and PNIPAAm

We used the PNIPAAm peak from the isopropyl $–CH_3$ groups (6 protons) to estimate the amount of this polymer relative to the amount of chitosan, which in turn was estimated using the GluN H2 proton signal and the DD value. It is clear from Figure 7.3 that PNIPAAm is undetectable for the samples treated under solvent conditions less favourable for swelling (iPrOH90 and iPrOH100). This means that the modification for low and non-swelling conditions, respectively, is much more superficial, as it would be expected. In turn, the relative amount of PNIPAAm is considerable high for iPrOH75 (5.3 wt. %) and only increases a little for iPrOH50 (5.5 wt. %), indicating a much higher modification depth of these membranes.

7.4.3 Surface analysis by X-Ray photoelectron spectroscopy (XPS)

The surface chemical composition of modified (iPrOH75 and iPrOH100) and non-modified membranes (CTS) was evaluated by XPS analysis. Table 7.1 shows the elemental composition of the surfaces (at%) extracted from the survey spectra. Carbon, oxygen and nitrogen appeared as major components for all the samples, as it was expected considering the chemical structure of chitosan and PNIPAAm (Figure 7.4). Some impurities (Ca, Cl and Zn) were also found, in very low percentage (< 0.5%) in the composition of some of the samples and were not considered for the element analysis. After the grafting, a polymer chain ($-CH_2-CH-$) is introduced on the membranes surface and as it was expected, the C1s percentage increased in the modified samples compared with the untreated one.

Table 7.1 Elemental composition (at%) of untreated chitosan membranes (CTS) and modified materials (iPrOH75 and iPrOH100) calculated from the XPS survey spectra

Element	CTS	iPrOH75	iPrOH100
C1s(at%)	65.13	77.49	74.29
O1s(at%)	29.15	21.01	22.47
N1s(at%)	5.72	1.50	3.24

Figure 7.5a shows the binding energy region corresponding to C1s peak (279.8-191.9 eV) for CTS samples. The peak-fitting was performed according with the chitosan chemical structure. The peak at 285.0 eV was assigned to C-H and C-C chemical bonds of the chitosan backbone. The second peak at 286.4 eV corresponded to C-OH, C-O and C-N-C=O carbons and, finally, the peak centred at 287.6 eV was assigned to O-C-O and N-C=O from the acetylated rings. It was not possible to perform the deconvolution of the band corresponding to C-NH_2 bond, because amines are reported to induce small chemical shifts (around 0.6 eV) [42] and the band should be superimposed by the band of the hydrocarbons chemical bonds in chitosan, observed at 285.0 eV.

In the case of linear PNIPAAm, it is expected a C1s spectra containing four peaks, allocated in the same position that chitosan peaks. Peaks at 285.0 eV and around 285.4 eV should be associated to hydrocarbons in the polymeric backbone. The peak corresponding to C-N-C=O should be situated around 286.5 eV and the carbon from the carbonyl group (N-C=O) should be allocated around 288.0 eV [43, 44].

Figures 7.5b and 7.5c show the C1s region for the samples iPrOH75 and iPrOH100, respectively. The intensity of the band corresponding to the hydrocarbon bonds increases in both cases compared with CTS (Table 7.2), providing evidence that PNIPAAm polymer chains have been introduced on the surface through the modification procedure. In the case of the sample iPrOH100, this result had not been possible to confirm using less surface sensitive techniques such as FTIR-ATR, showing that the PNIPAAm chains grafting occurred at a very superficial level (the FTIR-ATR penetration depth of the FTIR-ATR analysis is in the range of 1 - 5 μm [41]).

The binding energy region corresponding to O1s peak (394.0-404.0 eV) for chitosan is showed in Figure 7.5d. The peak at 531.5 eV was assigned to carbonyl oxygen (N-C=O) presented in the N-acetyl-glucosamine rings. Oxygen atoms involved in hydroxyl bonds (C-OH) were included in the peak appearing at 532.8 eV. The peak at 533.3 eV was identified as characteristic of the O-C-O bonds.

PNIPAAm only posses one oxygen atom per polymer molecule been involved in amide bonds (N-C=O). Therefore, after the grafting, it was expected an increase in the peak allocated around 531.5 eV relatively to the peaks contained single C-O bonds. As can be observed from values showed in Table 7.2, when the modification is performed using isopropanol at 75% (Figure 7.5e) the first peak became much more intense, corroborating the PNIPAAm grafting. On the other hand, when 100% isopropanol was used for the grafting reaction (Figure 7.5f), this increase was not so drastic showing that the grafting occurred but at lower extent.

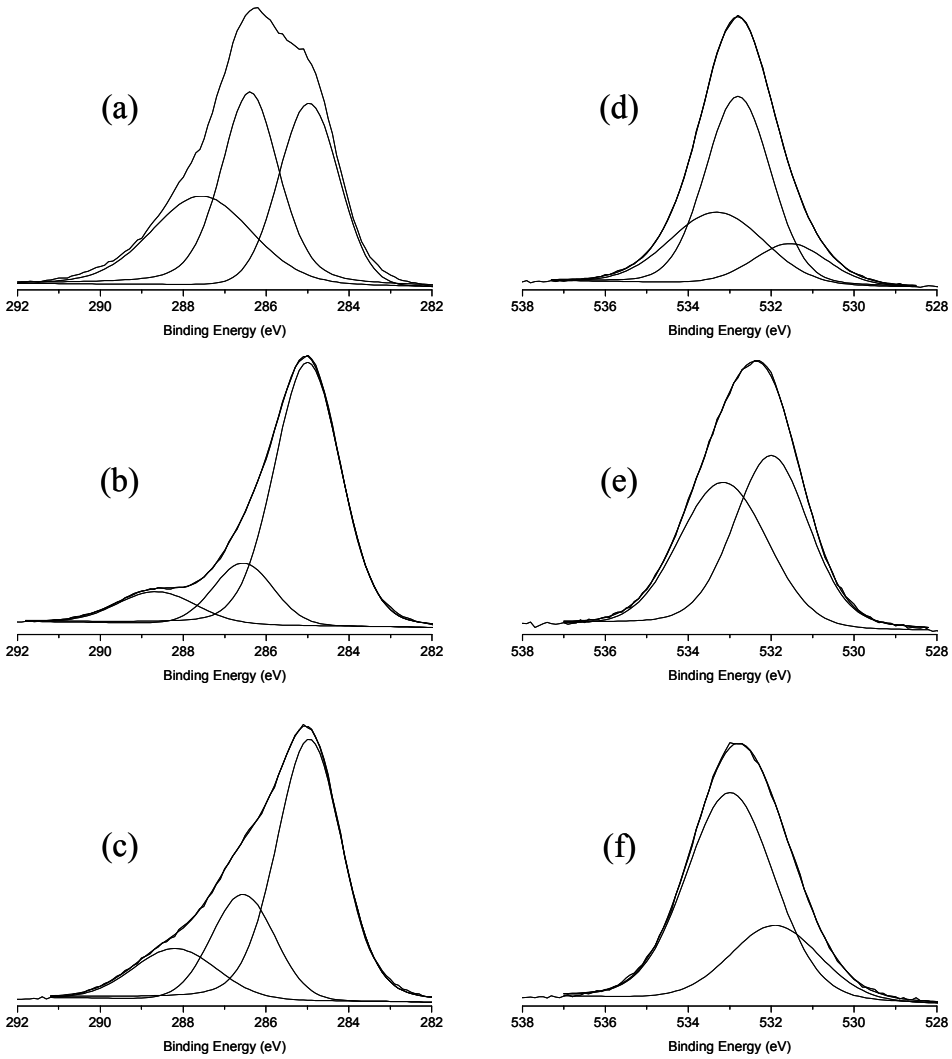

Figure 7.5 XPS high resolution spectra for C1s (left) and O1s (right). From top to down: CTS, iPrOH75 and iPrOH100

Table 7.2 C1s and O1s core levels composition (%) for CTS, iPrOH75 and iPrOH100

C1s core level				O1s core level			
Bond	**CTS**	**iPrOH75**	**iPrOH100**	**Bond**	**CTS**	**iPrOH75**	**iPrOH100**
C-C; C-H	33.0	75.3	63.4	N-C=O	14.0	52.8	27.0
C-O; C-N-C=O	38.8	14.8	22.4	C-OH	56.6	47.2	73.1
N-C=O; O-C-O	28.3	9.9	14.1	O-C-O	29.4	0.0	0.0

7.4.4 Chitosan membranes equilibrium hydration degree

The chitosan membranes water uptake kinetics (Figure 7.6) in PBS solution was very fast, the equilibrium hydration degree (WU_{eq}) being achieved in less than 5 min. It is interesting to notice that the non-modified chitosan membranes (CTS) presented the higher WU_{eq} of approx. 160% and that it decreases from iPrOH100 to iPrOH75, being lower for membranes polymerised at higher swelling solvent conditions. During the NIPAAm polymerisation the growing polymer chains predictably occupy the spaces created by the swelling in the reaction solvent. Being so, the conditions that induce higher swelling rates should allow for the entrance of higher amounts of newly formed polymer. Interestingly, the WU_{eq} is inversely related to the amount of PNIPAAm chains that entered the chitosan membranes pre-established molecular network.

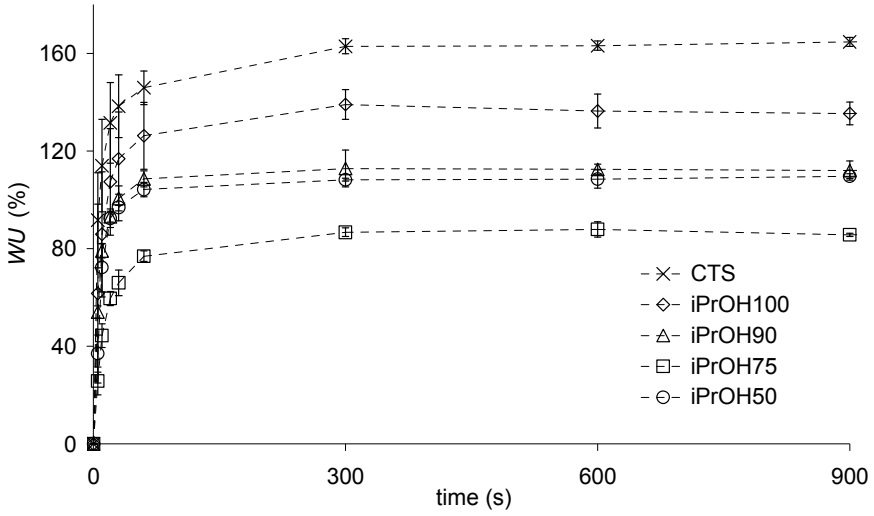

Figure 7.6 (a) Water uptake kinetics in PBS solution (37ºC) of non-grafted chitosan membranes (CTS) and grafted in mixtures of isopropanol and water at varying compositions (iPrOH100, iPrOH90, iPrOH75 and iPrOH50). Data represents mean ± standard deviation for n=3

On the other hand, the iPrOH50 equilibrium hydration degree was higher than that of iPrOH75, oppositely to what would be expected. Nevertheless, although the monomer and initiator are both soluble at the polymerisation conditions of isopropanol at 50% and 60ºC, the polymerised NIPAAm precipitates partially, which may explain such discontinuity in the tendency of equilibrium hydration degree. The precipitation of the newly formed PNIPAAm also explains why the bulk grafting yield calculated by ^{1}H-NMR is quite similar for both

iPrOH50 and iPrOH75 samples, although the swelling of the chitosan membranes in isopropanol at 50% is twice than that determined at 75%.

7.4.5 PNIPAAm covalent grafting versus chain entanglement

The immobilisation of PNIPAAm chains on the membranes may take place by means of covalent bonds, formed by transfer reactions of the growing PNIPAAm radicals to the side substituents of the pyranosyl groups of chitosan. In radical polymerisation, the growth of each radical proceeds by successive addiction of monomer units until interrupted by one of the chain termination mechanisms, such as for instance chain transfer. Chain transfer reactions may occur towards the solvents, initiator, monomers, impurities or other molecules present in the reaction system, in an extent that depends on the chain transfer constant of each individual component, according to the Mayo equation [45]. It has been reported that grafting of poly(vinyl acetate) to poly(vinyl alcohol) occurs through a chain transfer mechanism [46]. Moreover, it was found that poly(acrylic acid-co-acrylamide) chains may be grafted onto starch-based polysaccharides by transfer reactions of the growing radicals on the side substituents of the pyranosyl cycles [47]. In fact, chain transfer seems to be an important mechanism on the grafting of PNIPAAm onto chitosan membranes. The XPS core level spectra for C1s and O1s show that PNIPAAm is grafted on the surface of non-swollen chitosan membranes (iPrOH100), in which chain entanglement is not an expected mechanism for PNIPAAm chains immobilization. In fact, the non-swollen nature of these samples (iPrOH100) should not allow the penetration of the growing radical and the samples were thoroughly washed with water/acetone to remove the non-grafted PNIPAAm. In the other samples (iPrOH50, iPrOH75, P-iPrOH75 and iPrOH90), polymer chains physical entanglement can not be discharged as a possible mechanism for PNIPAAm immobilization. Nevertheless, according to the Mayo theory [45], grafting through chain transfer reaction should be favoured inside the membrane, because chitosan (chain transfer agent) concentration is much higher in the interior of the swollen members than at the surface level, oppositely to the solvent concentration, which is higher at the membranes surface.

7.4.6 Cell sheet detachment and assessment of the cell viability

The non-modified chitosan membranes (CTS) showed poor cell adhesion and proliferation (see Figure 7.7). The few viable cells adhered on the CTS sample surface after 10 days of culture did not present the typical fibroblast-like morphology, being quite round and sparsely

distributed. The poor cell adhesion and proliferation on chitosan membranes have been previously reported [32, 48]. The iPrOH50 membranes presented very similar results (not shown). In turn, the cells cultured on the membranes modified using solvent compositions varying from 75% to 100% of isopropanol presented the typical elongated fibroblastic morphology. Moreover, it was possible to observe regions on the surface of these samples where cells reach the confluence, but also regions with only few adhered cells. Although the modification with PNIPAAm improved the surface properties in terms of cell behaviour, they did not present adequate cell proliferation to reach confluence all over the samples surface, within the pre-determined culture period. As our aim is to be able to create cell sheets, which can be harvested by simply lowering the temperature, cell confluence is a critical parameter to achieve. In one of our previous works [32], plasma treatment was very effective on improving the viability and proliferation of osteoblast-like cells. In this sense, in this work we used the same PNIPAAm grafting procedure on plasma treated chitosan membranes (P-iPrOH75). Fully confluent and viable cell sheets were formed on this sample after 10 days of culture (see Figure 7.7). As it can be observed in Figure 7.8, the confluent cell sheets were harvested from the modified thermo-responsive chitosan membranes (P-iPrOH75) keeping the cultured cells at room temperature (c.a. 16ºC). Although it was not possible to reach 100% confluence on the other PNIPAAm modified chitosan membranes (iPrOH50, iPrOH75, iPrOH90 and iPrOH100), we were able to observe the low temperature detachment of some single cells and smaller patches of confluent cells.

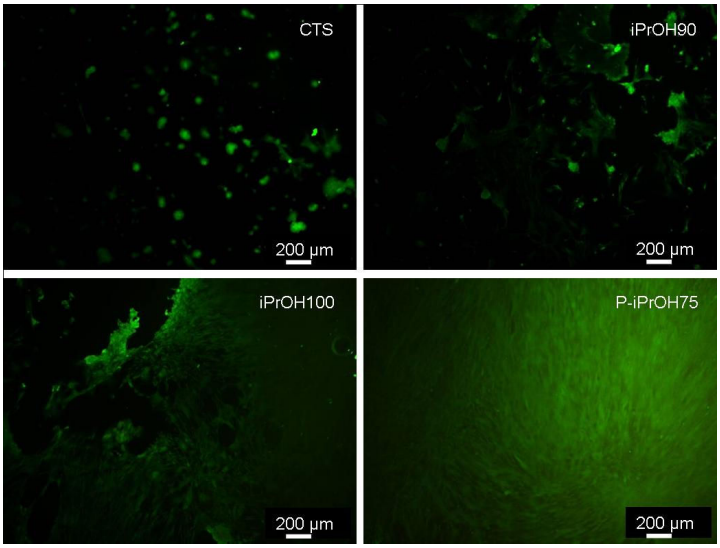

Figure 7.7 Fluorescence microscopy of viable human foetal lung fibroblast cells stained with Calcein AM solution in DMEM culture medium and after 10 days of culture on both non-modified chitosan membranes (CTS) and PNIPAAm grafted (iPrOH90, P-iPrOH75 and iPrOH100).

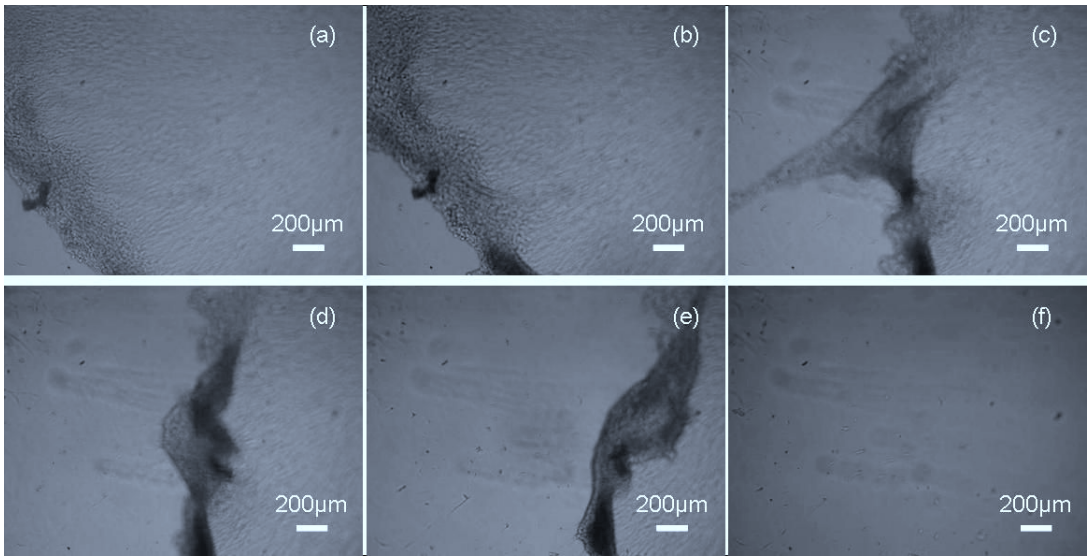

Figure 7.8 Light microscopy sequence **(a → f)** of the detachment, at room temperature (ca. 16ºC), of a confluent cell sheet grown on the PNIPAAm grafted chitosan membranes (P-iPrOH75).

7.5 Conclusions

The control of the swelling capability of the chitosan membranes could be tightly achieved by changing the composition of isopropanol and water mixtures, providing a suitable mean to tailor the modification yield and depth. The changes in the FTIR-ATR spectra point out to an increase in the amount of PNIPAAm in a superficial region of the membranes (1-5 µm) by means of increasing the polymerisation solvent swelling ratio. PNIPAAm was not detected in the ^{1}H-NMR spectra of the samples modified at low (iPrOH90) and non-swelling conditions (iPrOH100), revealing that the modification occurs mainly at superficial level, as it would be expected. In turn, the grafting yield calculated by ^{1}H-NMR is considerable high for iPrOH75 (5.3 wt. %) and iPrOH50 (5.5 wt. %), indicating a much deeper modification of these membranes. The XPS core level spectra for C1s and O1s show that PNIPAAm is grafted on the surface of non-swollen chitosan membranes (iPrOH100), in which chain entanglement is not an expected mechanism for PNIPAAm chains immobilization.

The immobilisation of PNIPAAm chains on these membranes should take place by transfer reactions of the growing PNIPAAm radicals to the side substituents of the pyranosyl groups of chitosan. In the other samples (iPrOH50, iPrOH75, P-iPrOH75 and iPrOH90), polymer chains physical entanglement can not be discharged as a concomitant mechanism for PNIPAAm immobilization.

The plasma treated chitosan membranes grafted with PNIPAAm (P-iPrOH75) produced fully confluent viable cell sheets after 10 days of culture. The confluent cell sheets were harvested from the thermo-responsive chitosan membranes (P-iPrOH75) by lowering the temperature. Although it was not possible to reach 100% confluence on the other PNIPAAm modified chitosan membranes, we were able to observe the low temperature detachment of some single cells and smaller patches of confluent cells.

The use of chitosan membranes, which possess adequate permeation properties for the rapid elimination or delivery of small molecules [38], would increase the mass transfer of nutrients and metabolic wastes, hopefully supporting the culture of thicker layered cell sheet constructs. Finally, fully hydrated chitosan membranes are flexible [30] and they should be easily adaptable to several anatomical shapes, facilitating the transfer of either single cell sheets or layered cell sheet constructs directly to the host site with minimal manipulation.

7.6 Acknowledgements

This work was partially supported by the Portuguese Foundation for Science and Technology (FCT), through funds from the POCTI and/or FEDER programmes and through the scholarship SFRH/BD/6862/2001 granted to Ricardo M. P. da Silva. Paula M. López-Pérez acknowledges EU Marie Curie Actions, Alea Jacta EST (MEST-CT-2004-008104) for providing her PhD Grant. This work was carried out under the scope of the European NoE EXPERTISSUES (NMP3-CT-2004-500283) and was also partially supported by the European Union funded STREP Project HIPPOCRATES (NMP3-CT-2003-505758).

7.7 References

1. Fujishige, S.; Kubota, K.; Ando, I., Phase-transition of aqueous-solutions of poly(*N*-isopropylacrylamide) and poly(*N*-isopropylmethacrylamide). *Journal of Physical Chemistry* **1989,** 93, (8), 3311-3313.

2. Kubota, K.; Fujishige, S.; Ando, I., Single-chain transition of poly(*N*-isopropylacrylamide) in water. *Journal of Physical Chemistry* **1990,** 94, (12), 5154-5158.

3. Scarpa, J. S.; Mueller, D. D.; Klotz, I. M., Slow hydrogen-deuterium exchange in a non-alfa-helical polyamide. *Journal of the American Chemical Society* **1967,** 89, (24), 6024-6030.

4. Baysal, B. M.; Karasz, F. E., Coil-globule collapse in flexible macromolecules. *Macromolecular Theory and Simulations* **2003,** 12, (9), 627-646.

5. Graziano, G., On the temperature-induced coil to globule transition of poly-*N*-isopropylacrylamide in dilute aqueous solutions. *International Journal of Biological Macromolecules* **2000,** 27, (1), 89-97.

6. da Silva, R. M. P.; Mano, J. F.; Reis, R. L., Smart thermoresponsive coatings and surfaces for tissue engineering: switching cell-material boundaries. *Trends in Biotechnology* **2007,** 25, (12), 577-583.

7. Yamato, M.; Konno, C.; Kushida, A.; Hirose, M.; Utsumi, M.; Kikuchi, A.; Okano, T., Release of adsorbed fibronectin from temperature-responsive culture surfaces requires cellular activity. *Biomaterials* **2000,** 21, (10), 981-986.

8. Huber, D. L.; Manginell, R. P.; Samara, M. A.; Kim, B. I.; Bunker, B. C., Programmed adsorption and release of proteins in a microfluidic device. *Science* **2003,** 301, (5631), 352-354.

9. Duracher, D.; Veyret, R.; Elaissari, A.; Pichot, C., Adsorption of bovine serum albumin protein onto amino-containing thermosensitive core-shell latexes. *Polymer International* **2004,** 53, (5), 618-626.

10. Shimizu, T.; Yamato, M.; Kikuchi, A.; Okano, T., Cell sheet engineering for myocardial tissue reconstruction. *Biomaterials* **2003,** 24, (13), 2309-2316.

11. Yang, J.; Yamato, M.; Kohno, C.; Nishimoto, A.; Sekine, H.; Fukai, F.; Okano, T., Cell sheet engineering: Recreating tissues without biodegradable scaffolds. *Biomaterials* **2005,** 26, (33), 6415-6422.

12. Kikuchi, A.; Okano, T., Nanostructured designs of biomedical materials: applications of cell sheet engineering to functional regenerative tissues and organs. *Journal of Controlled Release* **2005,** 101, (1-3), 69-84.

13. Yamada, N.; Okano, T.; Sakai, H.; Karikusa, F.; Sawasaki, Y.; Sakurai, Y., Thermoresponsive polymeric surfaces - control of attachment and detachment of cultured-cells. *Makromolekulare Chemie-Rapid Communications* **1990,** 11, (11), 571-576.

14. Ide, T.; Nishida, K.; Yamato, M.; Sumide, T.; Utsumi, M.; Nozaki, T.; Kikuchi, A.; Okano, T.; Tano, Y., Structural characterization of bioengineered human corneal endothelial cell sheets fabricated on temperature-responsive culture dishes. *Biomaterials* **2006,** 27, (4), 607-614.

15. Nakajima, K.; Honda, S.; Nakamura, Y.; Lopez-Redondo, F.; Kohsaka, S.; Yamato, M.; Kikuchi, A.; Okano, T., Intact microglia are cultured and non-invasively harvested without pathological activation using a novel cultured cell recovery method. *Biomaterials* **2001,** 22, (11), 1213-1223.

16. Von Recum, H. A.; Okano, T.; Kim, S. W.; Bernstein, P. S., Maintenance of retinoid metabolism in human retinal pigment epithelium cell culture. *Experimental Eye Research* **1999,** 69, (1), 97-107.

17. Canavan, H. E.; Cheng, X. H.; Graham, D. J.; Ratner, B. D.; Castner, D. G., Cell sheet detachment affects the extracellular matrix: a surface science study comparing thermal liftoff, enzymatic, and mechanical methods. *Journal of Biomedical Materials Research Part A* **2005,** 75A, (1), 1-13.

18. Kwon, O. H.; Kikuchi, A.; Yamato, M.; Sakurai, Y.; Okano, T., Rapid cell sheet detachment from poly(N-isopropylacrylamide)-grafted porous cell culture membranes. *Journal Of Biomedical Materials Research* **2000,** 50, (1), 82-89.

19. Kwon, O. H.; Kikuchi, A.; Yamato, M.; Okano, T., Accelerated cell sheet recovery by co-grafting of PEG with PIPAAm onto porous cell culture membranes. *Biomaterials* **2003,** 24, (7), 1223-1232.

20. Yamato, M.; Utsumi, M.; Kushida, A.; Konno, C.; Kikuchi, A.; Okano, T., Thermo-responsive culture dishes allow the intact harvest of multilayered keratinocyte sheets without dispase by reducing temperature. *Tissue Engineering* **2001,** 7, (4), 473-480.

21. Shimizu, T.; Yamato, M.; Kikuchi, A.; Okano, T., Two-dimensional manipulation of cardiac myocyte sheets utilizing temperature-responsive culture dishes augments the pulsatile amplitude. *Tissue Engineering* **2001,** 7, (2), 141-151.

22. Harimoto, M.; Yamato, M.; Hirose, M.; Takahashi, C.; Isoi, Y.; Kikuchi, A.; Okano, T., Novel approach for achieving double-layered cell sheets co-culture: overlaying endothelial cell sheets onto monolayer hepatocytes utilizing temperature-responsive culture dishes. *Journal of Biomedical Materials Research* **2002,** 62, (3), 464-470.

23. Nishida, K.; Yamato, M.; Hayashida, Y.; Watanabe, K.; Yamamoto, K.; Adachi, E.; Nagai, S.; Kikuchi, A.; Maeda, N.; Watanabe, H.; Okano, T.; Tano, Y., Corneal reconstruction with tissue-engineered cell sheets composed of autologous oral mucosal epithelium. *New England Journal Of Medicine* **2004,** 351, (12), 1187-1196.

24. Shimizu, T.; Yamato, M.; Isoi, Y.; Akutsu, T.; Setomaru, T.; Abe, K.; Kikuchi, A.; Umezu, M.; Okano, T., Fabrication of pulsatile cardiac tissue grafts using a novel 3-dimensional cell sheet manipulation technique and temperature-responsive cell culture surfaces. *Circulation Research* **2002,** 90, (3), E40-E48.

25. Kumar, M., A review of chitin and chitosan applications. *Reactive & Functional Polymers* **2000,** 46, (1), 1-27.

26. Wang, C.; Ye, W.; Zheng, Y.; Liu, X.; Tong, Z., Fabrication of drug-loaded biodegradable microcapsules for controlled release by combination of solvent evaporation and layer-by-layer self-assembly. *International Journal Of Pharmaceutics* **2007,** 338, (1-2), 165-173.

27. Prabaharan, M.; Mano, J. F., Chitosan-based particles as controlled drug delivery systems. *Drug Delivery* **2005,** 12, (1), 41-57.

28. Siddaramaiah; Kumar, P.; Divya, K. H.; Mhemavathi, B. T.; Manjula, D. S., Chitosan/HPMC polymer blends for developing transdermal drug delivery systems. *Journal Of Macromolecular Science-Pure And Applied Chemistry* **2006,** A43, (3), 601-607.

29. Thacharodi, D.; Panduranga Rao, K., Rate-controlling biopolymer membranes as transdermal delivery systems for nifedipine: Development and in vitro evaluations. *Biomaterials* **1996,** 17, (13), 1307.

30. Silva, R. M.; Silva, G. A.; Coutinho, O. P.; Mano, J. F.; Reis, R. L., Preparation and characterisation in simulated body conditions of glutaraldehyde crosslinked chitosan membranes. *Journal Of Materials Science-Materials In Medicine* **2004,** 15, (10), 1105-1112.

31. Silva, R. M.; Elvira, C.; Mano, J. F.; San Roman, J.; Reis, R. L., Influence of beta-radiation sterilisation in properties of new chitosan/soybean protein isolate membranes for guided bone regeneration. *Journal Of Materials Science-Materials In Medicine* **2004,** 15, (4), 523-528.

32. Lopez-Perez, P. M.; Marques, A. P.; da Silva, R. M. P.; Pashkuleva, I.; Reis, R. L., Effect of chitosan membranes' surface modification via plasma induced polymerization on the adhesion of Osteoblast-like cells. *Journal of Materials Chemistry* **2007,** 17, (38), 4064-4071.

33. Tuzlakoglu, K.; Alves, C. M.; Mano, J. F.; Reis, R. L., Production and characterization of chitosan fibers and 3-D fiber mesh scaffolds for tissue engineering applications. *Macromolecular Bioscience* **2004,** 4, (8), 811-819.

34. Silva, G. A.; Ducheyne, P.; Reis, R. L., Materials in particulate form for tissue engineering. 1. Basic concepts. *Journal of Tissue Engineering and Regenerative Medicine* **2007,** 1, (1), 4-24.

35. Baran, E. T.; Tuzlakoglu, K.; Salgado, A. J.; Reis, R. L., Multichannel mould processing of 3D structures from microporous coralline hydroxyapatite granules and chitosan support materials for guided tissue regeneration/engineering. *Journal of Materials Science-Materials in Medicine* **2004,** 15, (2), 161-165.

36. Patel, M.; Mao, L.; Wu, B.; VandeVord, P. J., GDNF-chitosan blended nerve guides: a functional study. *Journal of Tissue Engineering and Regenerative Medicine* **2007,** 1, (5), 360-367.

37. Mano, J. F.; Reis, R. L., Osteochondral defects: present situation and tissue engineering approaches. *Journal of Tissue Engineering and Regenerative Medicine* **2007,** 1, (4), 261-273.

38. da Silva, R. M. P.; Caridade, S. G.; San Roman, J.; Mano, J. F.; Reis, R. L., Transport of small anionic and neutral solutes through chitosan membranes: dependence on crosslinking and chelation of divalent cations. *Submitted* **2007**.

39. Terbojevich, M.; Cosani, A.; Muzzarelli, R. A. A., Molecular parameters of chitosans depolymerized with the aid of papain. *Carbohydrate Polymers* **1996,** 29, (1), 63-68.

40. da Silva, R.; Mano, J.; Reis, R., An exact mathematical description for the straightforward determination of the degree of N-acetylation of chitosan by the 1st derivative UV spectrophotometry. *Submitted* **2007**.

41. Ratner, B. D., Surface Properties of Materials. In *Biomaterials Science: An introduction to Materials in Medicine*, Ratner, B. D.; Hoffman, A. S.; Schoen, F. J.; Lemons, J. E., Eds. Academic Press: San Diego 1996; pp 21-35.

42. Briggs, D., *Surface analysis of polymers by XPS and static SIMS*. Cambridge University Press: 1998; p 47-87.

43. Adem, E.; Avalos-Borja, M.; Bucio, E.; Burillo, G.; Castillon, F. F.; Cota, L., Surface characterization of binary grafting of AAc/NIPAAm onto poly(tetrafluoroethylene) (PTFE). *Nuclear Instruments & Methods in Physics Research Section B-Beam Interactions with Materials and Atoms* **2005,** 234, (4), 471-476.

44. Bullett, N. A.; Talib, R. A.; Short, R. D.; McArthur, S. L.; Shard, A. G., Chemical and thermo-responsive characterisation of surfaces formed by plasma polymerisation of N-isopropyl acrylamide. *Surface and Interface Analysis* **2006,** 38, (7), 1109-1116.

45. Mayo, F. R., Chain Transfer in the Polymerization of Styrene: The Reaction of Solvents with Free Radicals. *J. Am. Chem. Soc.* **1943,** 65, (12), 2324-2329.

46. Okaya, T.; Fujita, H.; Suzuki, A.; Kikuchi, K., Study on chain transfer reaction of poly(vinyl acetate) radical with poly(vinyl alcohol) in a homogeneous system. *Designed Monomers and Polymers* **2004,** 7, (3), 269.

47. Elvira, C.; Mano, J. F.; San Roman, J.; Reis, R. L., Starch-based biodegradable hydrogels with potential biomedical applications as drug delivery systems. *Biomaterials* **2002,** 23, (9), 1955-1966.

48. Zhu, X.; Chian, K. S.; Chan-Park, M. B. E.; Lee, S. T., Effect of argon-plasma treatment on proliferation of human-skin-derived fibroblast on chitosan membrane in vitro. *Journal Of Biomedical Materials Research Part A* **2005,** 73A, (3), 264-274.

Chapter 8

General conclusions and final remarks

The inherent variability of natural materials demands the establishment of adequate purification and characterisation procedures for the natural origin raw-materials. Chitosan is a natural-derived polymer procuded by *N*-deacetylation of chitin, which can be obtained with a good purity. For this polymer, the *N*-deacetylation reaction can be other factor of variability, since producers often supply products with quite variable extents of *N*-deacetylation between batches. Although this might be regarded as a shortcoming, this problem can be relatively overcome by a careful examination of chitosan properties, such as the degree of *N*-acetylation (DA) and the molecular weight, and by keeping the same batch of purified materials throughout a closed set of experiments. It is also thought to be highly valuable to set up some correction measures of the raw-materials basic properties such as procedures for the selective *N*-acetylation or further *N*-deacetylation. This allows one not to be so dependent on the properties of the supplied chitosan raw-materials, as well as to tailor it to each specific application.

Chitosan was undoubtedly the centre of gravity of this thesis from the viewpoint of the materials in study, which justified a greater investment in its characterisation and to control its properties. In fact, one entire chapter (chapter 3) is dedicated to the determination of the degree of *N*-acetylation, in which the 1st derivative UV spectrophotometry method is improved and compared with the gold-standard ^{1}H-NMR methods. We derived a mathematical expression that avoids the use of empiric correction curves for the determination of the DA of highly deacetylated samples. The DA is determined directly from the mass concentration of chitosan solutions and the 1st derivative value of its UV spectra at 202 nm (the acetic acid solutions zero crossing point), over the entire range of chitosan DA. It was also defined a solid criterion for the absorbance range within which the method remains valid. A procedure was also proposed for the accurate mass determination of the hygroscopic chitosan. In our opinion, the 1st derivative UV spectrophotometry is a robust, accurate and precise technique for the determination of the DA of soluble chitosan samples. It presents several advantages such as: (i) it is relatively tolerant to the presence of residual acetic acid and protein contaminants; (ii) it only requires a small amount of sample, simple reagents and equipments; and (iii) the high value of the 1st derivative of the GluNAc molar absorptivity should assure a good accuracy on the determination of the GluNAc residues even at very low concentrations (high DA). The values of the DA for several chitosan samples for the entire range of the copolymer solubility confirmed the good precision of the

method with typical coefficients of variation around 1%. The comparison with an optimised ^{1}H-NMR determination reiterates the expected fine accuracy of the 1st derivative UV spectrophotometry. The proposed approach is important to automate the routine determination of the DA at large industrial scale, especially if taking into consideration the currently available potent multiwell microplate readers, which allow measuring hundreds of samples in just few minutes.

In what concerns to the applications for regenerative medicine, the first goal of this thesis was the development of biodegradable membranes based on chitosan and soybean protein isolate (SI) for guided bone regeneration (GBR). The GBR concept consists on the use of barrier membranes that prevent the in-growth of non-desired connective tissue, which in critical size defects inhibit the formation of new bone through the natural healing process. Membranes presenting very interesting morphology and properties could be obtained by combining chitosan and SI. The partial insolubility of SI at the processing pH, as well as its asymmetric distribution through the transversal section, being the SI insoluble particles more concentrated at the mould exposed surface, are desirable features to attain a controlled degradation rate *in vivo*. Furthermore, it can be foreseen a two-step degradation mechanism, eventually leading to *in situ* porous formation, which might be clinically useful. Moreover, since in general no remarkable differences were observed for the studied bulk and surface properties of the membranes, it might be possible to tailor their degradation and their biological response without changing their key properties, by means of controlling the blends' composition.

Although the chitosan-based membranes were initially thought for GBR, the key aim of the thesis (in the viewpoint of the envisaged applications for the developed materials) was a relatively new technology so-called cell sheet engineering. Even though relatively independent, chapter 5, 6 and 7 converge to that objective. The first two referred to chapters are related to the characterization of the chitosan membranes, in order to justify their use as underlying substrates to graft PNIPAAm for cell sheet engineering applications. Properties of those substrates such as permeability and elasticity can be advantageous to introduce new functionalities, like for instances combining with drug delivery strategies, conferring mechanical compatibility to the substrates, introducing mechanical stimulus, direct release of the cell sheet on the target place, etc. The remaining experimental chapter is specifically focused on the cell sheet engineering application.

In chapter 5, chitosan membranes were prepared, and in some cases crosslinked with glutaraldehyde, in order to obtain different degrees of crosslinking. A method was implemented to test the tensile mechanical properties of chitosan-based membranes in an aqueous solution environment, aiming at simulating physiological relevant conditions. This novel method is highly relevant to evaluate the mechanical performance of new biomaterials

that present high swelling ratios, since this evaluation both under static and dynamic solicitations at an air atmosphere is worthless. Actually, these test conditions are not representative of the physiological environments in which the swollen materials have a completely different mechanical behaviour. We found that the mechanical resistance to stretching decreased sharply when swollen in an aqueous environment, mainly due to the high hydration equilibrium degree of chitosan materials. Chitosan membranes and membranes crosslinked with small amounts of glutaraldehyde become more flexible, making them suitable for some biomedical applications. Moreover, dynamic mechanical analysis in temperature scan mode confirmed the mechanical stiffness dependence on the temperature of crosslinked chitosan membranes. This dependence increased with the crosslinking degree. All membrane formulations exhibit a viscoelastic behaviour which could have advantages in the mechanical compatibility with the tissues to be repaired. All formulations were found to be relatively stable in isotonic saline solution up to 60 days. In fact, the weight loss was never superior than 12% and the membranes have kept its mechanical integrity.

Another key aspect of biomaterials characterisation addressed in chapter 5 was the cytotoxicity screening. The preliminary cell culture cytotoxicity studies performed indicate that there is a good interaction of the tested materials with the fibroblast-like cells. The biochemical tests confirmed that the viability of cells in contact with the extracts is maintained. In some cases an increased biochemical activity of cells is observed, which can be correlated indirectly with cell proliferation. The biological performance of the membranes seems to pre-indicate that they are suitable to be used in biomedical applications.

In chapter 6, it was studied the transport of small anionic and neutral molecules across chitosan membranes. Chitosan membranes were prepared by solvent casting and crosslinked with glutaraldehyde at several ratios. The permeability experiments were conducted using a home designed side-by-side diffusion cell to determine the flux of small molecules of similar size, both holding different chemical moieties, both ionised at the physiological pH (benzoic acid, salicylic acid and phthalic acid) and neutral (2-phenylethanol). The permeability of the different model solutes revealed to be dependent on the affinity of these structurally similar molecules to chitosan, i.e., related to the partition coefficient determined in an independent experiment. The equilibrium swelling degree and the permeability of chitosan membranes showed a similar tendency, increasing until an intermediate crosslinking degree and then decreasing. This atypical behaviour is also described in chapter 5 and it was explained by a reduction in the crystallinity as the crosslinking degree increases. Finally, the permeability of the salicylate anion was enhanced by the presence of metal cations commonly present in biological fluids, such as calcium and magnesium, but remained unchanged for the neutral 2-phenylethanol. This effect was explained by the chelation of metal cations by the amine groups of chitosan, which increased

the partition coefficient. The change in the permeation properties of chitosan to anionic solutes in the present of these metallic cations is an important result and should be taken into consideration when trying to make *in vitro* predictions of the drug release from chitosan based controlled delivery systems.

In chapter 7, PNIPAAm was originally immobilised on chitosan membranes to render the membranes with thermo-responsive surface properties. The aim was to create membranes suitable for cell culture and in which confluent cell sheets can be recovered by lowering the temperature. The chitosan membranes were immersed in monomer solutions that were polymerised via radical initiation. The composition of the polymerisation reaction solvent, which was a mixture of a chitosan non-solvent (isopropanol) and a solvent (water), offered an interesting route to obtain a tight control over the chitosan membranes swelling capability, providing a suitable way of tailoring the modification yield and depth. It was hypothesised that the different swelling ratio, obtained at different solvent composition of the reaction mixture, should drive simultaneously the monomer solubility and diffusion into the polymeric matrix, polymerisation reaction rate, as well as eventual chain transfer reactions to the side substituents of the pyranosyl groups of chitosan. A combined analysis of the modified membranes chemistry by ^{1}H-NMR, FTIR-ATR and XPS showed that it was possible to control the chitosan modification yield and depth in the solvent composition range between 75% and 100% of isopropanol. The immobilisation of PNIPAAm chains on the membranes modified using 100% of isopropanol should take place by transfer reactions of the growing PNIPAAm radicals to the side substituents of the pyranosyl groups of chitosan. In the cases were some water was added to the reaction solvent, polymer chains physical entanglement can not be discharged as a concomitant mechanism for PNIPAAm immobilisation. Some of the membranes were subjected to oxygen plasma treatment before the PNIPAAm immobilisation. The plasma treated chitosan membranes grafted with PNIPAAm (using a reaction solvent with 75% of isopropanol) produced fully confluent viable cell sheets after 10 days of culture. The confluent cell sheets were harvested from the modified chitosan membranes lowering the temperature. Although it was not possible to reach the complete confluence on the other PNIPAAm modified chitosan membranes, it was also possible to observe the low temperature detachment of some single cells and smaller patches of confluent cells.

The hypothetic use of chitosan membranes, which were found to be permeable to small molecules, would increase the mass transfer of nutrients and metabolic wastes, hopefully supporting the culture of thicker layered cell sheet construct. Additionally, fully hydrated chitosan membranes are flexible and they should be easily adaptable to different anatomical shapes, facilitating the transfer of either single cell sheets or layered cell sheet constructs directly to the host site with minimal manipulation.

Future work

The scientific and technology development processes are a never-ended journey. Each closed research project opens a new range of questions and technological capabilities that can be exploited in multiple directions. The work developed in the scope of this thesis is not an exception. Herein, we do not intend, and we could never do so, to suggest exhaustively the possible directions for future work, but only to highlight some points that might be interesting and fruitful to exploit.

As a start point, we should say that, although confluent cell sheets have been successfully obtained using the developed thermo-responsive surfaces, further adjustments on the chemistry should be considered in order to improve the performance on what concerns to cell adhesion and proliferation. These improvements should decrease the time necessary for seeded cells to reach confluence and consequently to produce a cell sheet. Other work directions might include:

- To study the permeability of larger molecules and to determine the molecular weight cut-off of the chitosan membranes;
- To create full models to accurately describe the diffusional mass transfer across the membranes, taking into account the interactions' kinetics between the chitosan membranes matrix and the diffusing molecules;
- To combine the release of growth factors, differentiation factor or other bioactive agents with relevant cell types in cell sheet engineering approaches;
- To study how the mechanical properties of the underlying substrates affect the functionality of cell sheets created with cells of different phenotypes; for instance, which is the influence of the underlying substrates mechanical properties in the cardiomyocyte cell sheets pulsation;
- To set up methodologies to produce thermo-responsive culture dishes inserts at a larger scale to be used as routine research instruments.